

✓

**AN INVESTIGATION OF
THE MEDIAL BRANCHES OF THE
CERVICAL AND THORACIC SYMPATHETIC CHAIN**

by

NALINI PATHER

Submitted in partial fulfillment of the requirements for the degree

MASTERS OF MEDICAL SCIENCE

in the

Department of Anatomy
University of Durban-Westville
Durban
2001



To my husband Glen,

Son Rayuel,

My parents and family

*For you created my inmost being;
You knit me together in my mother's womb.
I praise you because I am fearfully and wonderfully made;
Your works are wonderful,
I know that full well.
Ps 139:13-14*

ABSTRACT

The number of peripheral segmental branches of the cervical and thoracic sympathetic chains are more variable and larger than assumed by textbooks and literature (Groen *et al.*, 1987). This investigation aims to clarify and update the variable patterns of the cervical sympathetic chain, the incidence of fused thoracic ganglia and the contributions of the cervical and thoracic sympathetic chain to the cardiac plexus. The study involved the macro and micro-dissection of 89 cadaveric sides (foetal, 60 and adult, 29).

The gross anatomy of the cervical sympathetic chain and variations is documented. This study confirms previous reports that the number of ganglia in the cervical region ranged from 2 (absent MCG) to four (double MCG) ganglia. A double MCG was found in 25.9%. This study reports the higher incidence of the normal/typical MCG (as per textbook definition) i.e. *Type II* MCG (46.6%) than the *Type I* MCG (27.6%) and *Type III* (32.8%). The number of thoracic ganglia in this study is 8-11. Fusion of ganglia was found to be more common in the lower thoracic chain than in the upper thoracic chain. This study reports the origin of cardiac rami from the thoracic sympathetic chain up to the interganglionic segment between T₅ and T₆ ganglia. The incidence if TCR₅ was 60.4%. In ¹⁵/₅₈ sides (25.9 %) TCR₅ arose from the interganglionic segment of the chain, either above or below the ganglion.

An accurate knowledge of the anatomy of the sympathetic nervous system and the adjacent structures is, inescapably a definite asset to the procedures used in interrupting the neural mechanism (Jamieson *et al.*, 1952). Successful sympathetic denervation of the heart, a field often beset with failure, is dependant on adequate morphological knowledge. It is hoped that this study using human foetuses as well as adult cadaveric specimens will draw the attention to important variations that are relevant to the surgeon.

The intricate anatomical relations presented in this study attest the complex anatomy of the sympathetic nervous system.

SUPPORTING SERVICES

In this research the statistical planning and analyses, and recommendations arising from these analyses have been done with the support of the Computer Services Department, and the University of Durban-Westville.

PREFACE

This study represents original work by the author and has not been submitted in any form to another University. Where use was made of the work of others, it has been duly acknowledged in the text.

The research described in this dissertation was supervised by Professor K S Satyapal and Dr P Partab of the Department of Anatomy, University of Durban-Westville) in which the research was conducted.

ACKNOWLEDGEMENTS

The author wishes to express her sincere gratitude to the following individuals and departments for their assistance in the preparation of this dissertation:

- My parents Dave and Radha Naidoo for their love, support and encouragement
- Professor K S Satyapal for his encouragement, motivation, assistance, skillful guidance, support and supervision
- Dr P Partab for his 'constructive criticism', scrupulous attention to detail, expert guidance and supervision
- Ms Lelika Ramsaroop for her friendship, assistance and most especially for being my 'teammate'
- Ms Nirusha Lachman for her friendship, advice, assistance, dedication and encouragement throughout this project
- Dr Y Omar, Professor MR Haffajee and Dr MAA Ebrahim for their kind support
- Mr G Mathura, Mr CE Chetty and the other technicians at the Department of Anatomy for their assistance through this project
- University of Durban-Westville for financial support
- Ms Indirani Naidoo from the IT Department, University of Durban-Westville for assistance in the statistical evaluation
- Dr A Bramdev and the technicians at the Lancet Laboratories, Lorne Street for their assistance in preparing and analyzing the histological specimens
- Reverend A L Hammond for his love, support, encouragement and inspiration
- My family at Trulite for their encouragement and love
- And most especially, my husband Glen for his love, professional assistance, thoughtfulness, support and encouragement; and my son Rayuel for his loving and understanding nature, without which this work would not have been possible

CONTENTS

	Page No.
Abstract	iii
Supporting Services	iv
Preface	v
Acknowledgements	vi
Contents	vii
List of Figures	x
List of Tables	xiii
List of Plates	xiv
 CHAPTER 1 INTRODUCTION.....	 1
 CHAPTER 2 REVIEW OF LITERATURE.....	 5
2.1 The sympathetic nervous system.....	11
2.2 Cervical sympathetic chain.....	18
2.2.1 Course and relations.....	19
2.2.2 Superior cervical ganglion.....	20
2.2.3 Middle cervical ganglion.....	22
2.2.4 Inferior cervical ganglion.....	27
2.2.5 Cervicothoracic ganglion.....	29
2.3 Thoracic sympathetic chain.....	33
2.3.1 Course and relations.....	33
2.3.2 Thoracic ganglia.....	36
2.4 Cardiac sympathetic nerves.....	41
2.5 Other medial branches.....	48
2.5.1 Splanchnic nerves.....	48
2.5.2 Vascular branches.....	52
2.5.3 Laryngo-pharyngeal branches.....	55
2.5.4 Pulmonary branches.....	55
2.5.5 Oesophageal branches.....	55
2.6 Embryology	56
 CHAPTER 3 MATERIALS AND METHODS.....	 62
3.1 Materials.....	63
3.2 Gross anatomical dissection.....	64
3.2.1 Thoracic dissection.....	64
3.2.2 Cervical dissection.....	65

5.5	Other medial branches.....	167
5.5.1	Splanchnic nerves.....	167
5.5.2	Vascular branches.....	171
5.5.3	Miscellaneous branches.....	173
CHAPTER 6	CONCLUSION.....	174
REFERENCES	178
APPENDIX A	Foetal and adult series.....	191
APPENDIX B	SCG length and width.....	192
APPENDIX C	MCG length and width.....	193
APPENDIX D	CTG length and width.....	194
APPENDIX E	Splanchnic nerve patterns.....	195
	Conference presentations and publications	196

3.3	Histology.....	66
3.4	Nomenclature.....	66
3.4.1	Identification of ganglia.....	66
3.4.2	Identification of cardiac rami.....	67
3.5	Statistical analysis.....	68
CHAPTER 4	RESULTS.....	69
4.1	Sample.....	70
4.2	Cervical Sympathetic Chain.....	72
4.2.1	Course and relations.....	72
4.2.2	Superior cervical ganglion.....	76
4.2.3	Middle cervical ganglion.....	79
4.2.4	Inferior cervical ganglion.....	90
4.2.5	Cervicothoracic ganglion.....	92
4.3	Thoracic sympathetic chain.....	98
4.3.1	Course and relations.....	98
4.3.2	Thoracic ganglia.....	100
4.4	Cardiac sympathetic nerves.....	104
4.4.1	Cervical cardiac rami.....	105
4.4.2	Cervicothoracic cardiac rami.....	113
4.4.3	Thoracic cardiac rami.....	118
4.5	Other medial branches.....	127
4.5.1	Splanchnic nerves.....	127
4.5.2	Vascular branches.....	133
4.5.3	Miscellaneous branches.....	139
4.6	Histological analysis.....	140
CHAPTER 5	DISCUSSION.....	142
5.1	Sample.....	143
5.2	Cervical Sympathetic Chain.....	144
5.2.1	Course and relations.....	144
5.2.2	Superior cervical ganglion.....	145
5.2.3	Middle cervical ganglion.....	148
5.2.4	Inferior cervical ganglion.....	154
5.2.5	Cervicothoracic ganglion.....	155
5.3	Thoracic sympathetic chain.....	158
5.3.1	Course and relations.....	158
5.3.2	Thoracic ganglia.....	159
5.4	Cardiac sympathetic nerves.....	164

LIST OF FIGURES

Figure 1	Diagram of the sympathetic and parasympathetic nervous distribution to the trunk.	Page 10
Figure 2	The thoracic and abdominal sympathetic trunks displaying thoracic and abdominal autonomic plexus	Page 12
Figure 3	Diagrammatic illustration of autonomic nervous pathways	Page 16
Figure 4	Relations of the cervical sympathetic chain.	Page 18
Figure 5	Diagrammatic illustration of MCG, ICG and the Ansa Subclavia	Page 22
Figure 6	Illustration of cervical chain displaying the varying locations of MCG	Page 24
Figure 7	Illustration of cervical sympathetic chain displaying an unfused ICG	Page 28
Figure 8	Relations of CTG	Page 30
Figure 9	Anterior view of the mediastinal relations of the right sympathetic chain	Page 34
Figure 10	Lateral view of the mediastinal relations of the left sympathetic chain	Page 35
Figure 11	The thoracic sympathetic chains and their relations	Page 37
Figure 12	Relations of TG in the intercostals space	Page 38
Figure 13	Diagrammatic illustration of the origin of the cardiac sympathetic nerves	Page 41
Figure 14	Cervical and thoracic cardiac sympathetic nerves	Page 44
Figure 15	Autonomic pathways to the heart	Page 47
Figure 16	Origin of splanchnic nerves from the thoracic sympathetic chain	Page 49
Figure 17	Autonomic pathway to the abdominal viscera	Page 51
Figure 18	Diagrammatic illustration of the sympathetic pathways to blood vessels	Page 52
Figure 19	Schema illustrating the development of possible variations of the	

	ganglionated chain from the primordial cell column	Page 57
Figure 20	The formation of two ventral motor (basal) columns and two dorsal sensory (alar) columns throughout most of the spinal cord	Page 59
Figure 21	Postganglionic fibres vascular fibres from cervical & thoracic chain ganglia to the head and pharynx and the heart and lungs	Page 61
Figure 22	Graphic representation of sample distribution (n=89)	Page 70
Figure 23	Graphical representation of the sample distribution of (n=89):	Page 71
Figure 24	Number of ganglia in the cervical chain	Page 74
Figure 25	Incidence of cervical ganglia	Page 75
Figure 26	Incidence of MCG variations	Page 80
Figure 27	Diagrammatic illustration cervical chain Types I, IIa and IIb	Page 85
Figure 28	Diagrammatic illustration cervical chain Types IIc, IIIa, IIIb and IIIc	Page 86
Figure 29	Illustration of mean distance of MCG (Types I & II) and CTG from SCG	Page 88
Figure 30	Illustration of location of CTG	Page 92
Figure 31	Summary of incidence of fused ganglia	Page 102
Figure 32	Summary of the incidence and origin of cardiac sympathetic nerves	Page 106
Figure 33	Incidence of origin of SCCR (n=58)	Page 109
Figure 34	Incidence and origin of MCCR (n=58)	Page 111
Figure 35	Incidence and origin of ICCR (n=9)	Page 113
Figure 36	Incidence and origin of CTCR	Page 115
Figure 37	Incidence of TCR	Page 118
Figure 38	Origin and incidence of TCR1	Page 119
Figure 39	Incidence and origin of TCR2	Page 121

Figure 40	Incidence and origin of TCR3	Page 123
Figure 41	Incidence and origin of TCR4	Page 124
Figure 42	Incidence and origin of TCR5	Page 125
Figure 43	Diagrammatic illustration of cervical chain types	Page 158
Figure 44	Types of ganglia	Page 161

LIST OF TABLES

Table 1	Lowest root of TCR	Page 45
Table 2	Foetal and adult sampling	Page 69
Table 3	Incidence of cervical ganglia	Page 74
Table 4	Vertebral location of SCG	Page 75
Table 5	Range of dimensions of SCG in the adult specimens	Page 76
Table 6	Vertebral location of MCG	Page 79
Table 7	Incidence of MCG in foetal and adult specimens	Page 82
Table 8	Range of dimensions of Types I, II and III MCG in the adult specimens	Page 88
Table 9	Incidence of different shapes of CTG	Page 93
Table 10	Range of dimensions of CTG in the adult specimens	Page 93
Table 11	Number of thoracic ganglia	Page 100
Table 12	Pervallence of fused ganglia	Page 101
Table 13	Summary of the origin and incidence of Cardiac sympathetic nerves	Page 104
Table 14	Incidence and origin of SCCR	Page 107
Table 15	Origin and incidence of MCCR	Page 111
Table 16	Origin and incidence of ICCR	Page 113
Table 17	Origin and incidence of CTTR	Page 114
Table 18	Origin and incidence of TCR1	Page 119
Table 19	Origin and incidence of TCR2	Page 121
Table 20	Origin and incidence of TCR3	Page 123
Table 21	Origin and incidence of TCR4	Page 124
Table 22	Origin and incidence of TCR5	Page 125
Table 23	Incidence of splanchnic nerves	Page 127
Table 24	Incidence of the number of roots of GSN	Page 130
Table 25	Range of root values for GSN, LSN, Isn	Page 130
Table 26	Incidence of highest root of GSN	Page 131

LIST OF PLATES

Plate 1	Antero-lateral view of left cervical sympathetic chain demonstrating its relations (adult)	Page 72
Plate 2	Antero-lateral view of right sympathetic chain demonstrating the split chain arising from the lower pole of SCG (adult)	Page 73
Plate 3	Antero-lateral view of left sympathetic chain demonstrating the relationship of SCG to the bifurcation of the common carotid artery (foetus)	Page 77
Plate 4	Antero-lateral view of left cervical sympathetic chain demonstrating the communicating ramus between SCG and the vagus nerve in a foetus	Page 78
Plate 5	Antero-lateral view of left sympathetic chain demonstrating Type II MCG (foetus)	Page 79
Plate 6	Antero-lateral view of left cervical sympathetic chain in a foetus demonstrating the relationship of the inferior thyroid artery to type ii MCG	Page 82
Plate 7	Antero-lateral view of left cervical sympathetic chain demonstrating the ICG in an adult specimen	Page 91
Plate 8	Antero-lateral view of right cervical sympathetic chain demonstrating the relations of CTG in a foetus.	Page 93
Plate 9	Antero-lateral view of left cervical chain demonstrating the rami communicantes to the brachial plexus in an adult	Page 95
Plate 10	Antero-lateral view of left sympathetic chain in a foetus demonstrating the formation of the ansa subclavian	Page 96
Plate 11	Antero-lateral view of Cervical Sympathetic Chain in an adult demonstrating the formation of the ansa subclavian	Page 97
Plate 12	Antero-lateral view of right thoracic sympathetic chain demonstrating the medial deviation of the chain inferiorly	Page 99
Plate 13	Antero-lateral view of right thoracic sympathetic chain demonstrating fused ganglia	Page 103

Plate 14	Anterior view of thoracic ganglion demonstrating the rami to the intervertebral disc and vertebral body	Page 104
Plate 15	Antero-lateral view of left cervical sympathetic chain demonstrating the ganglionic origin of SCCR in an adult.	Page 108
Plate 16	Antero-lateral view of left cervical sympathetic chain demonstrating the ganglionic origin of MCCR in an adult	Page 112
Plate 17	Antero-lateral view of adult cervical sympathetic chain demonstrating the ganglionic origin of CTCR in an adult	Page 116
Plate 18	Antero-lateral view of right sympathetic chain demonstrating the origin of the CTCR in an adult	Page 117
Plate 19	Antero-lateral view of right thoracic sympathetic chain demonstrating the origin of thoracic cardiac rami in a foetus	Page 122
Plate 20	Antero-lateral view of right sympathetic chain demonstrating the splanchnic nerves in a foetus with an accompany schematic diagram	Page 128
Plate 21	Antero-lateral view of left sympathetic chain demonstrating the splanchnic nerves in a adult	Page 129
Plate 22	Antero-lateral view of left thoracic sympathetic chain demonstrating the origin of GSN and LSN in a foetus	Page 132
Plate 23	Antero-lateral view of a foetal left cervical sympathetic chain demonstrating the vertebral nerve and branches to the common carotid artery	Page 134
Plate 24	Antero-lateral view of left sympathetic chain demonstrating the plexus around the subclavian artery	Page 136
Plate 25	Antero-lateral view of the left sympathetic chain demonstrating the aortic branches from the chain	Page 138
Plate 26	Antero-lateral view of left sympathetic chain demonstrating the pharyngeal branches arising from the SCG and the sympathetic cord (adult)	Page 139
Plate 27	Histological slides demonstrating the ganglionic cells (a) and a longitudinal section of the cardiac ramus (b)	Page 141

CHAPTER 1

INTRODUCTION

The number of peripheral segmental branches of the cervical and thoracic sympathetic chains exhibits great variability and is much larger than assumed by textbooks and literature (Groen *et al.*, 1987). Jit and Mukerjee (1960) and Bergman *et al.* (1988), without mentioning incidences, discuss numerous variations of the cervical and thoracic sympathetic ganglia with regards to their incidence, branches, distribution and connections. Baljet *et al.* (1985) reported the existence of many small visceral nerves in the human fetus, originating from every part of the thoracic sympathetic chain. However, the exact number, origin and direction of these small branches have not yet been described. Groen *et al.* (1987), having found similar variability in the pattern of the medial branches of the sympathetic trunk concluded, "thoracic sympathetic branches in man shows a complex, segmentally organized pattern."

The cardiac sympathetic rami constitute one of the major branches issuing from the medial aspect of the cervical and upper thoracic portions of the sympathetic chain. The cervical cardiac nerves have dominated literature accounts of the sympathetic nerves to the heart up to the middle of the 20th century (Kuntz and Morehouse, 1953). There are relatively fewer accounts of the thoracic cardiac rami. Saccomanno (1943) claimed that the thoracic cardiac rami, combined, contained twice as many fibres reaching the cardiac plexus as the larger cervical sympathetic cardiac rami. These nerves vary in size and numbers and in the manner in which they reach the cardiac plexus, in different specimens and bilaterally (Saccomanno, 1943). Ellison and Williams (1969) found thoracic cardiac rami arising from the upper four or five ganglia, slender rami running independently to the heart. The

literature reviewed is vague with regard to the incidence and course of the thoracic cardiac rami.

The cervical and thoracic sympathetic chains present various difficulties with regard to identification and nomenclature. Although standard anatomy textbooks (McMinn, 1994, Williams *et al.*, 1995) describe the cervical sympathetic chain as consisting of 3 ganglia, the incidence of a fourth cervical ganglion has been reported to be high enough (Axford, 1928; Kuntz and Morehouse, 1929; Alexander, 1933; Jamieson *et al.*, 1952; Mitchell, 1953, Ellison and Williams, 1969; Pick, 1970) to warrant a review of this standard generalised scheme of the cervical sympathetic chain. In the thoracic part of the sympathetic chain, ganglia usually vary in size and occasional fusion between ganglia is seen (Pick, 1970). Groen *et al.* (1987) reported the number of TG as varying between 8-10. Criteria for numbering TG require standardization.

Surgical intervention involving the sympathetic nervous system is becoming an increasingly popular option for pain relief. The increasing use of minimal access surgery warrants a review of the value of surgical operations and the manipulation of the sympathetic nervous system for symptomatic relief of such conditions as angina pectoralis, severe pain from acute myocardial infarction or the aorta. Proper application, however, requires a thorough knowledge of the complex anatomy of the sympathetic nervous system and its variations, which must be taken into account in surgical sympathetomies.

Detailed knowledge of the anatomy of the sympathetic ganglia and their branches is of utmost importance in providing insight into the identification of these fibres through a narrow operative field. This precise anatomic description will be invaluable to the endoscopic surgeon and the anaesthetist.

In view of the above, this study attempts to:

- Document the incidence and bony relations of the superior cervical (SCG), middle cervical (MCG), inferior cervical (ICG) and cervicothoracic (CTG) ganglia.
- Re-evaluate the nomenclature and identification of cervical sympathetic ganglia
- Determine the incidence of fused thoracic ganglia
- Determine the origin and incidence of the cardiac sympathetic nerves
- In addition, the origin and incidence of other branches issuing from the medial aspect of the cervical and thoracic chain (including the splanchnic nerves and vascular rami in the neck) will be documented.

CHAPTER 2

REVIEW OF LITERATURE

A Historical Introduction

The history of the autonomic nervous system must go back to the days when man first became aware that extreme heat or cold, sustained physical effort and emotions (such as fear or rage and love or hate) could quicken the heart beat, hasten the rate of breathing, redden or blanch the complexion, dry the mouth and moisten the skin. The first relevant scientific data however, was recorded by Galen of Pergamon (AD 129-199), the Prince of Physicians (later known as the Pioneer of Anatomy), when he introduced the experimental method of performing original anatomical dissections and then correlating them to physiological observations. He was amongst the first to appreciate the sympathetic trunks, identifying them as “costal” branches of the “6th pair of cerebral nerves” (today recognized as the glossopharyngeal, vagus and spinal accessory nerves) (Mitchell, 1956). According to O'Malley (1964), the so called ‘human anatomy’ of Galen, is based almost entirely on dissections of the Barbary ape; having occasionally glanced at human internal organs when he tended to the wounds of the Gladiators in Pergamon and Rome. However, subsequent anatomists, up to and including Versalius in 1555, adopted his description.

The vagus and sympathetic nerves were clearly recognised as two separate structures first by Estienne in 1545 and later by Eustachio, whose copper plates were engraved around 1552 but not published until 1714 (Pick, 1970). These reveal that he had a clearer concept of the sympathetic trunks and their branches than that of his predecessors. He described the sympathetic trunks as arising within the skull, from the abducent nerves, and he sketched a number of ganglia along their course with various

rami communicantes. Their relationships to the vertebrae, brachial, and sacral plexuses were clearly depicted, and inferiorly, they were represented as converging towards the lower end of the sacrum. Numerous branches arising from and interconnecting the trunks were visible, especially in the abdomen (Mitchell, 1953).

Willis (1621-1675), a neuroanatomist, made important strides to our present day anatomical knowledge and functional concepts of the autonomic nervous system. He was the first to notice some delicate vascular filaments on the walls of the arterial circle, at the base of the brain that bears his name (Pick, 1970). In 1664, he depicted the sympathetic trunk as a branch of the abducent nerve and called the ganglionated chain the “intercostal” nerve after Reid, in 1616, had given it the name ‘intercostalis’ because it linked over the ribs (Sheehan, 1936). Willis gave the first detailed and reasonably accurate description of the branches of the sympathetic trunk, including the rami communicantes, ansa subclavian, the prevertebral sympathetic plexuses and their branches, and the origin and distribution of the thoracic splanchnic nerves (Pick, 1970). He represented the greater thoracic nerve as bifurcating to end partly in the coeliac and aortico-renal ganglia. On the right of his plate, both the lesser and least splanchnic nerves were shown ending in the aortico-renal ganglion.

Important advances to our present day concept of the autonomic nervous system were made in short succession during the 18th century. Francois-Pourfour de Petit concluded in 1727 that the ‘intercostal nerve’ originated below the cranium (Mitchell, 1953). He thereby disproved the erroneous idea of the cerebral origin, which had been held by anatomists from the time of Galen until Du Petit’s publication. He was the first to describe the Claude-Bernaud-Horner syndrome when he described how the ‘intercostal’

nerves carried the 'spirits' to the eyes after he excised the superior cervical ganglion in a dog (Mitchell, 1953).

With the development of neurology, the notion of widespread nervous control of the body functions emerged. Winslow (1732) (after whom the opening into the lesser peritoneal sac is named) studied in detail the morphology of the ganglia and coined the term "*nervi sympathici majores/maximi*" for those nerves that he thought carried the "sympathies" far and wide in the body (Pick, 1970). His was an anatomical breakthrough, which obscured Willis' 'intercostal nerve' and Versalius' 'cranial nerve'.

This notion was developed amongst others by Johnstone in 1764 who arrived, with the aid of some very accurate anatomical observations, at the problem of the nervous influence on visceral motion and sensitivity (Pick, 1970). By the end of the 18th century, it was clear with Bichat (1800), that what he called 'sympathetic nervous system' controlled visceral functions while somatic functions were under the direct control of the brain and spinal cord (this idea still prevails).

During the 19th century, the advent of the microscope as a tool of anatomical research, hailed rapid advances in the physiological and histological fields, many of which provided direct and indirect evidence about the anatomical arrangement of the visceral nervous system (Pick, 1970). Ehrenberg, in 1833, identified cell bodies in the sympathetic ganglia and Valentin, in 1843, provided a better account of the cells and ganglia, differentiating the fibres of the white and grey rami, and noting that certain fibres ended in the ganglia while others passed through them (Mitchell, 1953).

In 1846, Beck reported that the sympathetic ganglia were connected with the cervical and sacral nerves by grey communicating rami only, while in 1885, Gaskell recognized that white rami communicantes connected the sympathetic trunks to the spinal cord. In 1886, Gaskell further postulated that the sympathetic outflow from the spinal cord came from a column of cells in the lateral horn (Sheehan, 1936).

A new impetus was provided when Langley and Dickinson, in 1889, discovered the paralyzing action of nicotine on cells of the sympathetic ganglia. From this, it became possible to determine the positions of cell stations or synapses, and the distribution of 'preganglionic' and 'postganglionic' fibres – terms first coined by Langley in 1893. The afferent fibres accompanying autonomic nerves were indistinguishable from other afferent nerves; hence, he excluded them from the autonomic nervous system, which he considered purely efferent or motor, although he acknowledged the importance of the afferent stimuli in modifying visceral activities (Mitchell, 1953).

Today, it is well established that the two divisions of the autonomic nervous systems are, at tract levels, very close and interaction between these two systems and the central nervous system, especially at supra-spinal levels; is an everyday experience [*figure 1*]. Moreover, the two systems share many basic structural, physiological and pharmacological properties (Pick, 1970).

The last two centuries have seen great advances in the knowledge of the sympathetic nervous system and at the dawn of the 21st century, deemed the minimal access era, the attention of anatomists and surgeons has already been refocused on the morphology of the sympathetic trunks and their branches. The need for visualization of the finer

branches of the sympathetic trunks has prompted this anatomical study to document the variations in the cervical and thoracic sympathetic trunks and their distribution with respect to incidence, origin, course and relations to the cardiac plexus. It is postulated that these variations form the basis for the varied and inconsistent results in surgical procedures involving these nerves.

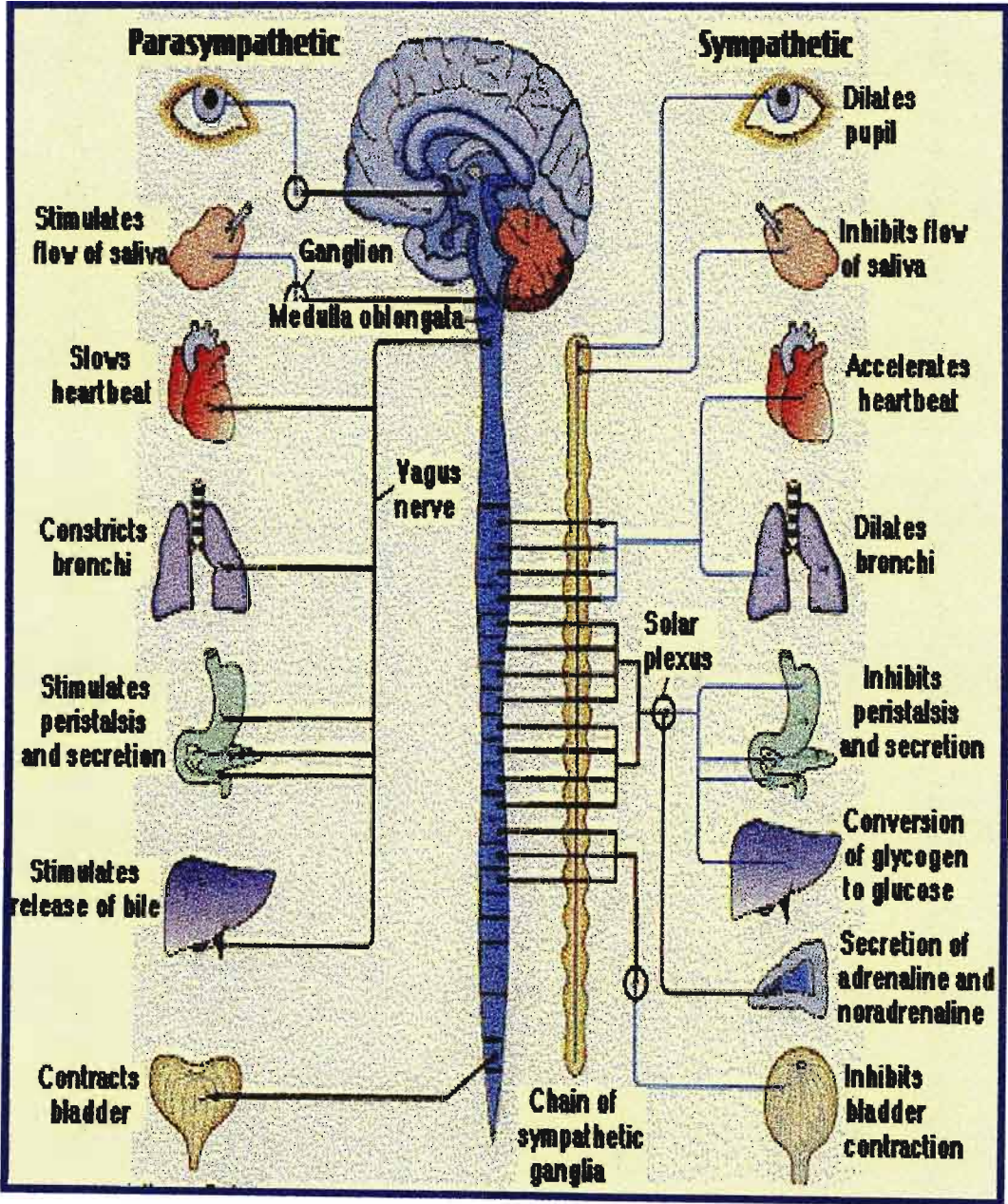


Figure 1: Diagram of sympathetic and parasympathetic nervous distribution to the trunk [Martini and Timmons, 1997]

2.1. THE SYMPATHETIC NERVOUS SYSTEM

The sympathetic nervous system, the larger division of the autonomic nervous system, includes the two paravertebral ganglionated trunks, their branches, plexuses and subsidiary ganglia [figure 2]. It has a much wider distribution than the parasympathetic system, for it innervates all the sweat glands of the skin, arrector muscles of the hair, the muscular walls of many blood vessels, the heart, lungs and abdomino-pelvic viscera (Williams *et al.*, 1995).

The ganglionated nerve cords extend from the base of the skull to the coccyx (McMinn, 1994). In the neck, the trunk is posterior to the carotid sheath and anterior to the transverse processes of the cervical vertebrae; in the thorax, it is anterior to the heads of the ribs; in the abdomen, it is antero-lateral to the vertebral bodies of the lumbar vertebrae and in the pelvis it is anterior to the sacrum and medial to the anterior sacral foramina (Williams *et al.*, 1995). Anterior to the coccyx, the two trunks meet each other in the unpaired terminal ganglion impar (McMinn, 1994).

The ganglia of the sympathetic nervous system can be divided into 2 main categories, paravertebral and prevertebral.

The *paravertebral ganglia* are situated bilaterally along the ventero-lateral aspect of the vertebral column; with their connecting trunks forming the sympathetic chains, which extend from the base of the skull to the sacrum (Williams *et al.*, 1995). The *prevertebral ganglia* lie close to the medial sagittal plane of the body ventral to the abdominal aorta, e.g. coeliac ganglion [figure 2] (Williams *et al.*, 1995). In addition to

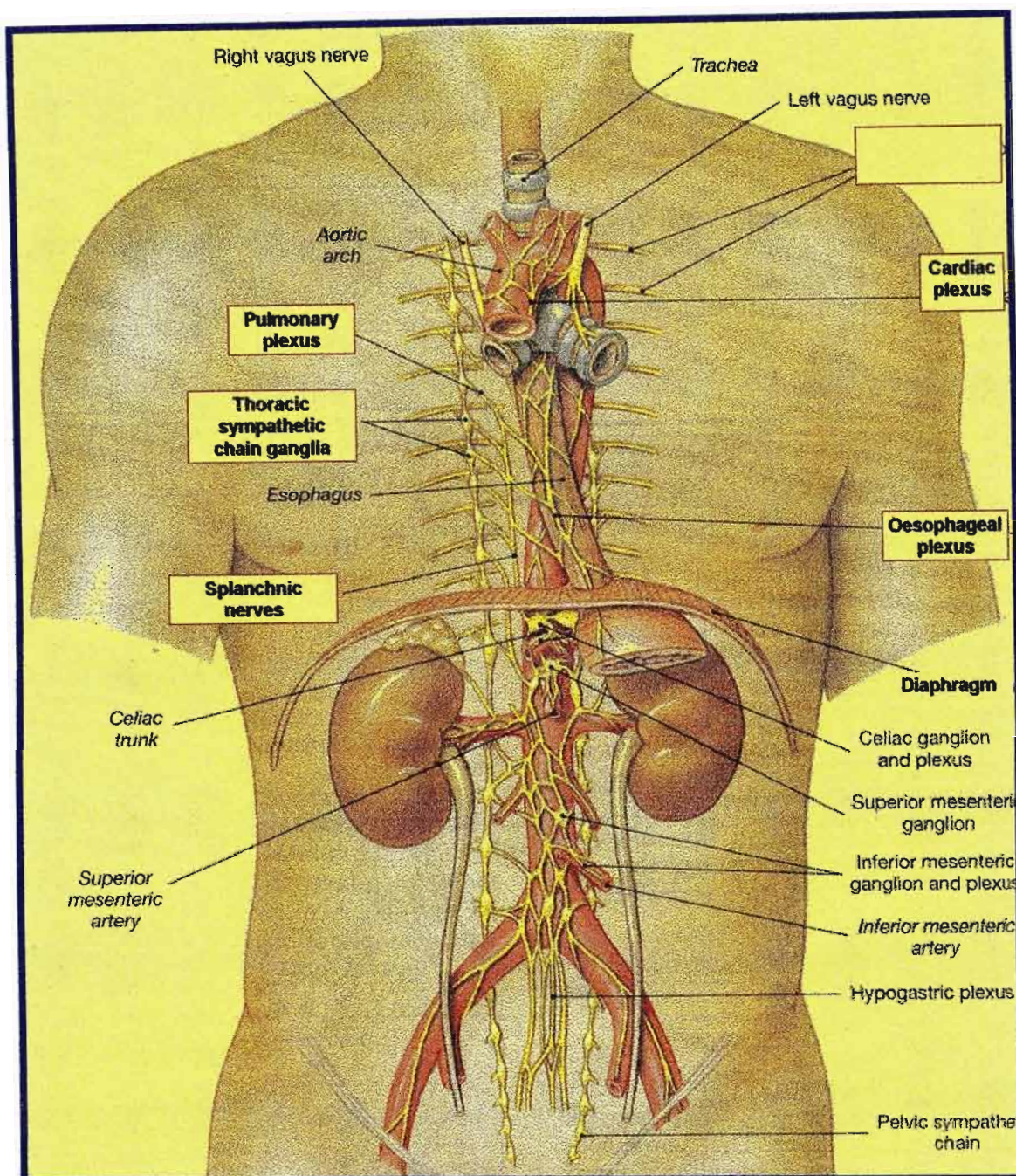


Figure 2: The thoracic and abdominal sympathetic trunks displaying thoracic and abdominal autonomic plexus [Adapted from Martini and Timmons, 1996]

the paravertebral and prevertebral ganglia, sympathetic neurons are found in paravisceral ganglia and intramural ganglia (Gabella, 1976). Other sympathetic ganglia which are neither paravertebral nor prevertebral nor part of the above-mentioned group,

are known as “*intermediate ganglia*” and are mainly associated with the white and (more frequently) the grey rami communicantes and sometimes with the ventral spinal roots (Wrete, 1941, 1959; Skoog, 1947; Boyd, 1957). Although very variable in number and size, they are consistently found in the cervical and uppermost thoracic segments, whereas they are often absent in the mid-thoracic and sacral segments (Boyd, 1957). Ganglia of similar structure, and presumably equivalent nature, are present along the carotid artery and the cavernous sinus and in the orbit (Boyd, 1957).

Originally, the ganglia on the sympathetic trunks correspond numerically to the ganglia on the dorsal roots of the spinal nerves, but fusion of adjoining ganglia occurred and in man, there are rarely more than 22 or 23 ganglia (Pick, 1970). In the thoracic and lumbar regions, ganglia of the sympathetic chain are numbered after the spinal nerve with which they have major connections, not on sequential order (Williams et al, 1995). Variations in the number, size and distribution of the sympathetic ganglia between different species and individuals are common, and in man, the variations in the pattern of the ganglia are particularly obvious in the neck (Becker & Grunt, 1957, Mitchell, 1953, Pick, 1970). Subsidiary ganglia in the autonomic plexuses (e.g. celiac ganglion, superior mesenteric ganglion) are derivatives of the ganglia on the sympathetic trunks [figure 2].

Structure of the sympathetic ganglia

The structural and functional characteristics of the sympathetic ganglia have been a subject of an increasing number of experiments and observations in recent decades.

A capsule of connective tissue, which is continuous with the epineurium of the nerve trunks, invests the ganglia, while connective tissue septa divide groups of ganglion cells. The stroma is particularly thick in man (Pick, 1970): the capsule of the SCG represents $\pm 30\%$ of the weight of the ganglion.

Collagen fibrils (50nm in diameter) invest each individual ganglion cell and its satellite cells. Among the collagen fibrils there are bundles of microfilaments (<20nm in diameter) and amorphous material. A few fibroblasts and blood vessels are also present in sympathetic ganglia. Chromaffin and mast cells are also found, of which there are about 24 000 in the SCG (Gabella, 1976). The total number of sympathetic ganglion cells has not been counted in any species, but neurons have been counted in individual ganglia, particularly in the SCG. This ganglion has been preferred by most investigators because it is easily identified and dissected, has clear-cut limits and neat pre- and post-ganglionic nerves (Gabella, 1976).

The great majority of nerve cells are multipolar, with the somatic dimensions ranging from about 25 to 50 μ m in man. A smaller type of cell (diameter: 15-20 μ m) with a less pronounced multipolar shape occurs in smaller numbers and probably corresponds to SIF cells (Williams *et al.*, 1995). While varying in size, the multipolar neurons display a

more marked variation in the distribution and form of their dendritic arrays (McLachland, 1974).

The axons of the principle ganglion cells are usually fine, non-myelinated and constitute the postganglionic fibres, which are distributed to effector organs in a variety of ways. According to Williams *et al.* (1995), the postganglionic fibres from the sympathetic trunk may [*figure 3*]:

- a. Pass back to corresponding spinal nerve through a 'grey rami communicantes' (GRC); usually joining the spinal nerve trunk just proximal to 'white rami communicantes' (WRC). Its fibres are distributed to the ventral and dorsal rami of the spinal nerves and their branches to blood vessels, sweat glands and hair in their zone of supply;
- b. Pass in a medial branch of the ganglion to be distributed to viscera;
- c. Pass to blood vessels in the neighbourhood of the sympathetic trunk and supply these or may be carried along the vessels and their branches to the peripheral distribution;
- d. Ascend to higher level or descend to a lower level before leaving the sympathetic trunk either in one of its medial branches, in a GRC or along an adjacent blood vessel.

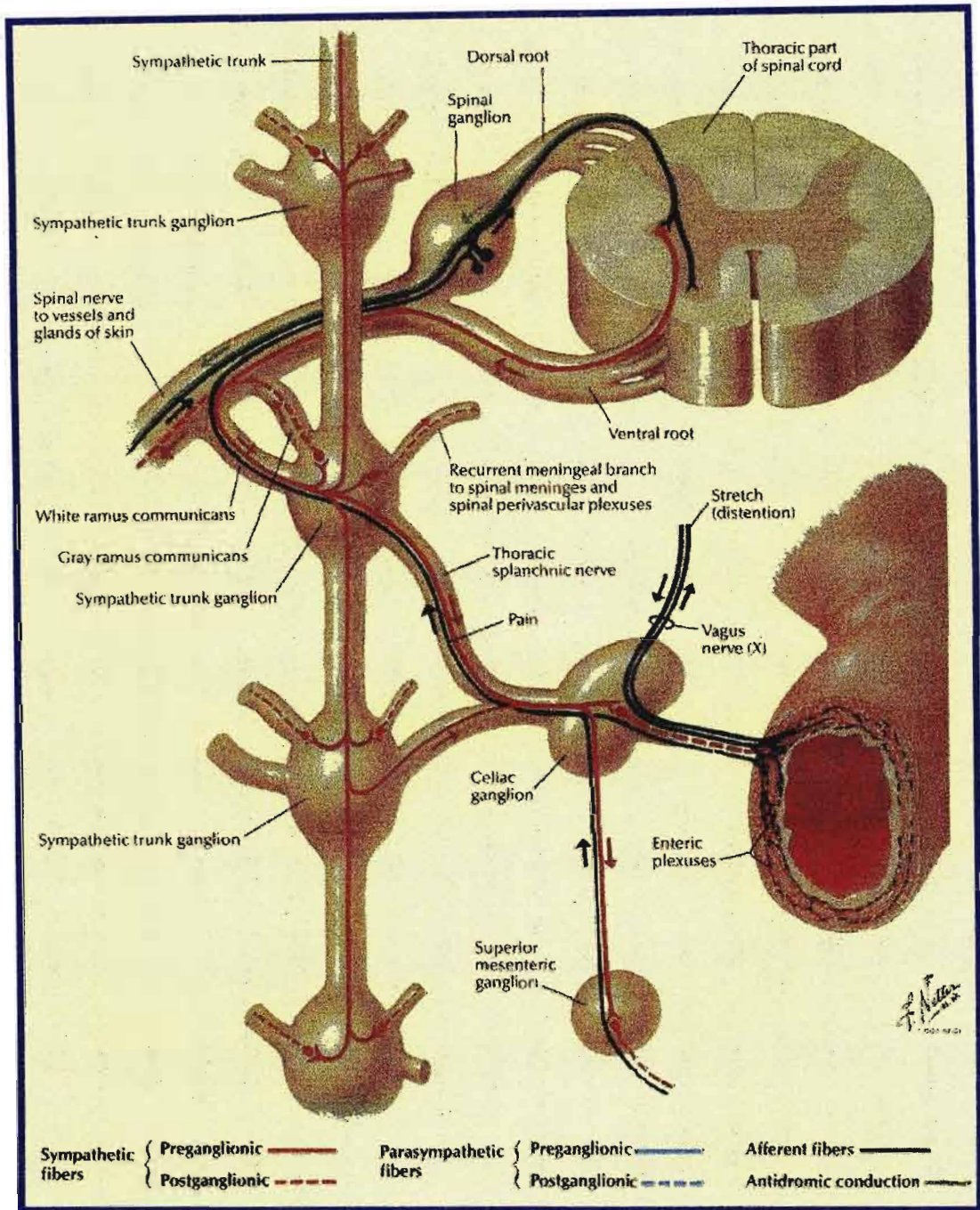


Figure 3: Diagrammatic illustration of autonomic nervous pathways
(NOTE: sympathetic pathways in red) [Adapted from Netter, 1990]

In addition to WRC and GRC, mixed RC have been found. Some of these in the thoracic region represent fusion of WRC and GRC, but some found in the cervical region contain bundles of thick myelinated fibres, which are somatic efferent in character and utilize the GRC as a convenient route to reach prevertebral muscles (Williams *et al.*, 1995).

Functional significance

The efferent postganglionic fibres, which pass in the GRC to the spinal nerve, supply vasoconstrictors to blood vessels, secretomotor fibres to sweat glands and motor fibres to arrectores pilorum muscles, in the areas supplied by the corresponding spinal nerve. Those that accompany the motor nerves to voluntary muscles are probably distributed only to blood vessels supplying muscles. Thus, most, if not all, peripheral spinal nerve branches contain postganglionic sympathetic fibres. Those that pass to the viscera and other structures are concerned with vasoconstriction, dilatation of the pupils or bronchioles, glandular secretions and peristaltic movements of GIT and GUT (Williams *et al.*, 1995).

The peripheral autonomic nervous system is controlled by the activities of the higher levels in the brainstem and cerebral hemispheres, viz. brainstem reticular formation, various thalamic and hypothalamic nuclei, limbic lobe, prefrontal neocortex, and a variety of projection pathways that connect these regions of the CNS (Williams *et al.*, 1995).

2.2 CERVICAL SYMPATHETIC CHAIN

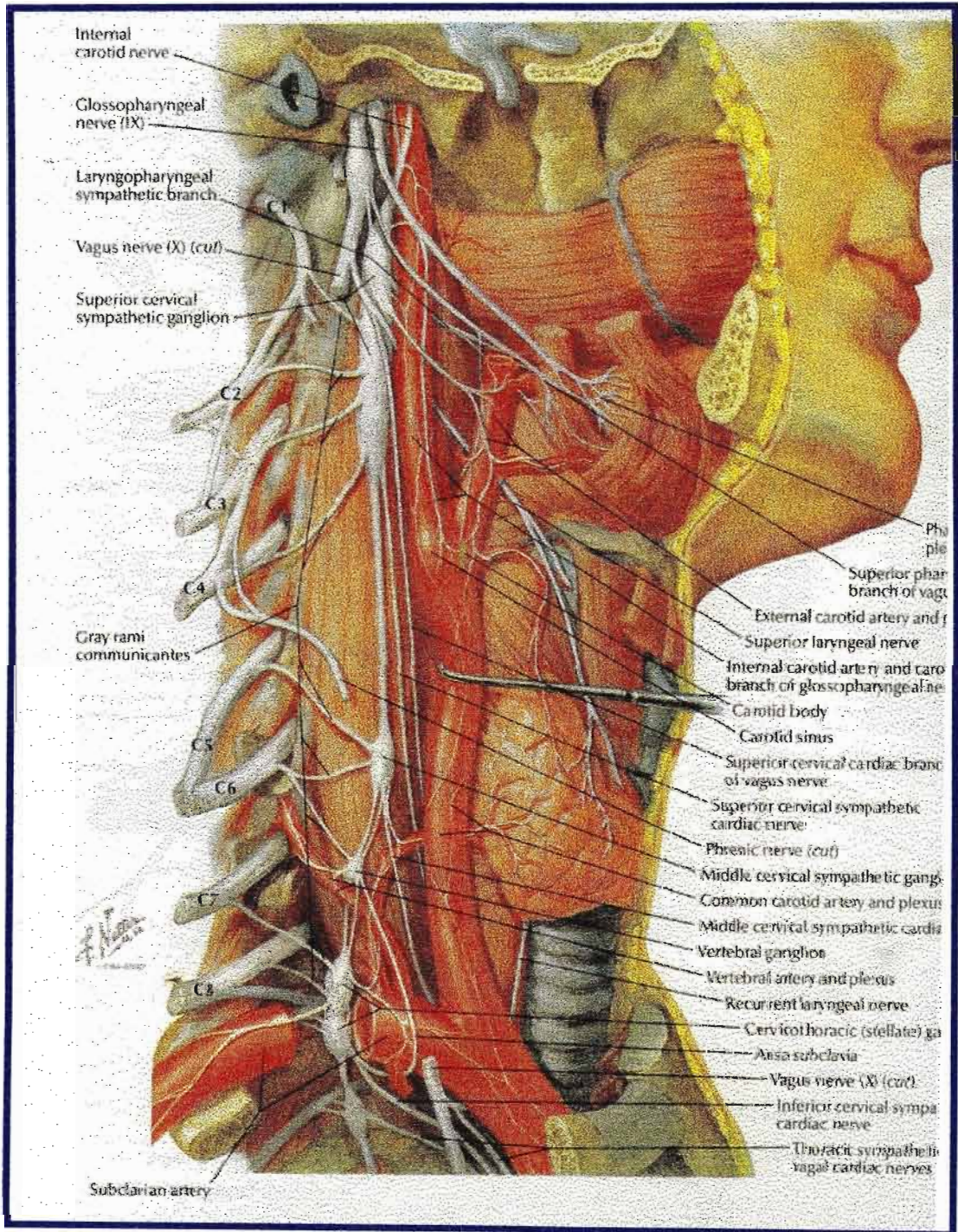


Figure 4: Relations of the cervical sympathetic chain
[Netter, 1990]

2.2.1 COURSE AND RELATIONS

Standard anatomy textbooks (McMinn, 1994; Williams *et al.*, 1995) describe the cervical sympathetic chain as consisting of 3 ganglia, distinguished according to their relative positions as the superior cervical ganglion (SCG), middle cervical ganglion (MCG) and inferior cervical ganglion (ICG) which is often fused with the first thoracic ganglion to form the cervicothoracic or stellate ganglion (CTG). The incidence of a fourth cervical ganglion has been reported to be high enough (Axford, 1928; Kuntz and Morehouse, 1929; Alexander, 1933; Jamieson *et al.*, 1952; Mitchell, 1953; Ellison and Williams, 1969; Pick, 1970) to warrant a review of this standard generalised scheme of the cervical sympathetic chain.

The cervical sympathetic trunk lies embedded in prevertebral fascia (Pick, 1970), postero-medial to the internal carotid artery and the common carotid artery and anterior to the transverse processes of the cervical vertebrae [figure 4]. The intersegmental chain, connecting the ganglia, is usually single, although Mitchell (1953) describes it as 'sometimes double'. Pick (1970) observed a double strand only in the formation of a loop around the inferior thyroid and subclavian arteries, between MCG and ICG or CTG.

2.2.2 SUPERIOR CERVICAL GANGLIA (SCG)

SCG is the largest of the cervical ganglia [figure 4]. The literature reviewed revealed much uniformity amongst anatomists with regard to the anatomy of SCG: although with differing ranges, the average reported length (adult) is 2.8cm (Becker & Grunt, 1957; Pick, 1970); constantly present bilaterally (Potts, 1925, Jamieson *et al.*, 1952); and commonly associated with the internal jugular vein and the internal carotid artery (Becker & Grunt, 1957; Pick, 1970). Only Bergman *et al.* (1988) reported a double SCG. The SCG extends from the base of the skull (Pick, 1970; Williams *et al.*, 1995) to the 2nd or 3rd cervical vertebra (Potts, 1925). Mitchell (1956) described SCG lying between the 2nd to 4th cervical transverse processes. Becker and Grunt (1957) describe, in a series of 100 adult sides, a variable relation of SCG to the cervical vertebrae: C₁₋₂ (29%); C₁₋₃ (61%); C₂₋₃ (6%); C₁ (1%); C₂ (1%); C₂₋₄ (2%).

It is believed to be formed by the coalescence of four ganglia, corresponding to the upper four cranial nerves. It is related anteriorly, to the sheath around the internal carotid artery and posteriorly, to the longus capitis and longus colli muscles. The internal carotid nerve ascends from the upper pole of the ganglion to the cranial cavity while the lower pole is united by the connecting trunk to the MCG or CTG (Williams *et al.*, 1995). It may communicate with the vertebral neural plexus and the descendens cervicales nerves (Ellison and Williams, 1969). The branches of the ganglion may be divided into medial, lateral and anterior groups (Williams *et al.*, 1995).

Lateral branches: These consist of GRC to the upper four cervical nerves and to certain cranial nerves (Williams *et al.*, 1995), viz. filaments run to the inferior ganglion

of the vagus, hypoglossal, spinal accessory and glossopharyngeal nerves and some fibres are distributed to the meninges in the posterior cranial fossa (Mitchell, 1956; Pick, 1970).

Medial branches: These are the laryngopharyngeal and the cardiac branches. The *laryngopharyngeal* branches supply the carotid body and pass to the side of the pharynx where they join branches of the glossopharyngeal and vagus nerves to form the pharyngeal plexus. The *cardiac* branch arises by two or more filaments from the lower pole of SCG.

Anterior branches: The anterior branches ramify onto the common carotid and external carotid arteries and their branches.

2.2.3 MIDDLE CERVICAL GANGLION (MCG)

It is in respect to the ganglia lying between the SCG and CTG (or if unfused, ICG) that the most diversification of opinion exists. MCG is the smallest of the three cervical ganglia and varies greatly in its occurrence, shape and position (Pick, 1970). It is occasionally absent, as such, being replaced by minute ganglia in the sympathetic trunk; or it may be fused with the SCG (Williams *et al.*, 1995). "It is usually at the level of the 6th cervical vertebra, anterior to the inferior thyroid artery [figure 5], or it may lie opposite the CTG" (Williams *et al.*, 1995). It is probably formed by the coalescence of the 5th and 6th cervical segments, judging by the postganglionic rami which pass to the 5th and 6th cervical nerves, but also the 4th and 7th.

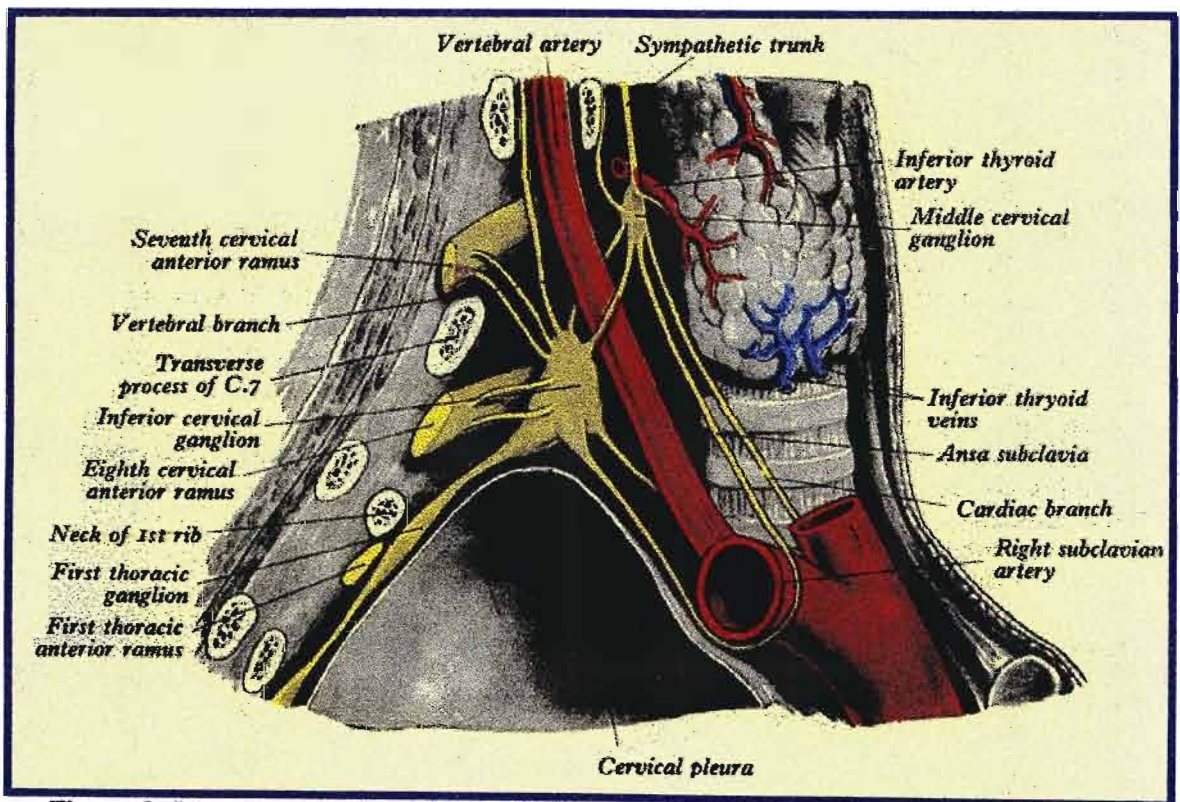


Figure 5: Diagrammatic illustration of MCG, ICG and the formation of the Ansa Subclavia
 (NOTE: The relationship of MCG and the inferior thyroid artery)
 [Adapted from Williams *et al.*, 1995]

MCG may be absent entirely (Potts, 1925; Axford, 1928; Pick and Sheehan, 1946; Bergman *et al.*, 1988; Williams *et al.*, 1995), or it may occur as a single or double structure (Potts, 1925; Axford, 1928; Pick and Sheehan, 1946; Pick, 1970; Williams *et al.*, 1995). In the literature reviewed, there exists indefinite references to a “high” and a “low” MCG; “thyroid ganglion of Haller (or Krause)”, “MCG of Arnold (or Luschka)” “intermediate ganglion of Jonnesco” and the vertebral ganglion (Axford, 1928; Kuntz and Morehouse, 1929; Alexander, 1933; Jamieson *et al.*, 1952; Mitchell, 1953, Ellison and Williams, 1969; Pick, 1970; Bergman *et al.*, 1988); many authors feeling that *only* one, or the other type, is present in any single chain.

Interestingly, literature is vague with regards to the ‘normal or typical’ MCG, located *at* the level of the 6th cervical vertebra, as described in standard textbooks. Jamieson *et al.* (1952) reported the varying location of this ganglion from C₅-T₁ vertebrae. He differentiated a MCG from an ICG by the intimate association of the MCG with the inferior thyroid artery as it intersects the cervical sympathetic chain [figure 5]. He also defined a ‘high’ type MCG as one “lying completely or partially at the level of the transverse process of C6 vertebrae or at a slightly higher level; while a ganglion, which lies entirely inferior to this transverse process, is considered a ‘low’ type MCG”. Axford (1928) reported the higher incidence of the ‘low’ MCG than the ‘high’ which he described as “an ovoid thickening on longus colli muscle, at the level of the 5th or 6th cervical transverse process, being most often related to the carotid tubercle of Chassaignae” [figure 6].

According to Pick (1970), MCG may be located anywhere between the 4th and 6th vertebra but rarely at the level of the 3rd and 7th. He further describes a vertebral

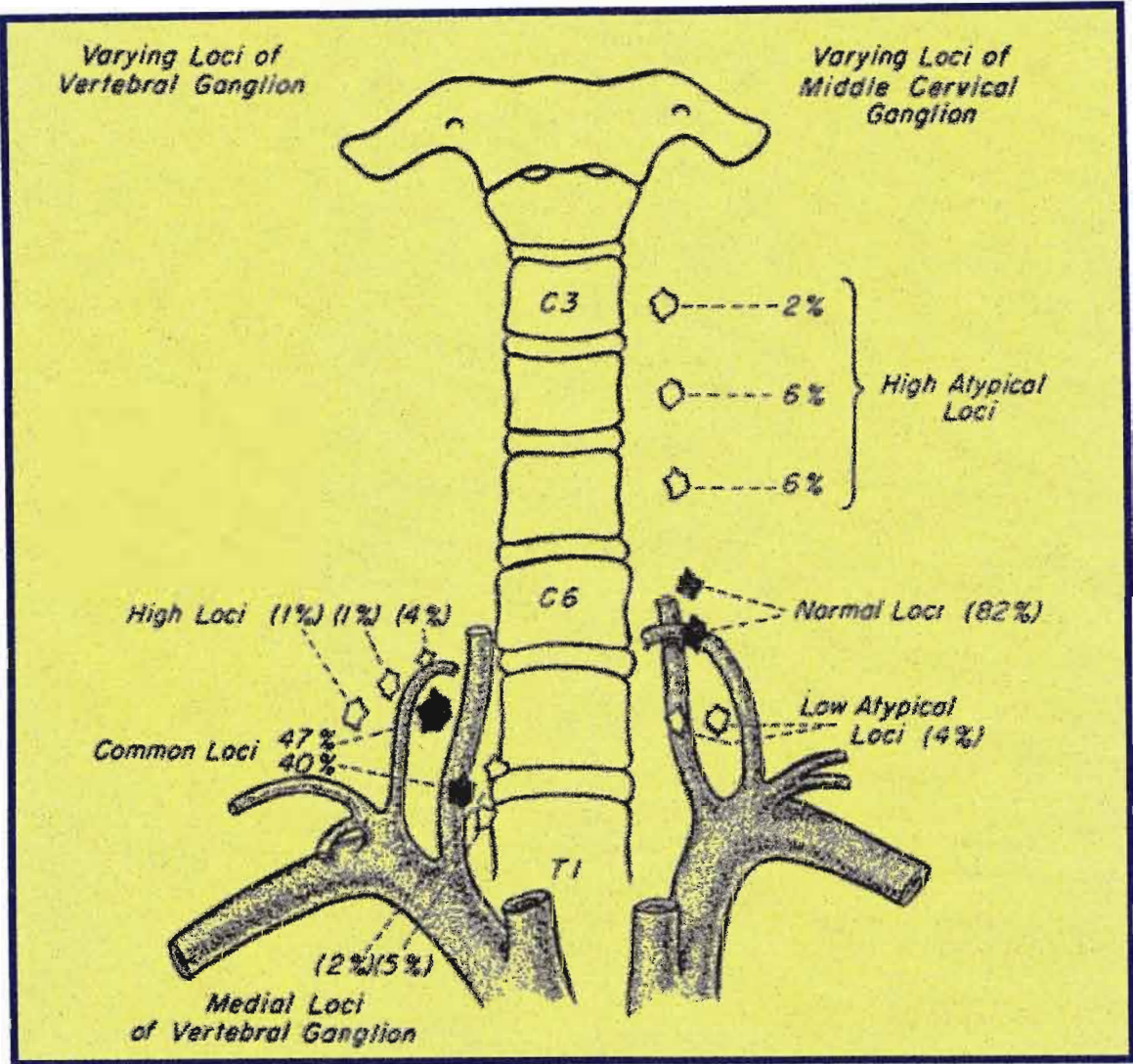


Figure 6: Illustration of cervical chain displaying the varying locations of MCG
 [Adapted from Becker and Grant, 1957]

ganglion (corresponding to the ‘low’ MCG) lying on the vertebral ansa, at the level of the 7th cervical vertebra, which is formed on the posterior loop of the ansa subclavia and issues the vertebral nerve. It does not give off rami communicans. Ellison and Williams (1969), however, describe this ganglion as almost constantly present; “although usually single, it maybe found in two parts: one closely related to the vertebral artery and the other antero-medial or antero-lateral to it”. The vertebral ganglion may communicate with the vagus or phrenic nerves and may give rise to the middle cervical cardiac sympathetic nerve (Mitchell, 1956). It gives grey rami to the 6th

and 7th spinal nerves. Mitchell (1953) describes the vertebral ganglion as constantly present on one or the other of the cords interconnecting MCG and ICG.

Some authors (Axford, 1928; Wollard and Norrish, 1933) have suggested that the 'low' MCG is a detached portion of either a 'high' MCG or ICG. Mitchell (1956) however, reported that the dimensions of the 'low' MCG however, did not vary inversely in size with the absence or presence of the 'high' MCG or ICG which should be expected were it a detached portion of one or the other.

Several authors (Axford, 1928; Sheehan, 1933; Woollard and Norrish, 1933; Saccomanno, 1943; Bonica, 1953) comment on the higher incidence of the 'low' MCG or vertebral ganglion, even though they refer to it by varying terminology. In the literature reviewed however, actual numerical incidences of the different types of MCG are seldom cited. It is assumed that this is the same ganglion described by Jonnesco, in 1923, as the "intermediate" ganglion, but as previously reported by Pick (1970), this term is inappropriate as it is used to describe ganglia on RC or on ventral nerve roots. Lazorthes and Cassan in 1939 suggested that the vertebral ganglion and CTG be described together as CTG but Pick (1970) responds: "vertebral ganglion is entirely cervical and never cervico-thoracic."

Literature reports varying relationships of MCG to the inferior thyroid artery: located anterior and slightly superior to the inferior thyroid artery (Mitchell, 1956; Becker and Grunt, 1957; Williams *et al*, 1995); posterior to the inferior thyroid artery (White and Smithwick, 1942; Pick, 1970). Jamieson *et al* (1952) reported the intersection of the inferior thyroid artery and the cervical chain to occur at or below the level of the 7th

cervical vertebra, thus related to the 'low' MCG. In his series of 100 sides, the artery passed posterior to the sympathetic chain in 55% and anterior in 41% of cases.

MCG, when situated at the level of the 6th cervical vertebra, usually supplies rami to the 5th and 6th cervical nerves, and at times also to the 4th and 7th (Williams *et al.*, 1995). When this ganglion is absent or in close proximity to ICG, these cervical nerves derive their rami directly from the sympathetic trunk. When the ganglion lies close to ICG, it plays a subsidiary role of furnishing rami, its chief function being to supply the cardiac plexus (Potts, 1925).

MCG also gives off thyroid and cardiac branches. The cardiac branch, the largest of the sympathetic cardiac branches is derived from the ganglion itself or more frequently from the sympathetic trunk cranial or caudal to it (Williams *et al.*, 1995). It is connected to the CTG by two or more cords, which are very variable in their disposition (Mitchell, 1956). The posterior cord usually splits to enclose the vertebral artery, thus forming the *vertebral ansa* [figures 4 and 5]. The anterior cord loops down anterior and then, inferior to the first part of the subclavian artery, medial to the origin of the internal thoracic artery and supplies rami to them (Pick, 1970). This loop is called the *ansa subclavia* [figures 4 and 5]. It is intimately related to the cervical pleural and generally consists of more than one filament.

2.2.4 INFERIOR CERVICAL GANGLION (ICG)

ICG, when unfused, lies the level of C7 vertebra or the area opposite the upper part of the thoracic vertebra [*figures 5 and 7*]. It is commonly situated just behind the subclavian artery usually at the point of origin of the vertebral artery. It is imperfectly separated from the first thoracic ganglion and is most times fused with the latter (Kuntz, 1929). This ganglion supplies rami to the 7th and 8th cervical nerves and to the 1st thoracic nerve.

The incidence of an unfused ICG varies in the literature reviewed. Most authors report an incidence in the range of 12.5%-20%: Perlow and Vehe (1935), $\frac{8}{48}$ sides (16.7%); Jamieson et al. (1952), $\frac{18}{100}$ sides (18%); Pick & Sheehan (1946), $\frac{5}{25}$ sides (20%); Jit and Mukerjee, $\frac{20}{100}$ sides (20%) and Ellison and Williams (1969), $\frac{3}{24}$ sides (12.5%). Becker and Grunt (1957) however reported the presence of an unfused ICG in $\frac{71}{114}$ sides (62.3%), thus explaining their most frequent pattern of cervical chain differing from the classical concept [*figure 7*].

Lazorthes and Cassan in 1939 suggested that the vertebral ganglion and ICG be described together as CTG but Pick (1970) responds: "ICG is entirely cervical and never cervico-thoracic."

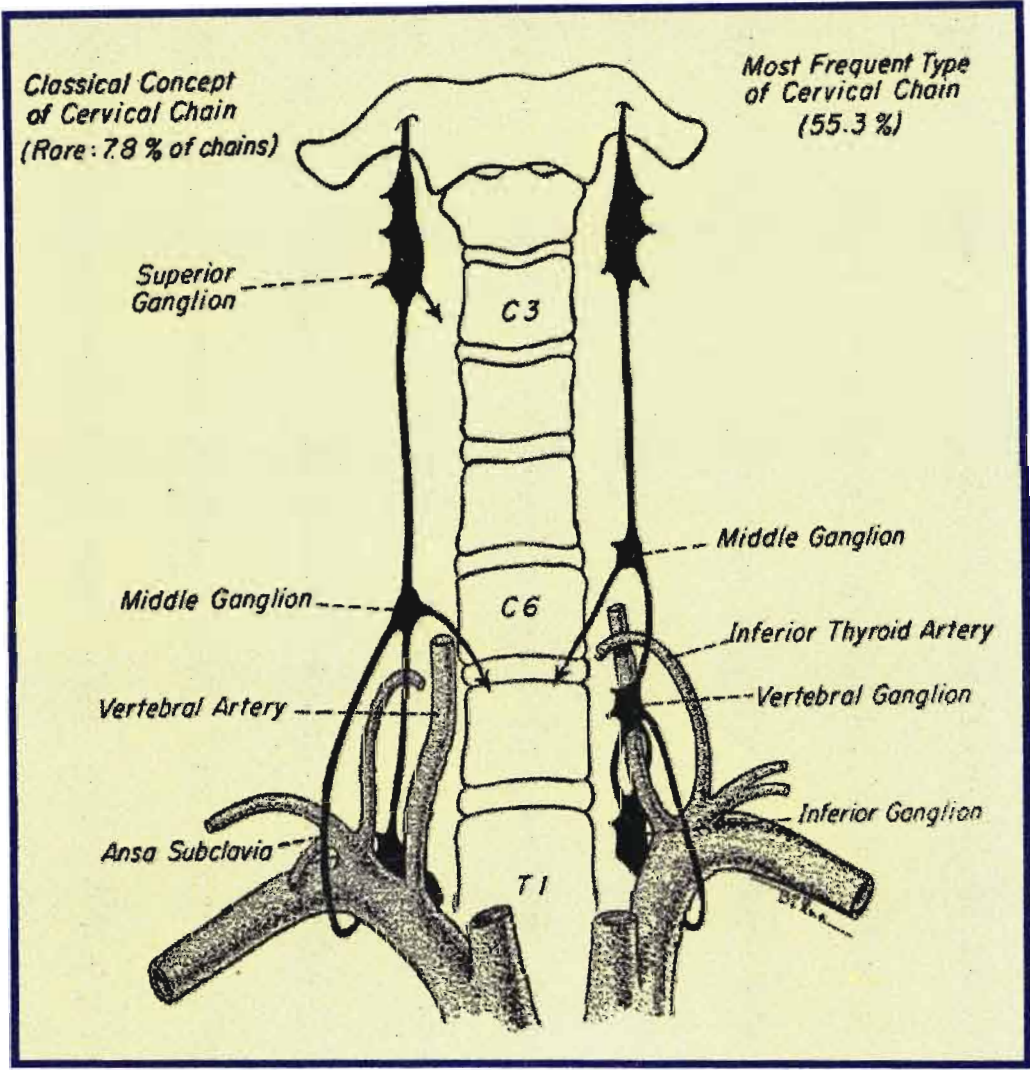


Figure 7: Illustration of cervical sympathetic chain displaying an unfused ICG on the left side (Note: this was the most common pattern of cervical chain noted by Becker and Grunt, 1957) [Adapted from Becker and Grunt, 1957]

2.2.5 CERVICO-THORACIC GANGLION (CTG)

This is an irregular shaped ganglion [figure 4], much larger than the MCG, being probably formed by the coalescence of the lower 2 cervical segmental ganglia (typically forming ICG) with the first thoracic ganglion. Sometimes this fusion may include the second thoracic ganglion (Kuntz, 1927, Saccomanno, 1943, Pick and Sheehan, 1946; Jit and Mukerjee, 1960, Ellison and Williams, 1969; Pick, 1970). The 'low' MCG, ICG, 1st and 2nd thoracic ganglia were reported to be fused to form an unusually large CTG by Jit and Mukerjee (1960).

The reported incidence of CTG varies amongst authors; most authors citing an incidence between 75%-88%: Mitchell (1953), 70%; Pick & Sheehan (1946), 80%; Jit & Mukerjee (1960), 80%; Jamieson *et al.* (1952), 82%; Perlow & Vehe (1935), 83.3%; Ellison & Williams (1969), 88%; however, Becker and Grunt (1957) report an incidence of 37.7%. In addition, some authors do not distinguish between an ICG and CTG (Groen *et al.*, 1987).

CTG lies at the junction of the cervical and thoracic portions of the sympathetic trunk. The ganglion rests against the transverse process of C7 vertebra, the neck of the first rib, the first intercostal space and occasionally, in the upper portion of the neck of the 2nd rib. The ganglion lies immediately lateral to the lateral border of the longus colli and between the base of the transverse process of the 7th cervical vertebra and the neck of the first rib, which is posterior to it.

White *et al.* (1952) described a definite isthmus (a macroscopically visible union between the ICG and T1 components of CTG) [figure 4] in all specimens in his series, while Becker & Grunt reported the incidence of a definite isthmus or 'waist' to be only 37.7% ($^{43}/_{114}$ sides).

The major portion of the ganglion lies medial to the costocervical trunk of the subclavian artery and is commonly pressed against the C7 and T1 spinal nerves (Jamieson *et al.*, 1952). The vertebral artery and its associated veins lie anterior to it. Variations of the relationship of CTG to the vertebral artery to have been reported by Perlow and Vehe (1935): anterior, 4.2%; medial, 47.9%; anteromedial, 33.3%; posterior, 4.2% and posteromedial, 10.4%.

The interganglionic cord joins CTG with MCG above and the 2nd thoracic ganglion, below. Inferiorly, it is separated from the posterior aspect of the cervical pleura by the

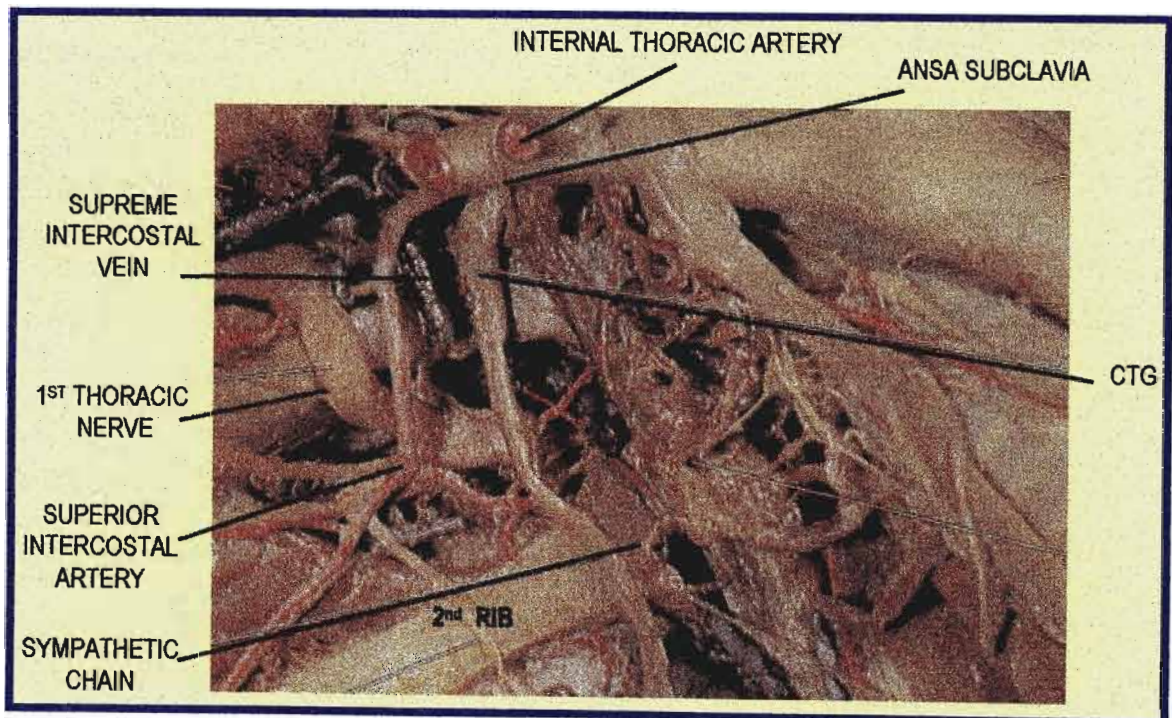


Figure 8: Relations of CTG [Adapted from Netter, 1990]

suprapleural membrane; while the branches of the costocervical trunk lie near its lower pole. Passing down the lateral side of CTG is the supreme intercostal vein and the superior intercostal artery (Williams *et al.*, 1995) [figure 8].

CTG sends GRC to the 7th and 8th cervical, and the 1st thoracic nerves; GRC to the 7th cervical nerve may vary from one to five in number, with 2 being the usual number (Williams *et al.*, 1995). Pelow and Vehe (1935) describe rami from CTG to C8 and T1, only.

CTG also gives off a ramus that ascends medial to the vertebral artery and anterior to the transverse process of the 7th cervical vertebra and after communicating with the 7th nerve, sends a branch upwards through foramen transversarium to the seventh vertebrae (Williams *et al.*, 1995). This is presumably the vertebral nerve.

The Ansa Subclavian (AS)

According to Pick (1970), the transition of the cervical and thoracic sympathetic chains is marked by the loop around the subclavian artery (the ansa subclavia). Classically, AS has been described as arising from the MCG, looping the subclavian artery and terminating in either the ICG or CTG (Becker and Grunt, 1957) [figures 4, 5 and 7]. The posterior loop of the AS is double and forms a loop around the origin of the vertebral artery (Sacomanno, 1943). AS is seldom single and usually consists of two or more filaments of varying size (Mitchell, 1953). The posterior cord usually splits to enclose the vertebral artery and “often contains the vertebral ganglion” (Ellison and Williams, 1969). The anterior cord loops down anterior to and then posterior to the 1st

part of the subclavian artery, which it supplies (Jamieson *et al.*, 1952). Becker and Grunt (1957) reported AS terminating superiorly in the ‘low’ MCG/vertebral ganglion (70.9%) and the ‘high’ MCG (23.3%). In a few cases, it arose from the upper pole of the ICG or CTG, “looped around the subclavian artery, and returned to the parent ganglion and even less frequently, directly from the sympathetic trunk” (Becker and Grunt, 1957).

2.3 THORACIC SYMPATHETIC CHAIN

2.3.1 COURSE AND RELATIONS

The thoracic portion of the sympathetic chain is continuous at the root of the neck, behind the vertebral and subclavian arteries, with the cervical sympathetic chain. It lies anterior to the heads of the ribs for most of its extent [*figures 9 and 10*]. In the lower part of the thorax, it inclines medially to lie on the sides of the bodies of the lower 2 thoracic vertebrae. It leaves the thorax behind the medial lumbocostal arch to become continuous with the lumbar sympathetic chain (Hollinshead, 1956).

The sympathetic trunk lies lateral to the hemiazygos system of veins on the left side [*figure 10*] and the azygos vein of the right side [*figure 9*]. Both chains lie immediately against the pleura and, usually, in front of the intercostal vessels; thus facilitating the removal of the chain without injury to the vessels (Hollinshead, 1956). The venous pattern however may be variable and in the upper part of the thorax, the first intercostal vein typically passes in front of the chain (Hollinshead, 1956).

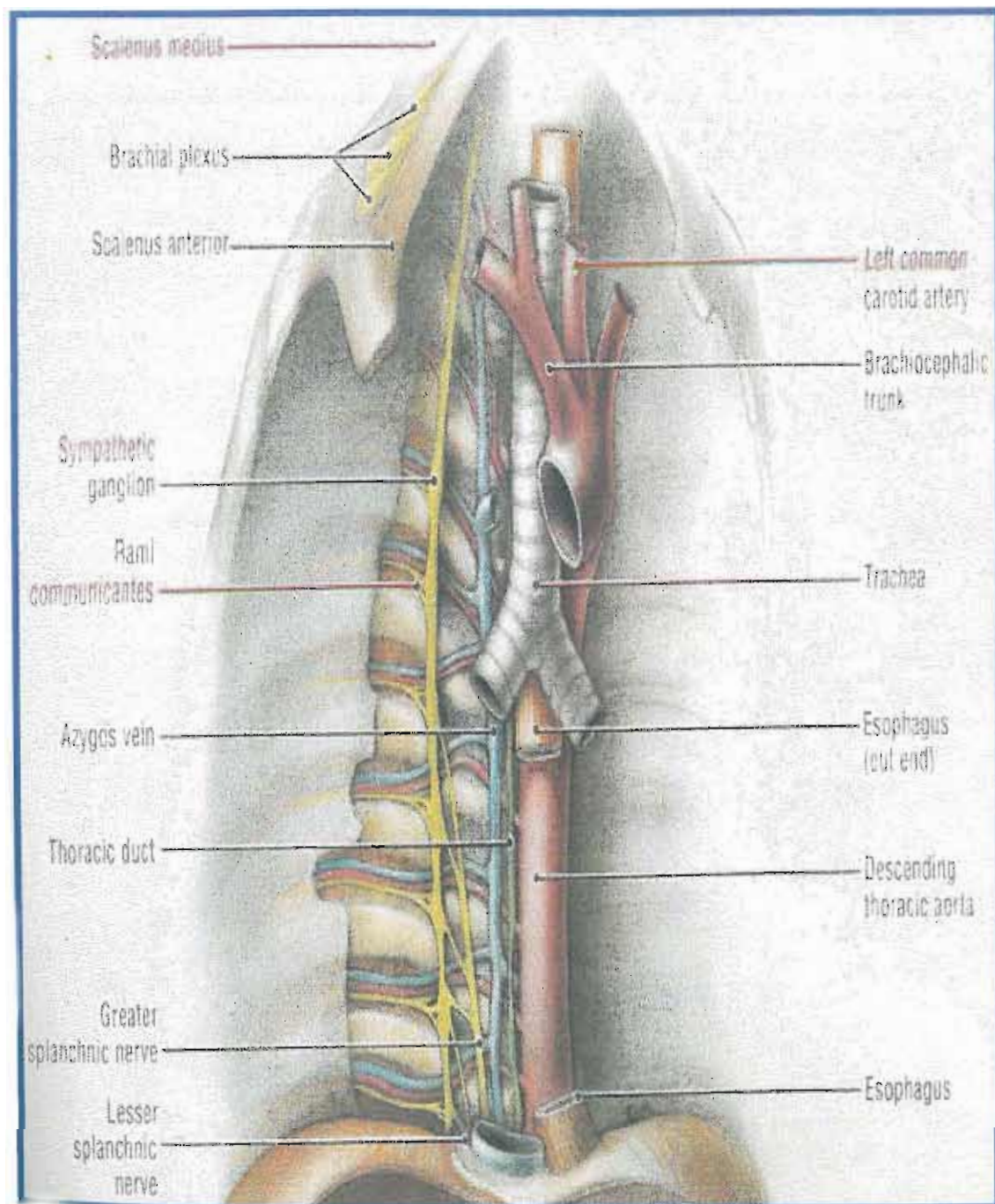


Figure 9: Anterior view of the mediastinal relations of the right sympathetic chain
[Agur, 1991]

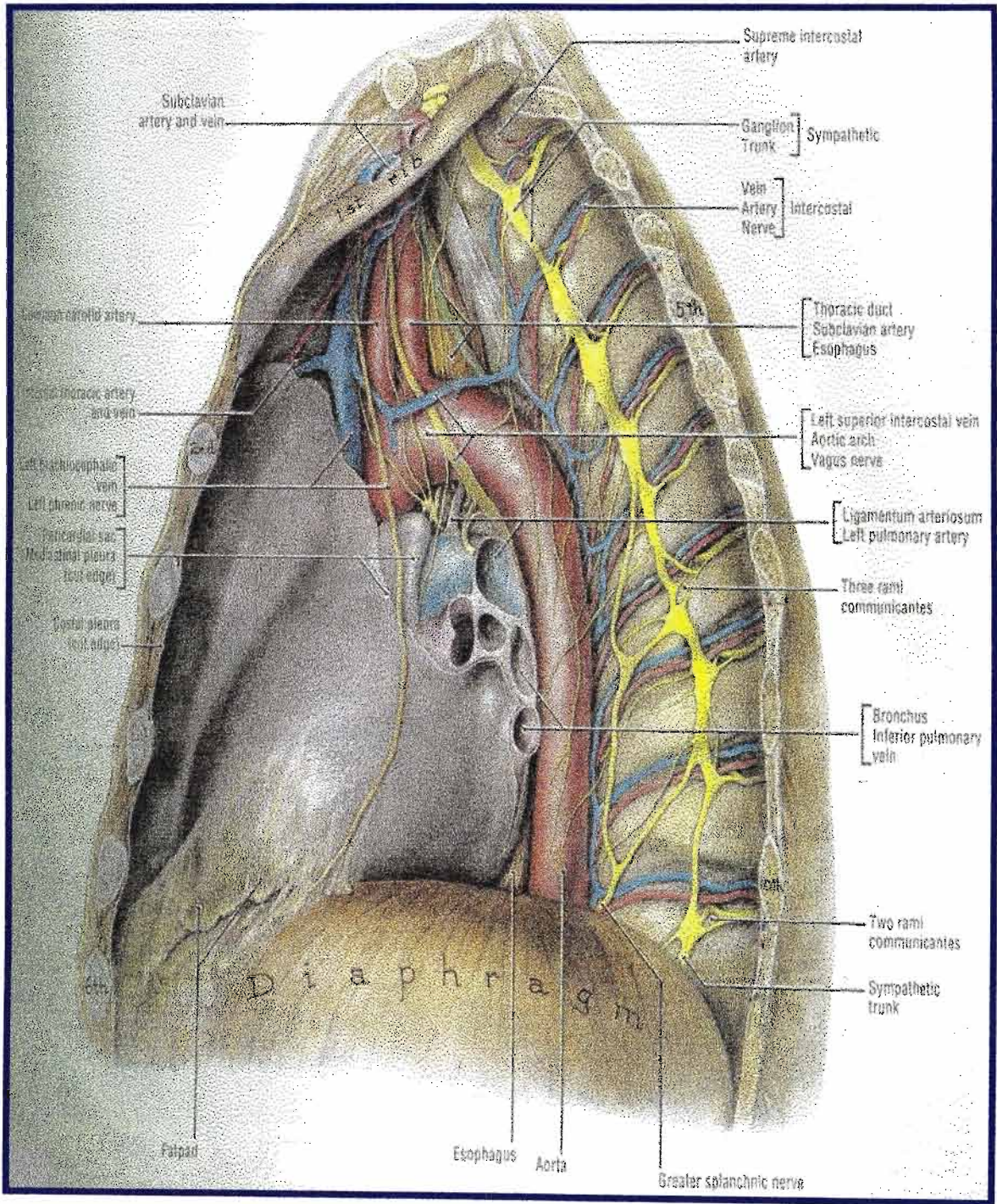


Figure 10: Lateral view of the mediastinal relations of the left sympathetic chain
[Agur, 1991]

2.3.2 THORACIC GANGLIA (TG)

The thoracic region is characterized by a segmental arrangement of the sympathetic ganglia; and further, by grey and white rami to each thoracic nerve (Potts, 1925). Beginning below the second thoracic ganglion (T₂G) of the sympathetic chain, ganglia tend to be rather regularly segmental at least as low as the 10th. TG usually vary in size and occasional fusion between ganglia is seen (Pick, 1970). Groen *et al.* (1987) reported the number of TG as varying between 8-10. Fusion of ganglia affects the point of entry of rami to the sympathetic trunk or ganglia (Potts, 1925).

Criteria for numbering TG require standardization. Since rami and the splanchnic nerves do not always originate from the sympathetic ganglia of the chain but also from the interganglionic segments (Potts, 1925; Braeucker, 1927; Pick and Sheehan, 1946; Kuntz, 1953; Mitchell, 1953; Wrete, 1959; Pick, 1957, 1970) and since the variability in the number, size and location of the ganglia is well known (Groen *et al.* 1987); a direct determination of segmental connections is difficult [figure 11]. Various investigators have numbered TG according to:

- a) The spinal nerve to which they are attached via:
 - i) WRC (Zuckerman, 1937; Sheehan and Pick, 1943);
 - ii) GRC (Langley, 1896);
 - iii) Both WRC and GRC (Groen *et al.* 1987);

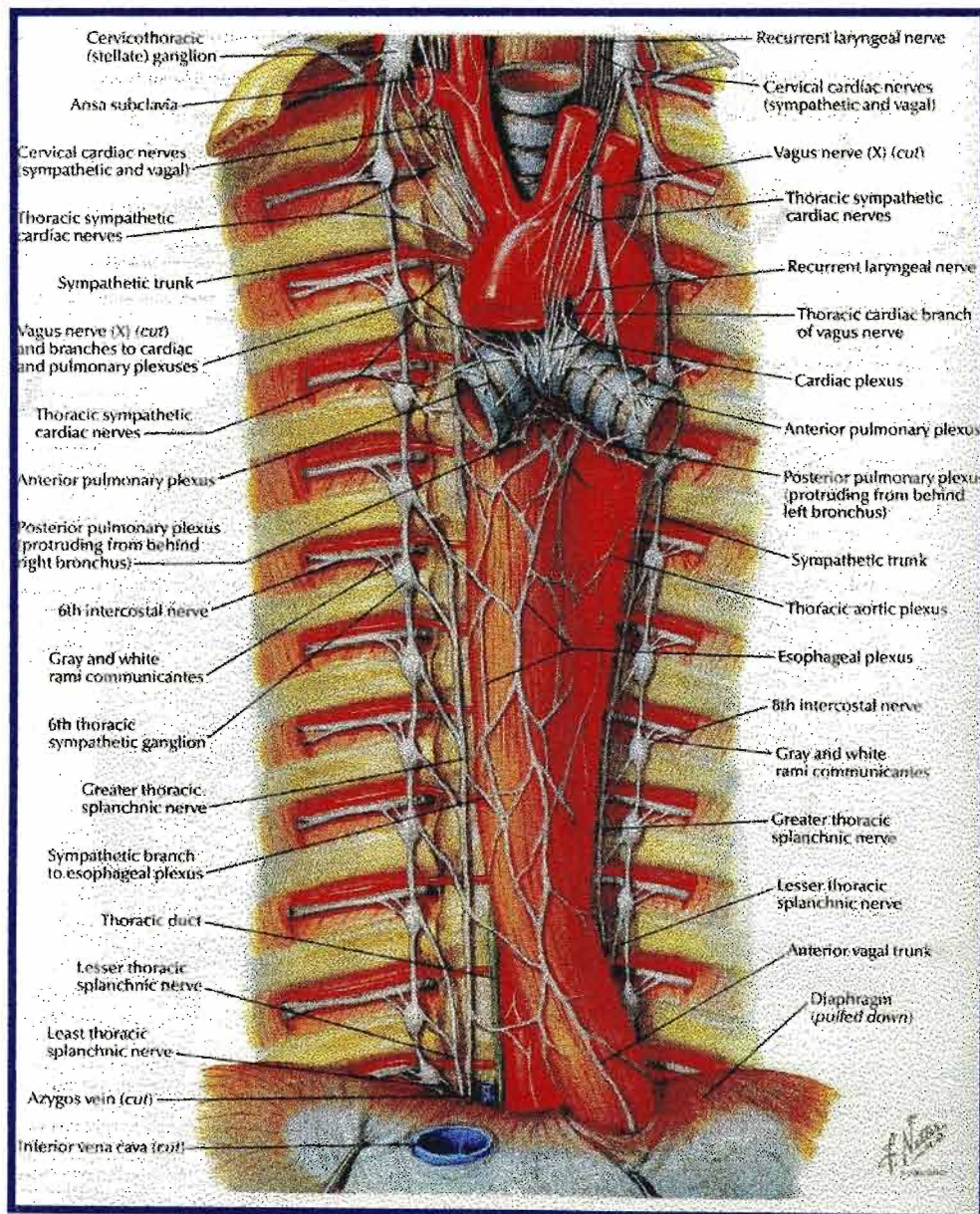


Figure 11: *The thoracic sympathetic chains and their relations [Netter, 1990]*

- b) The closest segmental artery (Wrete, 1959);
- c) Sequentially, after identifying:
 - i) The CTG (Jit and Mukerjee, 1960);
 - ii) The third thoracic ganglion (Sheehan and Pick, 1942).

The ganglia lies slightly below the level of the intercostal nerve and therefore the rami run somewhat upwards and laterally (Hollinshead, 1956)[figure 12]. Standard textbooks however still distinguish the rami more lateral to be usually the WRC, consisting of preganglionic fibres coming to the chain; while the more medial ramus as the GRC formed by the postganglionic fibres leaving the chain to join the thoracic nerve (Williams *et al.*, 1995). Sometimes grey and white rami may be fused to form a single

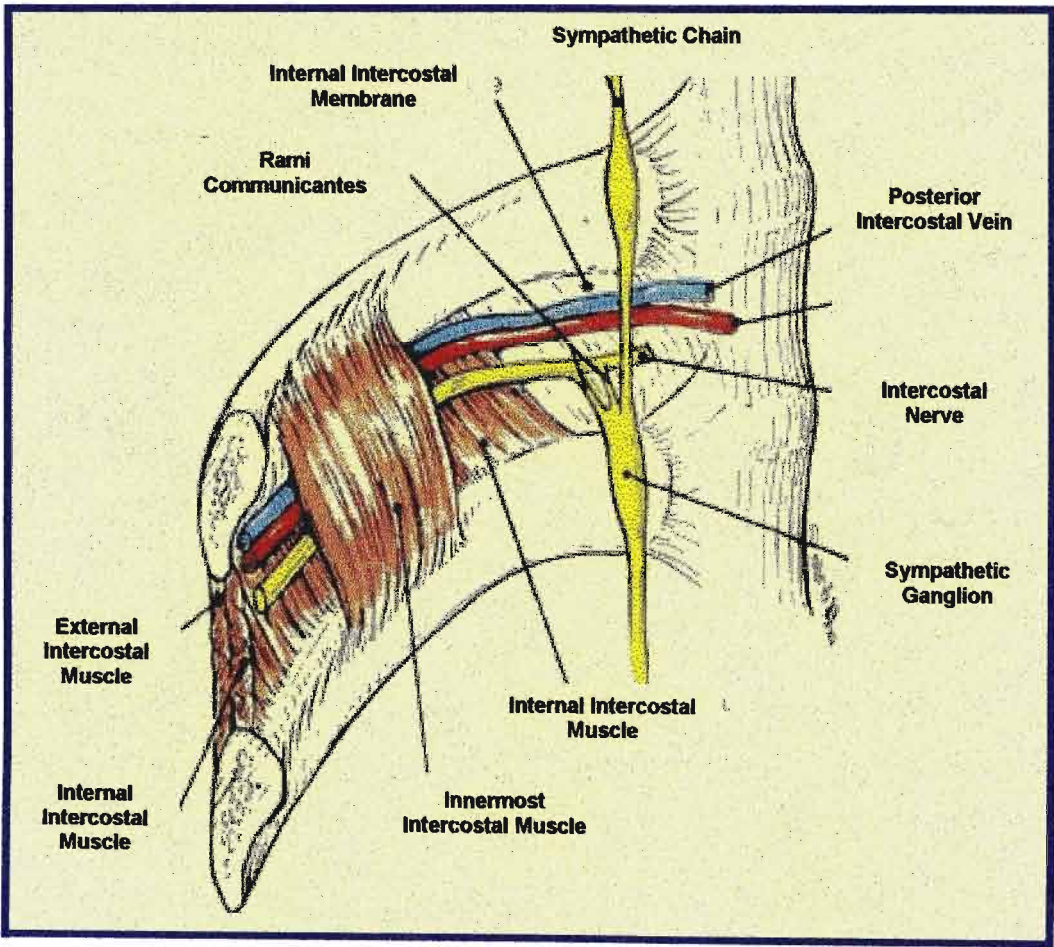


Figure 12: Relations of TG in the intercostals space [Adapted from Moore, 1995]

‘mixed’ rami communicantes (Pick, 1970; Groen *et al.*, 1987).

In gross dissection, it is impossible to distinguish white from gray rami due to variations in location, composition and number of rami communicantes. Furthermore, histological differentiation is based on the ratio of myelinated to unmyelinated fibres within gray and white rami (Pick, 1970; Groen *et al.*, 1987). This remains technically difficult. Wrete (1959) reported that GRC and WRC could only be distinguished macroscopically, with much difficulty, in fresh tissue. In addition, the identification of TG macroscopically, is further complicated by ganglionic fusion and anomalies in segmental arterial patterns (Groen *et al.*, 1987).

Groen *et al.* (1987) defined a thoracic segment as that part of the thoracic sympathetic trunk, which is connected via RC with one spinal nerve, without discriminating between grey and white rami communicantes. RC are subject to variation in size and direction towards the spinal nerve (Hovalaque, 1927, Kuntz, 1953, Mitchell, 1953, White and Sweet, 1969), although Sheehan and Pick (1943), Pick and Sheehan (1946) and Pick (1957, 1970) distinguish in the adult a fixed pattern of these rami, especially in the cranial part of the thoracic sympathetic chain (Groen *et al.*, 1987). Groen *et al.* (1987) differentiated three types of rami based on their course towards the spinal nerve (*viz.* ascending, descending, transverse), noting no distinct pattern and inter- and intra-individual variations.

In the thoracic region, there tend to be two RC to each sympathetic ganglion except at the two extremes [figure 12]. Occasionally these RC are combined to form a single trunk, and occasionally there may be more than two RC (Hollinshead, 1956). In the lower part of the thoracic sympathetic chain, the ganglia tend to be connected not only to the corresponding nerve but also to the nerve below. Pick and Sheehan (1946) found this to especially true in more than 50% of cases for the 10th thoracic ganglion.

According to Pearson and Sauter (1971), GRC of the upper thoracic ganglia often split into 2 bundles, the larger bundle joining the corresponding nerve while the smaller ascends behind the neck of the rib above and joins the next higher nerve.

Rami communicantes to the upper thoracic portion of the chain vary more than anywhere else in the thorax (Hollinshead, 1956). Johnson and Mason (1921) found, for instance, that while there were always at least two RC attached to the first thoracic nerve, there were sometimes as many as five. Perlow and Vehe (1935) found that in 3 out of 38 sides the 1st thoracic nerve received a grey ramus from the 2nd thoracic ganglion (presumably, the nerves of Kuntz). Ehlich and Alexander (1951) stated that most bodies show such a connection. The nerve of Kuntz was originally described as an inconstant intrathoracic ramus, which joined the second intercostal nerve to the ventral ramus of the first thoracic nerve, proximal to the point where the latter gave a large branch to the brachial plexus (Kuntz, 1927). Subsequently, a variety of sympathetic interneuronal connections up to the fifth intercostal space were reported and described as the Nerves of Kuntz (Ramsaroop *et al.*, in press).

In addition to RC, which connects the chain or ganglia to the spinal nerves, the thoracic sympathetic chain gives off a series of visceral or splanchnic branches. Thus, a variable number of thoracic splanchnic nerves leave the chains especially in the upper part of the thorax. They are very fine branches.

The medial branches of the upper five ganglia are very small: they supply filaments to the thoracic aorta and its branches. On the aorta, they form a delicate plexus (thoracic aortic plexus) together with filaments from the greater splanchnic nerve. Twigs from the 2nd to the 5th ganglia pass to the deep part of the cardiac plexus (Hollinshead, 1956).

Medial branches of the lower seven ganglia are large; they distribute filaments to the aorta, and unite to form the greater, lesser and lowest splanchnic nerves, the last of which is always not identifiable.

2.4 CARDIAC SYMPATHETIC NERVES

The sympathetic cardiac nerves may be conveniently divided into cervical and thoracic cardiac nerves (Kuntz and Morehouse, 1930). The literature reviewed reports cardiac sympathetic nerves to be highly variable in their topography (Kuntz and Morehouse, 1930; Mizeres, 1972).

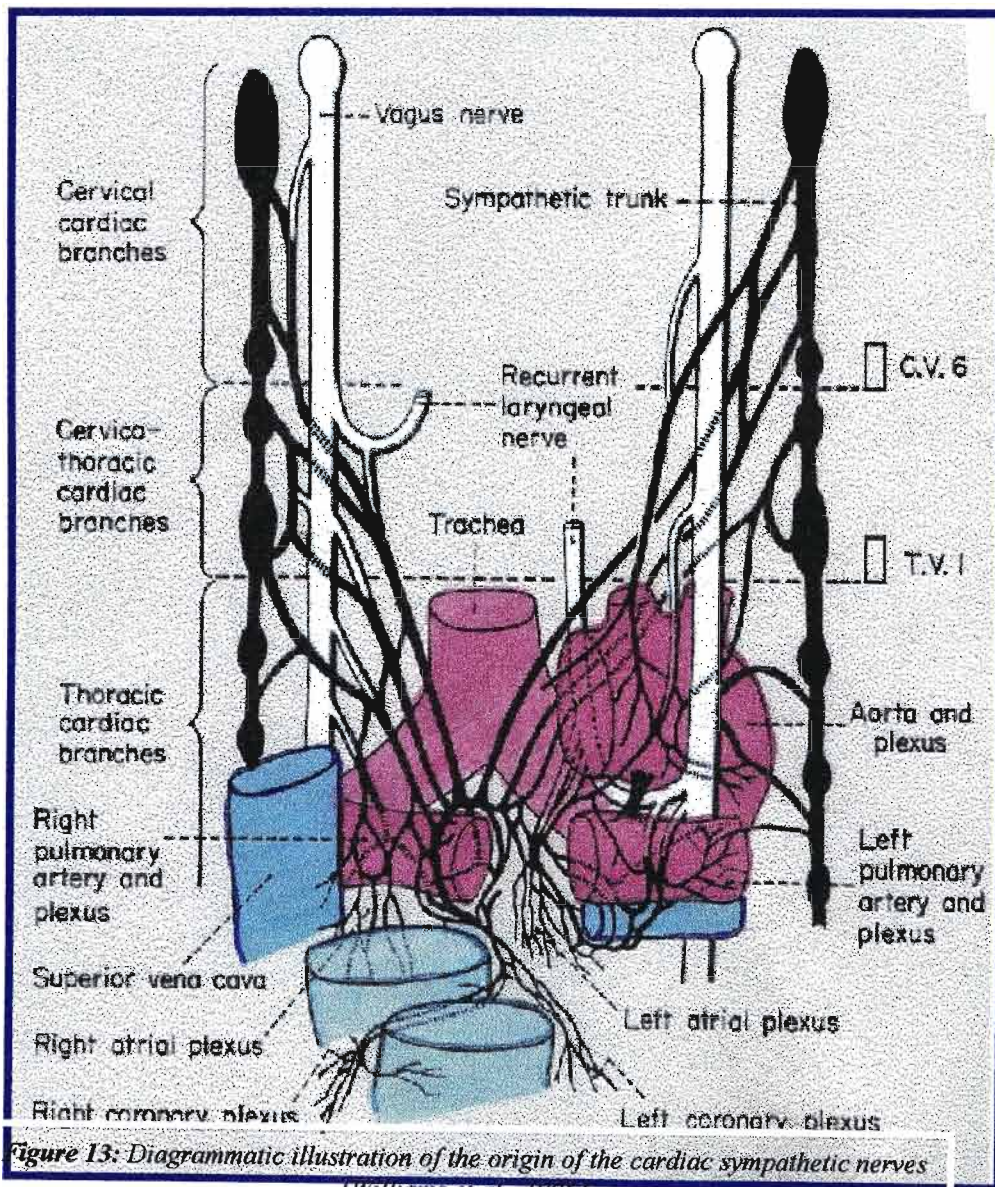


Figure 13: Diagrammatic illustration of the origin of the cardiac sympathetic nerves
[Williams et al., 1995]

The cervical cardiac nerves have dominated literature accounts of the sympathetic nerves to the heart up to the middle of the 20th century (Kuntz and Morehouse, 1953). The cervical cardiac nerves descend through the cervical region, enter the thorax and then join the cardiac plexus [figure 13].

The thoracic cardiac rami (TCR), in general, are arranged segmentally and only those arising from the upper four or five thoracic segments enter the cardiac plexus directly (Saccomanno, 1943) and contain, combined, twice as many fibres reaching the cardiac plexus as the larger cervical sympathetic cardiac rami. These nerves vary in size and number and in the manner in which they reach the cardiac plexus, in different specimens and bilaterally (Saccomanno, 1943).

The *superior cervical cardiac sympathetic ramus* arises by two or more filaments from the lower pole of SCG [figure 14]. It is believed to contain only efferent fibres; the preganglionic outflow being from the upper thoracic segments of the spinal cord; and to be devoid of any visceral pain fibres from the heart [figure 15]. It runs down the neck behind the common carotid artery and in front of longus colli muscle; it crosses in front of the inferior thyroid artery and recurrent laryngeal nerves. The intra-thoracic course on the right side then differs slightly from the left. The right nerve, at the root of the neck, passes posterior to the subclavian artery and postero-lateral to the brachiocephalic trunk to reach the posterior aspect of the arch of the aorta, where it joins the deep part of the cardiac plexus (Williams *et al.*, 1995). The left nerve, in the thorax, runs in front of the left common carotid artery and across the left side of the arch of the aorta to join the superficial part of the cardiac plexus (Williams *et al.*, 1995).

The *middle cervical cardiac ramus*, the largest of the sympathetic cardiac branches is derived from the MCG itself or more frequently from the sympathetic trunk cranial or caudal to it (Mitchell, 1956). On the right side, it descends behind the common carotid artery and at the root of the neck runs either in front of or behind the subclavian artery. It then descends on the trachea and joins the right half of the deep cardiac plexus (Williams *et al.*, 1995). The vertebral ganglion may give rise to the middle cervical cardiac sympathetic nerve (Potts, 1925).

An *inferior cervical cardiac ramus* arises from the CTG. It descends behind the subclavian artery and along the front of the trachea to join the deep part of the cardiac plexus. Behind the subclavian artery, it communicates with the middle cardiac nerve. It is often replaced by a varying number of fine filaments from the CTG and the ansa subclavia (Williams *et al.*, 1995).

When the 1st thoracic ganglion is unfused it also gives off cardiac filaments but when a CTG is present its cardiac branches contain rami from both ganglia (Mitchell, 1953). The presence of cardiac nerves arising from the upper four TG was first recorded by Weber, in 1815, on a dissection of a calf (Pick, 1970) while Mitchell (1953) accords its discovery in man, to Swan in 1830. It was, subsequently, rediscovered almost a century later, by Baeucker in 1927. Ionesco and Enachescu (1927) found them to be best developed in the Artiodactyla (lambs and calf). They dissected human fetuses and 2 adult cadavers and came to the conclusion that these nerves arise from the 2nd to the 5th thoracic sympathetic ganglia, bilaterally.

Jit and Mukerjee (1960) describe one or two cardiac branches from CTG to the deep

plexus and from T₂G or the immediate cord (above/below), in the majority of cases and in 3 cases from the left T₃G and in one case T₄G. Kuntz and Morehouse (1929), having dissected still born fetuses, young cadavers and one adult cadaver, reported cardiac rami form the 2nd and 3rd TG below CTG, and 'in many instances' from the 4th and

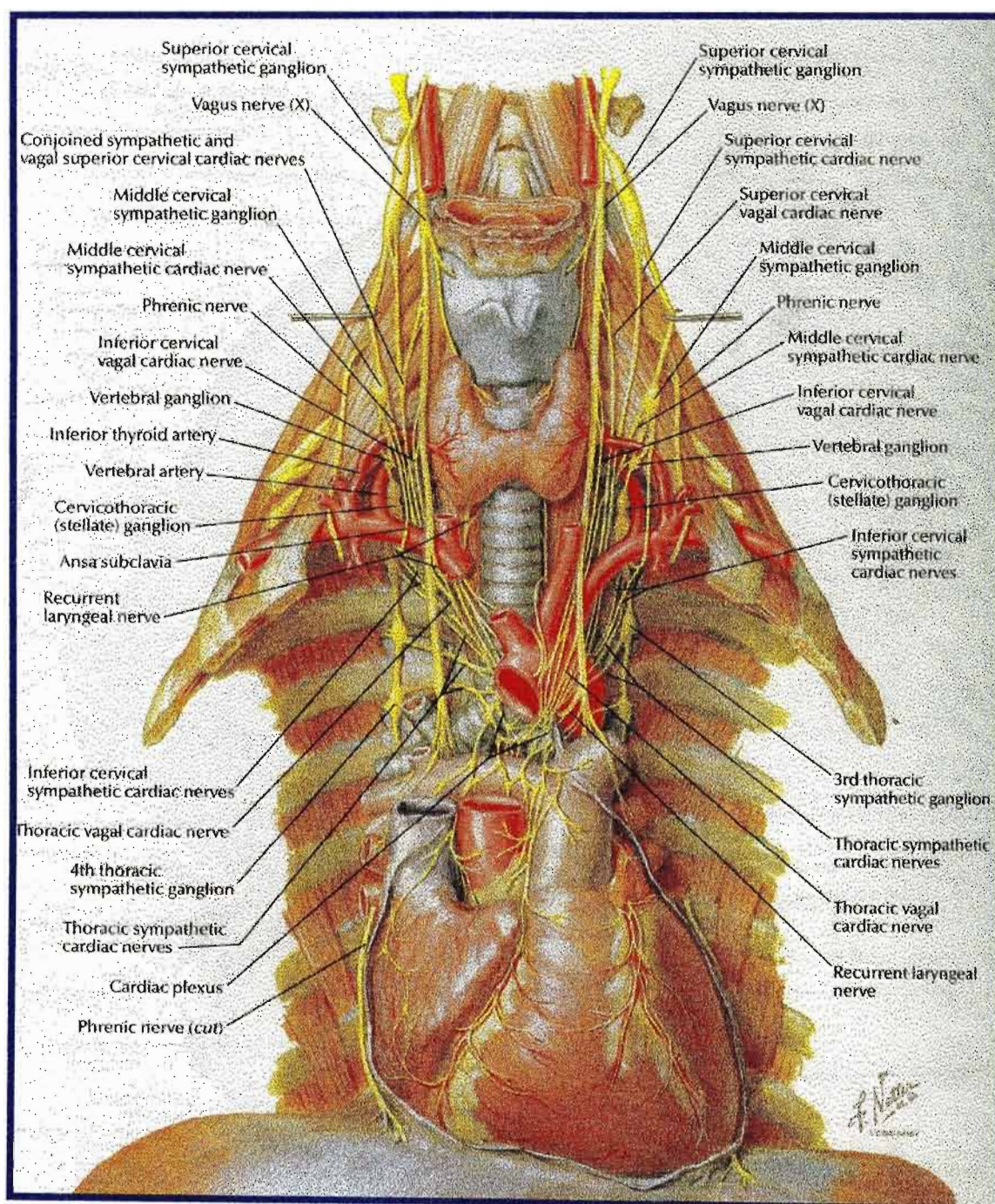


Figure 14: Cervical and thoracic cardiac sympathetic nerves
[Netter, 1990]

sometimes from the right 5th TG. Kuntz (1933) described cardiac nerves from the upper four TG in the rhesus monkey. Mitchell (1953) also describes the origin of thoracic cardiac nerves from the second to the fourth ganglia and occasionally from the fifth TG; however, the frequency of this origin is not stated. Perman (1924) traced the cardiac nerves in the calf and lamb from the third to the sixth thoracic ganglia but failed to trace any cardiac nerves below the level of the second TG in man. Anufriew (1926) and Schurawlew (1927) observed cardiac nerves arising from up to the T₂G on the left side. Riegele (1926) in the ape found cardiac nerves from up to the T₄G on the right side. Alexander (1933) reported fibres running to the heart from the dorsal ganglia as low as the fifth. Cannon *et al.* (1926) demonstrated nerves arising from the medial aspect of the chain up to 3 or 4 ganglia below CTG. Ellison and Williams (1969) found thoracic cardiac rami arising from the upper four or five ganglia, slender rami running independently to the heart. The literature reviewed is vague with regard to the incidence and course of the TCR.

Table 1: Lowest root of TCR

Author	Year	Material	Lowest Root
Weber	1815	Calf	T ₄
Perman	1924	Calf	T ₃ – T ₆
		Man	T ₂
Regiele	1925	Ape	T ₄
Anufriew	1925	Man	T ₂
Cannon <i>et al.</i>	1926	Man	T ₄ -T ₅
Schurawlew	1927	Man	T ₂
Lonesco and Enachesco	1927	Foetus and Adult	T ₂₋₅
Alexander	1933	Man	T ₅
Kuntz	1933	Rhesus Monkey	T ₄
Mitchell	1953	Man	T ₄ (rarely T ₅)
Jit and Mukerjee	1960	Man	T ₂ (100%); T ₃ (3%); T ₄ (1%)
Ellison and Williams	1969	Foetus	T ₄ -T ₅

The cardiac plexus is situated at the base of the heart, and is divided into superficial and deep parts, which are closely connected (Mitchell, 1956). Mizeres (1963) has emphasized the unity of the cardiac plexus, division of which into the superficial and deep parts, he considered an artefact of dissection.

Successful sympathetic denervation of the heart, for the relief of pain, a field often beset with failure, is dependant on adequate morphological knowledge of cervical and thoracic cardiac rami (Ellison and Williams, 1969). There is presently an increased interest in the anatomy of the cardiac contributions from the thoracic sympathetic chain and its role in cardiac pain pathways.

Angina of effort is similar in origin to intermittent claudication, just as the sympathetic nerves, which conduct pain impulses to the brain, are similar to the somatic sensory fibres (Ross, 1958)[*figure 15*]. They arise from peri-arterial and epicardial nerve endings in the heart and pass by way of the deep and superficial cardiac plexuses and the middle and inferior cervical nerves to the MCG and ICG through which they pass without interruption and continue down the ganglionated trunks to enter the spinal cord by way of the white rami communicates of the upper 4 or 5 thoracic roots (Ross, 1958). It is probable that other routes exist, running directly from the deep plexus to the upper four or five thoracic ganglia, but little is known of these alternate pathways (Ross, 1958).

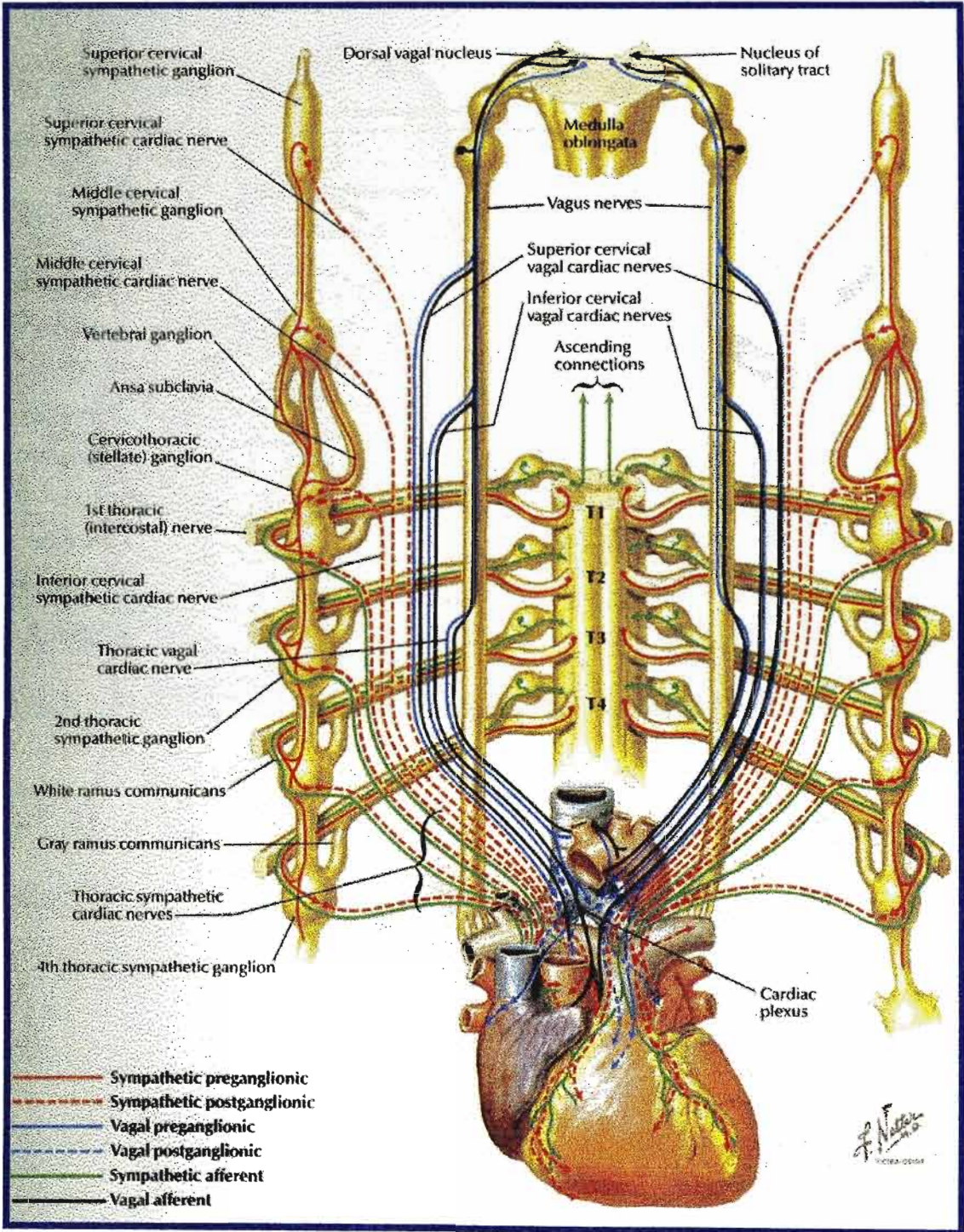


Figure 15: Autonomic pathways to the heart [Netter, 1990]

2.5 OTHER MEDIAL BRANCHES

2.5.1 SPLANCHNIC NERVES

The thoracic sympathetic chain gives rise to three splanchnic nerves 'proper' which arise from the lower eight ganglia [figure 16]. The greater splanchnic nerve (GSN) is formed by branches of the T5-9 sympathetic ganglia, the lesser splanchnic nerve (LSN) from T10-11 ganglia and the least splanchnic nerve (lsn) from T12 ganglion. These splanchnic nerves contain predominantly visceral efferent fibres as well as pain conducting visceral afferent fibres (McMinn, 1994).

The GSN consists mostly of myelinated, preganglionic, visceral afferent fibres. It is formed by branches of the 5th to the 9th or 10th thoracic ganglia; but fibres in the higher branches may be traced upwards in the sympathetic trunk as far as the 1st/2nd ganglion (Hollinshead, 1956). Its roots of origin may vary from 1 to 8, with 4 being the most usual (Jit and Mukerjee, 1960; Groen *et al.*, 1987). It descends obliquely on the bodies of the vertebrae, supplies fine branches to the descending aorta and perforates the crus of the diaphragm and ends mainly in the coeliac ganglion, but partly in the aortico-renal ganglion and suprarenal glands (Jit and Mukerjee, 1960).

Filaments from the 9th and 10th and sometimes the 10th and 11th ganglia form the LSN, which pierces the diaphragm with the GSN and joins the aortico-renal ganglion (Jit and Mukerjee, 1960).

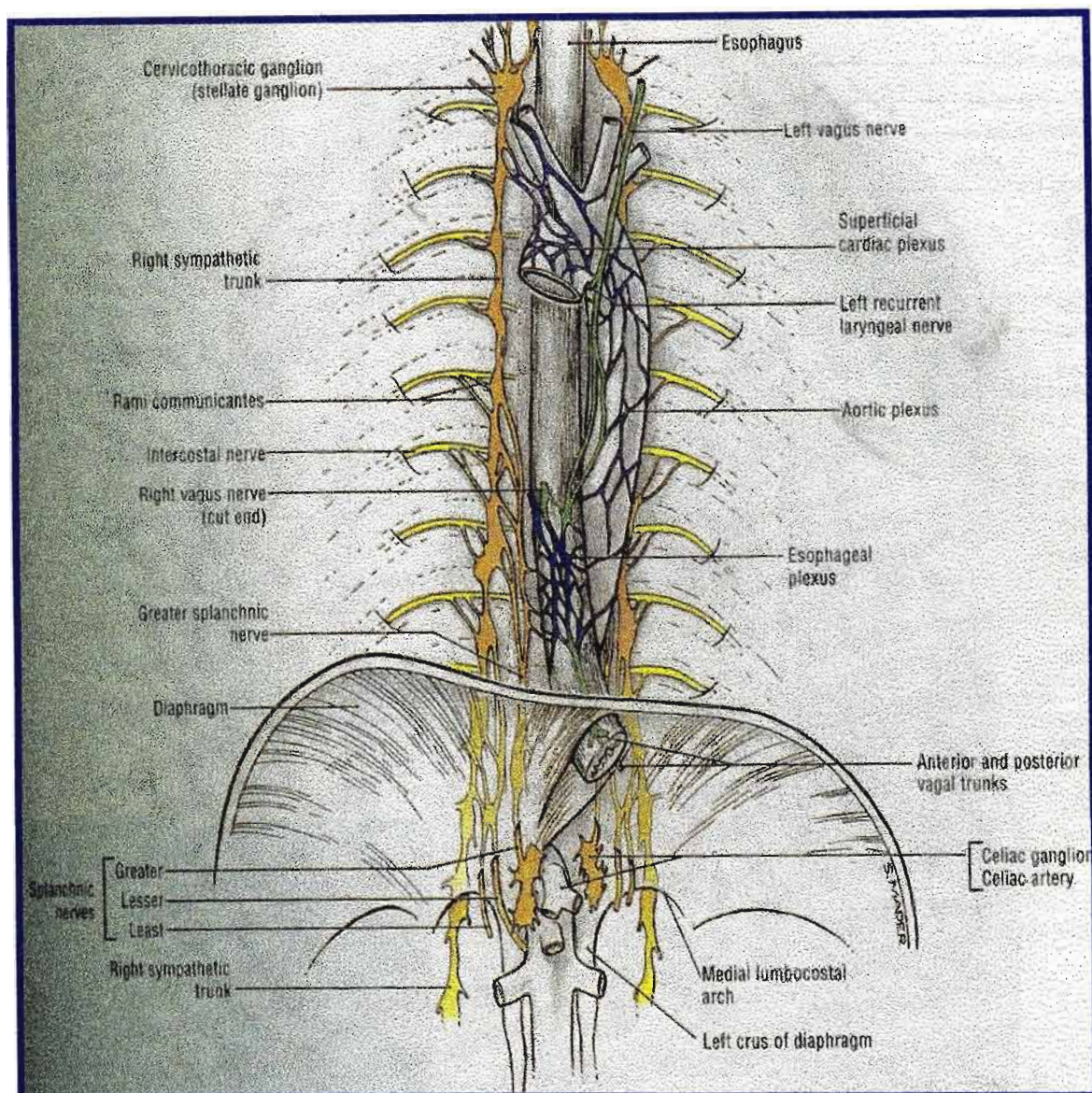


Figure 16: Origin of splanchnic nerves from the thoracic sympathetic chain
[Agur, 1991]

The Isn or 'renal nerve' arises from the last thoracic ganglion (Mitchell, 1956). It enters the abdomen with the sympathetic trunk and ends in the renal plexus (Jit and Mukerjee, 1960). De Sousa (1955) has further described a fourth (accessory) splanchnic nerve but its existence has yet, not been confirmed and is doubtful (Mitchell, 1956).

The uppermost root of GSN is reported to be from T₄G or T₅G ganglion (Kuntz, 1934; Mitchell, 1953; Reed, 1951; Jit and Mukerjee, 1960), while its lowest root can be as low

as T₁₂G ganglion (Hollinshead, 1956).

Edwards and Baker (1940) noted the origin of the LSN as high as T₇G, with the origin from T₁₀G and T₁₁G, being most frequent. Reed (1951) however, in an adult series, reported the origin of the LSN to be from T₉G-T₁₂G; and the origin of lsn to be from either T₁₁G and/or T₁₂G. Jit and Mukerjee (1960) found lsn arising predominantly from a single root in 37% of cases. Pain fibres of the upper abdominal viscera reach the sympathetic chain via the GSN and LSN from coeliac plexus. It is postulated however, that pancreatic pain fibres through the coeliac and superior mesenteric plexuses (Hiraoka et al., 1986) [*figure 17*].

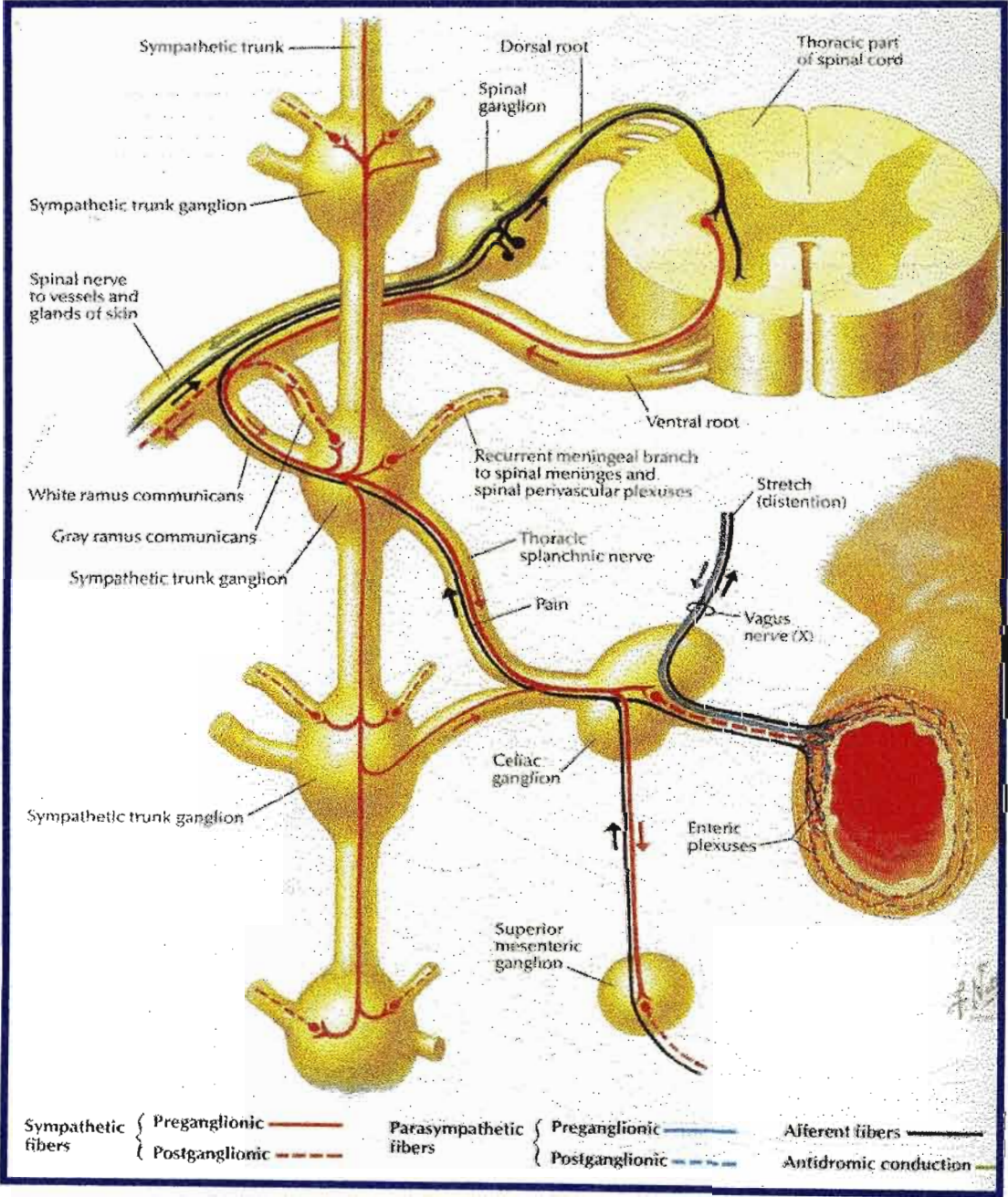


Figure 17: Autonomic pathway to the abdominal viscera [Netter, 1990]

2.5.2 VASCULAR BRANCHES

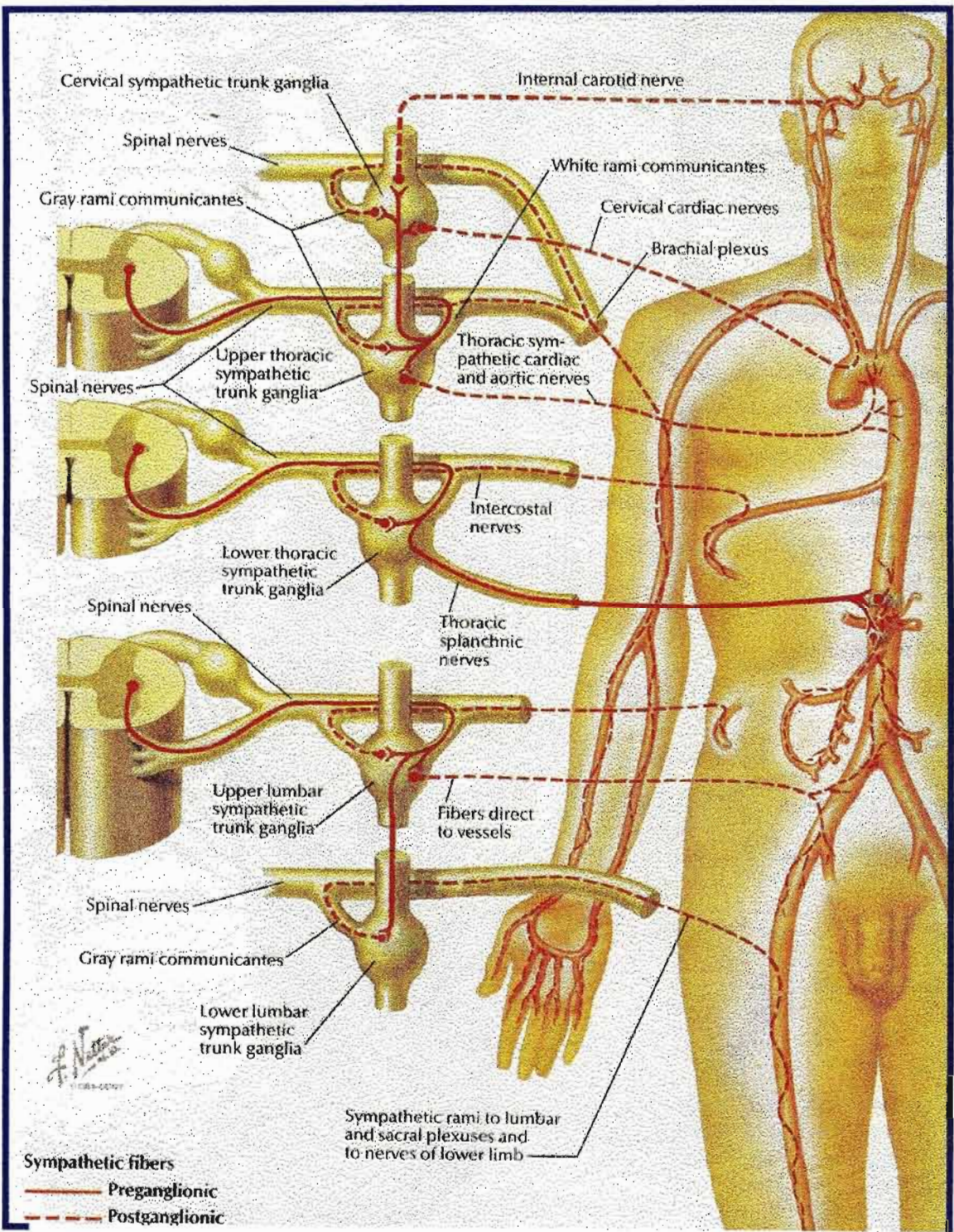


Figure 18: Diagrammatic illustration of the sympathetic pathways to blood vessels [Netter, 1990]

Postganglionic fibres may reach blood vessels at the cervicothoracic inlet, directly or may be carried through branches of the brachial plexus for variable distances before passing to more peripheral vessels in the upper limb. In man the levels of outflow of preganglionic fibres is not known, but most observers place the segmental limits between T₂G–T₃G and T₆G–T₇G segments [figure 18].

SCG supplies vascular branches to the internal and external carotid arteries (Mitchell, 1956). The branches from SCG to the external carotid artery arise four to six filaments that form a rich plexus around the artery and its branches. The internal carotid nerve is the direct upward continuation of the upper pole of SCG (Williams *et al.*, 1995)

MCG supplies vascular branches to the external carotid, common carotid, thyrocervical trunk, inferior thyroid, ascending cervical and vertebral arteries (Mitchell, 1956; Pick, 1970). In addition, Mitchell (1956) describes the vertebral ganglion (also known as the 'low' MCG) distributing filaments to the vertebral and subclavian arteries (Mitchell, 1956). Classically, the ansa subclavia is described as arising from the MCG, looping around the subclavian artery and terminating in either the ICG or SG (Becker and Grunt, 1957) via two or more cords (Williams *et al.*, 1995).

CTG contributes branches to the blood vessels, which form the plexus on the subclavian artery, and its branches (Pick, 1970). The plexus around the subclavian artery is derived from these branches and the ansa subclavia; extends to the first part of the axillary artery but fibres may extend further, though not in large numbers (Mitchell, 1970). According to Pearson and Sauter (1971) the extension of the subclavian plexus, which passes to the internal thoracic artery, is joined by a branch from the phrenic nerve. The plexus on the vertebral artery is derived mainly from a thick branch from CTG, which

ascends behind the vertebral artery to foramen transversarium of the sixth cervical vertebra, reinforced by branches from the cervical sympathetic trunk (Jit and Mukerjee, 1960).

Aortic Plexus

“The walls of the thoracic aorta are invested by a conspicuous network of nerves. However, it is not known to what extent these nerves actually terminate in the aorta or are just conveyed along the course of this blood vessel to other destinations” (Pick, 1970).

The arch and ascending aorta are supplied by the cardiac rami (Pick, 1970). The thoracic sympathetic trunks contribute a number of branches to the descending aorta. The medial branches of the upper five thoracic ganglia are very small: they supply filaments to the thoracic aorta and its branches. On the aorta, they form a delicate plexus (thoracic aortic plexus) together with filaments from the greater splanchnic nerve (Hollinshead, 1956). The aortic plexus is usually described as continuing through the diaphragm to join the coeliac or the abdominal aortic plexus, but to what extent this is true is not clear. Some surgeons have suspected that this may be important contribution to the abdominal innervation, but it should be emphasized that anatomically the thoracic aortic plexus is extremely poorly developed, and is in no manner comparable to the density to that about the abdominal aorta (Hollinshead, 1956).

2.5.3. LARYNGO-PHARYNGEAL BRANCHES

The *laryngo-pharyngeal* branches, arise from the SCG and the chain immediately below. These supply the carotid body and pass to the side of the pharynx where they join branches of the glossopharyngeal and vagus nerves to form the pharyngeal plexus. These communicate in a plexiform manner on the connective tissue of the external to the pharyngeal constrictors. From here rami extend cranially and caudally to be distributed to the larynx and pharynx (Williams *et al.*, 1995).

2.5.4 PULMONARY BRANCHES

The pulmonary plexus lies on the anterior and posterior aspects of the bronchial and vascular structures in the hila of the lungs, the anterior plexus being much smaller than the posterior plexus. According to Mizeres (1963), these plexuses are continuous extensions of the cardiac plexus being distributed along the right and left pulmonary arteries. The efferent sympathetic fibres are postganglionic fibres from the 2nd to the 5th thoracic ganglia of the sympathetic trunk. The anterior part of pulmonary plexus is formed by branches of cardiac sympathetic nerves as well as direct sources from the trunk. The posterior part of the pulmonary plexus is formed by rami of the cardiac plexus as well as 2nd to the 5th or 6th thoracic ganglia (Williams *et al.*, 1995).

2.5.5 OESOPHAGEAL PLEXUS

The oesophageal plexus is formed largely from filaments from the vagal trunks. The sympathetic contribution to the oesophageal plexus is minor and arises from the GSN and thoracic aortic plexus (Pick, 1970).

2.7 EMBRYOLOGY

As regards the embryology of the peripheral visceral afferent neurons, it is now widely, though not uniformly accepted that their cells of origin develop from the primordial spinal and cranial ganglia, which are derivatives of the neural crest (Pick, 1970).

This theory, first postulated by Kuntz, believes in an outgrowth of the sympathetic cells from the neural tube along the ventral roots and rami communicantes. Within the pale mesoderm, the primordia of the ganglia of the sympathetic trunks are present in the form of aggregates of large and deep stained cells in the lower thoracic and upper abdominal regions along the dorso-lateral aspects of the aorta. The sympathetic trunks form continuous columns extending from the rostral to the sacral regions of the embryo. Rami communicantes are also present during this stage. Cells, with an appearance identical to that of the primordia sympathetic trunks, derived partly from the neural tube and partly from the spinal ganglia pass along the ventral and dorsal spinal roots to form the primordial sympathetic trunks (Mitchell, 1953).

According to Kuntz (1953), the cervical sympathetic trunk does not develop from the primordial cervical spinal segments but is formed from a cranial extension of the thoracic sympathetic trunk, as well as by local cell proliferation. The segmentation of the thoracic and abdominal sympathetic, which begins in human embryos at 10mm in length, is not apparent in the cervical region of those of 15mm in length but may clearly be recognized in human embryos of 10mm in length in which individual sympathetic ganglia are connected by distinct internodal rami (Kuntz, 1953).

During the early stages of development the sympathetic primordial, due to the curvature of the embryo is in such close proximity to each other that they appear to be continuous column of loosely aggregated cells. Secondary segmentation and the formation of internodal rami occurs later; the details of this process is not certain, especially in the lower thoracic and lumbar regions, where irregularity in the number and position of sympathetic ganglia is a well known fact (Pick, 1970). According to Pick and Sheehan (1946), each primordial ganglionic mass divides into a cranial and caudal portion, and the ultimate fate of these portions determines the number and position of the sympathetic ganglia at various spinal levels [figure 19]:

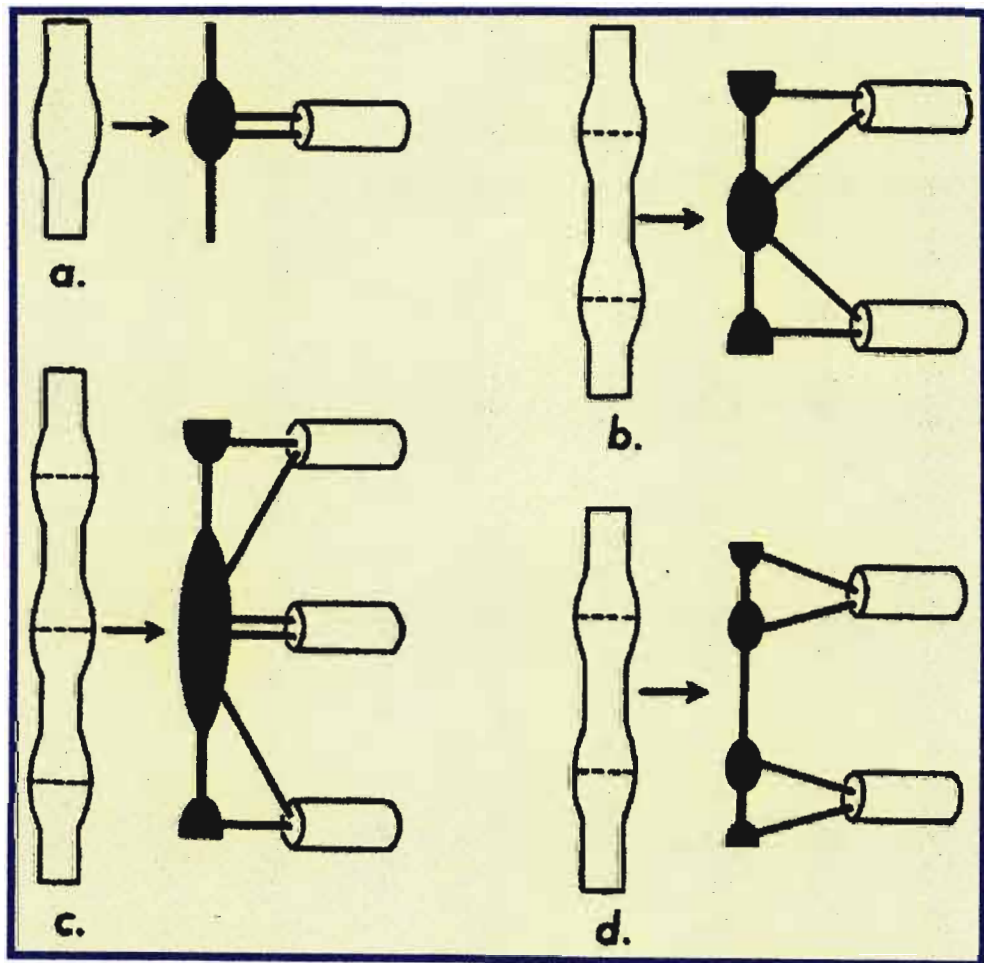


Figure 19: Schema illustrating the development of possible variations of the ganglionated chain from the primordial cell column [Pick, 1970]

- a. The two portions merge together again (or really never divide), forming a single ganglion with connections to only one spinal nerve, a type of ganglion truly segmental and most commonly occurring in the upper thoracic regions;
- b. A 2nd possibility would be the fusion of the caudal half of one primordial mass with the cranial half of the next lower mass, resulting in ganglia with connections to 2 spinal nerves. Such ganglia are not segmental and are typically in the lower thoracic regions in man.
- c. Thirdly, the fusion of positions of more than two primordial masses may take place and result in the formation of ganglia with connections to three or more spinal nerves. This arrangement is exemplified best by SCG and ICG, and is likewise common in the lumbar region in man.
- d. A fourth arrangement would result from the persistence of one or both portions of the primordial mass as a separate ganglion, thereby producing additional ganglia or complete duplication. Finally, an entire primordia mass or part of it may seemingly be absent when the rami communicantes usually connected with it are issued directly from the internodal ramus of the sympathetic trunk.

The primordia of the prevertebral plexus appears in the rostral abdominal region, in human embryos of 6mm in length, as a result of the ventral outgrowth of the primordial sympathetic trunks along the lateral aspects of the aorta (Pick, 1970). A similar displacement of cells from the upper thoracic primordial sympathetic trunks towards these prevertebral plexuses takes place at some later stage. Thus in the human embryos of 10mm in length an anlage of prevertebral plexuses, including the splanchnic nerves are quite conspicuous (Pick, 1970). The autonomic ganglia and ganglionic

plexus of the cranial region have, according to Kuntz (1953), a similar embryological history.

Starting at the end of the fourth week, the neuroblasts in the mantle layer of the spinal cord become organized into four columns that run the length of the cord: a pair of dorsal/alar columns and a pair of ventral/basal columns [figure 20]. Laterally the alar and basal columns are separated by a groove called the sulcus limitans; dorsally and

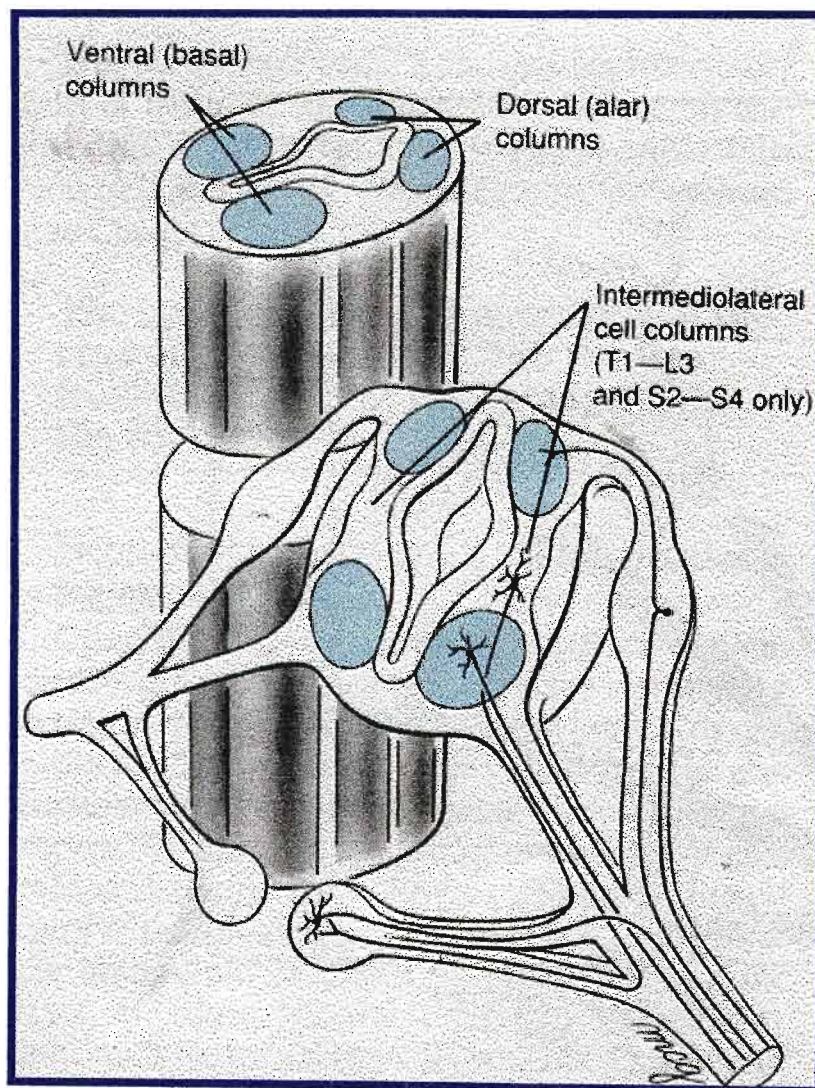


Figure 20: The formation of two ventral motor (basal) columns and two dorsal sensory (alar) columns throughout most of the spinal cord [Larsen, 1993]

ventrally they are separated by acute thinning of the neural tissue called, respectively, the roof plate and the floor plate. The cells of the dorsal column develop in association neurons, which will interconnect the motor neurons of the ventral columns with the neuronal processes that soon grow into the cord from the sensory neurons of the dorsal root ganglia. In most regions of the cord-at all 12 thoracic levels, at the lumbar levels (L1-3) and at the sacral regions (S2-4)- the neuroblasts in more dorsal regions of the basal columns segregate to form distinct intermedio-lateral cell columns [figure 19]. The thoracic and lumbar intermedio-lateral cell columns contain central autonomic motor neurons of the sympathetic nervous system, whereas the intermedio-lateral cell column in the sacral region contain central autonomic motor neurons in the parasympathetic system.

Not all peripheral sympathetic neurons are located in the chain ganglia. The peripheral ganglia of some specialized sympathetic pathways develop from neural crest cells that congregate next to major branches of the dorsal aorta. One pair of these prevertebral and pre-aortic ganglia originates from the cervical neural crest and forms at the root of the celiac trunk. Other, more diffuse ganglia develop in association with the superior mesenteric artery, the renal arteries, and the inferior mesenteric artery. These are formed by thoracic and lumbar neural crest cells [figure 21].

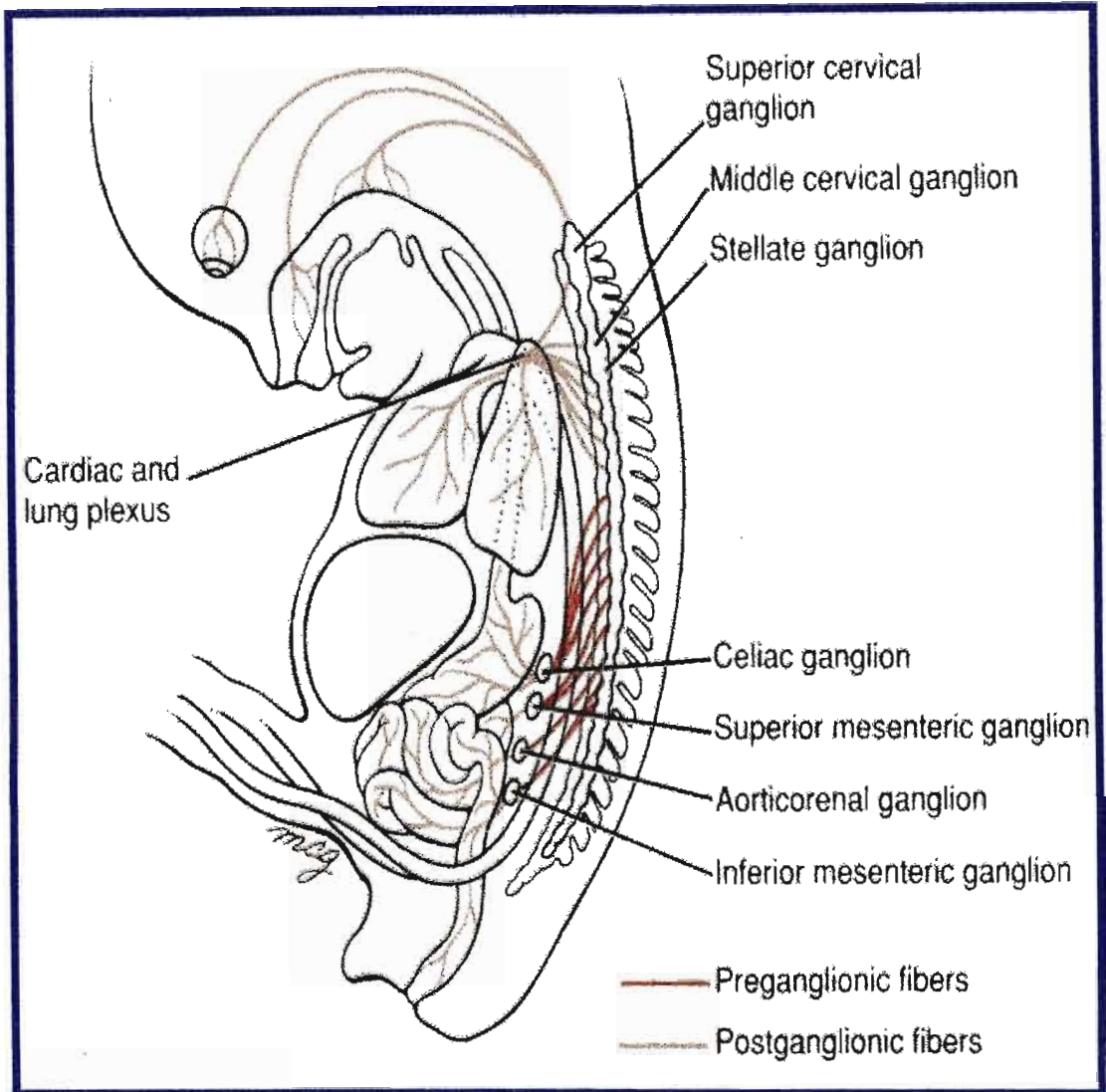


Figure 21: Postganglionic fibres emanating from cervical and thoracic chain ganglia follow blood vessels to structures in the head and pharynx and the heart and lungs
[Adapted from Larsen, 1993]

CHAPTER 3

MATERIALS AND METHODS

GENERAL

The cadaveric material used in this study of the medial branches of the cervical and thoracic sympathetic chains (in accordance with the Human Tissue Act, 51 of 1989) was obtained from the Department of Anatomy at the Universities of Durban-Westville and Natal and the Department of Human Biology, Technikon Natal.

The research was conducted at the Department of Anatomy, University of Durban-Westville, with clearance from both the Ethics Committee and Research Committee of the University of Durban-Westville.

3.1 MATERIALS

This study utilised 48 cadavers: 31 preserved fetuses without morphological abnormalities (gestational ages: 16 weeks to full term) and 17 adult cadavers [n=89 sides: right, 43 (foetal, 30; adult 13); left, 46 (foetal 30; adult, 16)]. Five adult sides (4 right and 1 left) were undissected due to pleural adhesions and 2 foetal sides (1 right and 1 left) were undissected due to tissue damage.

The dissections were conducted at both macroscopic and microscopic levels using surgical equipment and micro-dissectors, with the use of a light dissecting microscope and loupe lens.

This sample was used in this investigation as follows:

- Cervical ganglia and the cervical sympathetic chain [n=58 sides: foetal, 42; adult, 16]
- Thoracic ganglia [n=85 sides: foetal, 56; adult, 29]
- Cardiac rami [n= 58 sides: foetal, 42; adult, 16]
- Splanchnic nerves [n=48 sides: foetal, 32; adult, 16]

3.2 GROSS ANATOMICAL DISSECTION

3.2.1 THORACIC DISSECTION

The thoracic dissection was performed prior to any cervical dissection.

A midline vertical incision was made from the jugular notch to the umbilicus. Two transverse skin incisions were then made:

- i) From the jugular notch to the shoulder tip;
- ii) From the xiphoid process of the sternum, along the inferior border of the rib cage as far laterally as the mid-axillary line.

The skin flaps were reflected laterally and the muscle attachments along the mid-axillary line on the rib cage were removed. The intervening intercostal muscles were cut, followed by the ribs, in the mid-axillary line. The rib cage was then reflected superiorly.

The sterno-clavicular and the 1st sterno-costal joints were mobilized. The attachments of the scalene muscles on the first rib were detached. The anterior rib cage was removed.

The lungs were removed by excision of the pulmonary vessels and bronchi at the hilum. All fatty tissue was disposed off and the supra-pleural membrane and costal pleura overlying the sympathetic chain was stripped away, from the first rib to the costo-diaphragmatic recess (at the level of T10/11 vertebra). The diaphragm was excised as close to its costal and pleural attachments as possible. In the foetuses the abdomen was then eviscerated while in the adults the specimen was divided at the level of the umbilicus (for ease of use).

3.2.2 CERVICAL DISSECTION

In 21 foetuses and 8 adult specimens the cervical sympathetic chain was further dissected [n=58 sides: right, 29 (foetal, 21; adult 8); left, 29 (foetal, 21; adult, 8)].

A midline skin incision was made from the midpoint of the body of the mandible to the midpoint of first transverse incision of the thoracic dissection. The skin and fascia was reflected as far laterally as possible. The sternocleidomastoid and strap muscles of the neck were removed. The contents of the carotid sheath were mobilized. The major venous structures, viz. the subclavian vein and brachiocephalic trunk, were removed. The cervical plexus was identified. The cervical sympathetic chain was then followed upwards from the thoracic inlet and micro-dissected to reveal the finer branches of the sympathetic chain.

The medial branches from the cervical and thoracic segments of the chain were traced. Detailed drawings were made of each chain as it was studied *in situ*.

3.3 HISTOLOGY

Fused ganglia, segments of cardiac rami and of the interganglionic segments between the ICG, T1 and T2, were biopsied and stained using haematoxylin and eosin (*H and E*) by the technicians at the Lancet Laboratories in Lorne Street, Durban. The authenticity of the biopsied structures was confirmed histologically.

3.3 NOMENCLATURE

3.3.1 IDENTIFICATION OF GANGLIA

Cervical Ganglia

The superior cervical ganglion, a constantly occurring ganglion, was identified as the uppermost cervical ganglion located near the base of the skull (Glabella, 1976). The cervicothoracic ganglion or the inferior cervical ganglion was identified by its location and macroscopic connections (Jit and Mukerjee, 1960). All ganglia residing on the cervical sympathetic chain between these ganglia were regarded as middle cervical ganglia (Axford, 1928; Becker and Grunt, 1957).

Thoracic Ganglia

Thoracic ganglia were identified, according to the method proposed by Groen et al. (1987), by their macroscopic spinal nerve contributions (i.e. rami communicantes) without differentiating between grey and white rami. By naming ganglia according to their distribution to spinal nerves one is effectively designating a ganglion according to its developmental origin (Bradley, 1951). In instances where a ganglion contributed rami communicantes to more than one spinal nerve, it was regarded as a fused ganglion.

3.3.2 IDENTIFICATION OF CARDIAC RAMI

The cardiac rami were named according to the ganglion from which they arose. The rami arising from the inter-ganglionic segments of the sympathetic chain were named after the closest ganglion located on the sympathetic chain.

3.4 STATISTICAL ANALYSIS

In addition to the incidence (right and left) of all medial branches observed, the following morphometric parameters were documented:

- Length (foetal and adult specimens) and width (adult specimens) of cervical ganglia (SCG, MCG, ICG and CTG)
- Length of the interganglionic chain (in adult specimens) between: SCG and MCG, SCG and CTG, MCG and CTG.

For statistical comparisons of measurements and incidence, standard deviations and *p*-values were calculated using *t-test: two-sample assuming equal variances* with Microsoft Excel Office-2000. A *p*-value < 0.05 was considered significant in all statistical comparisons.

Weighted means were calculated from incidence and sample sizes cited in literature using the following formula:

$$\frac{\sum nx}{\sum n}$$

CHAPTER 4

RESULTS

4.1 SAMPLE

Thirty-one foetal and seventeen adults were included in this study with a total of eighty-nine sides (right, 43 and left, 46), as indicated in table 2 [figures 22 and 23].

Table 2: Foetal and adult sampling

	RIGHT	LEFT	TOTAL
Foetal	30	30	60
Adult	13	16	29
Total	43	46	89

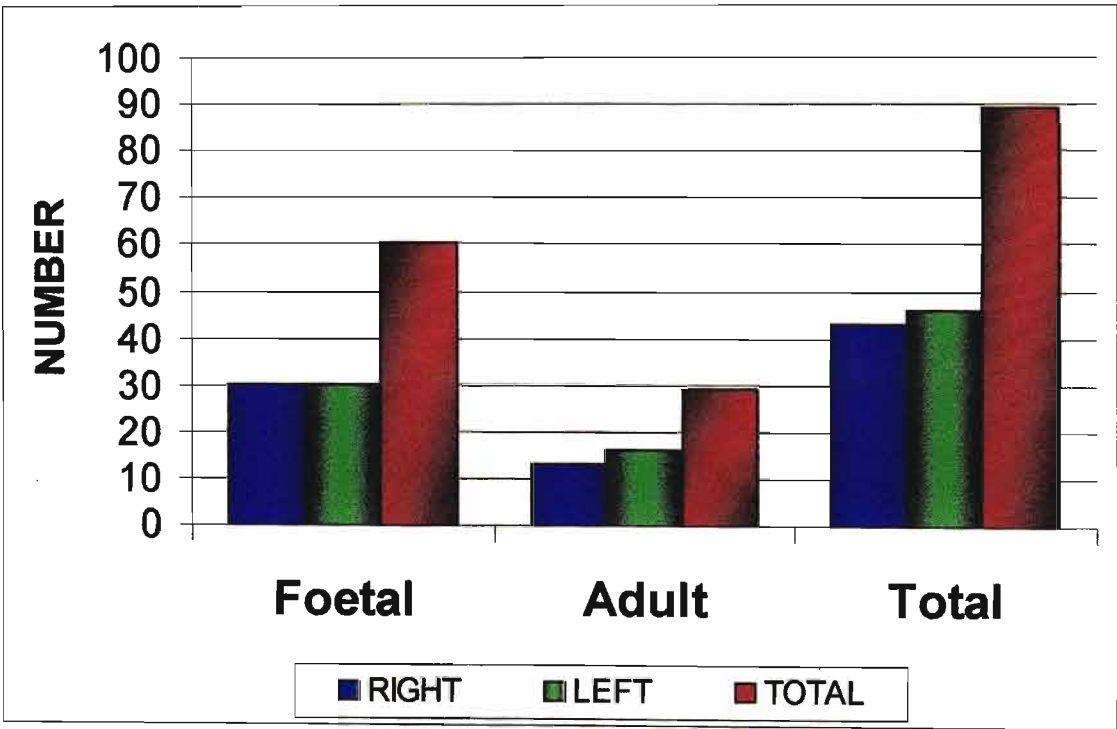


Figure 22: Graphic representation of sample distribution (n=89)

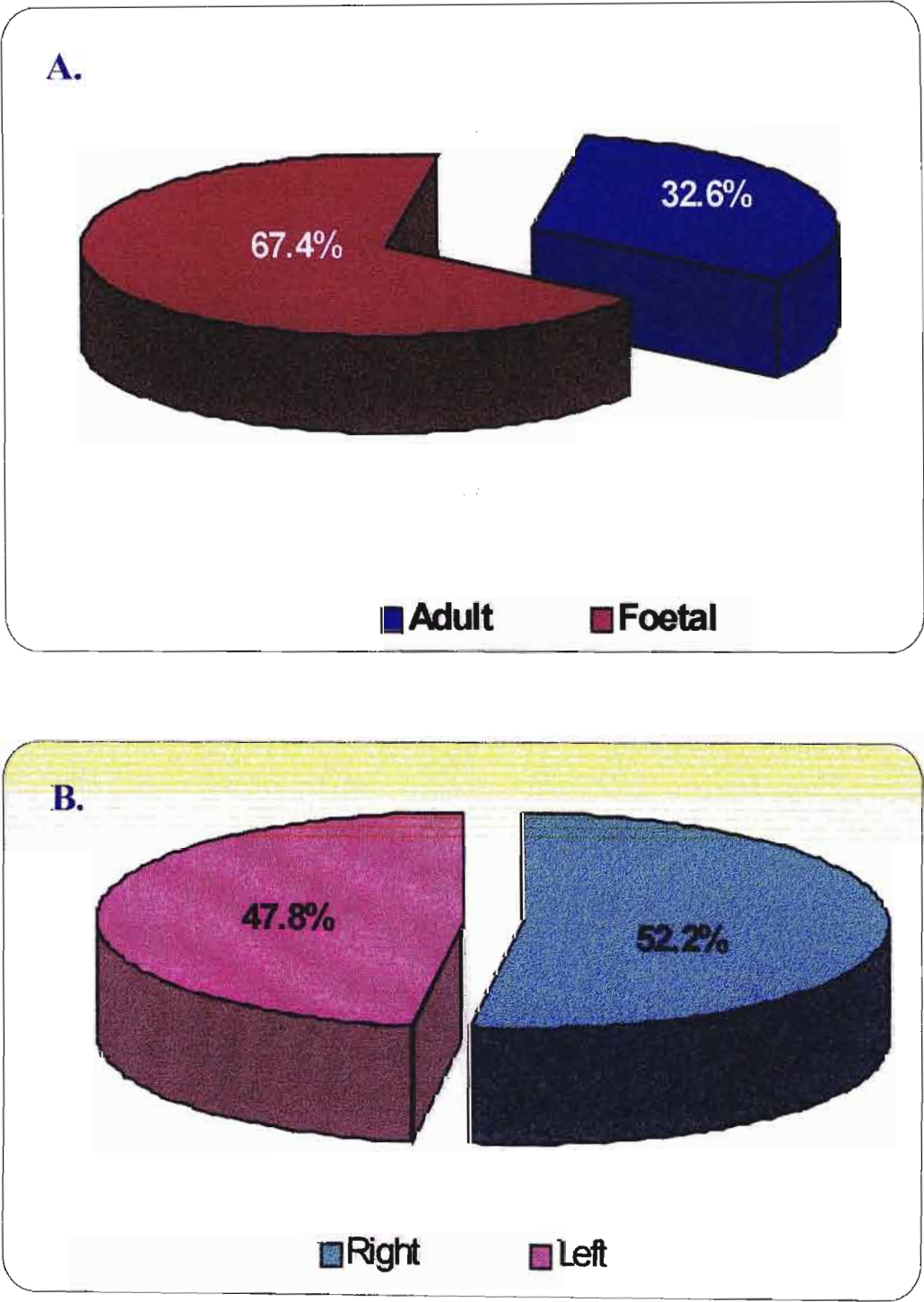


Figure 23: Graphic representation of the sample distribution of (n=89):
A) foetal vs. adult, and B) right vs. left

4.2 CERVICAL SYMPATHETIC CHAIN

The cervical sympathetic chain was examined in 29 specimens [n=58 sides: right, 29 (foetal, 21; adult, 8); left, 29 (foetal, 21; adult, 8)].

4.2.1 COURSE AND RELATIONS

The cervical part of the sympathetic chain was found to be located anterior to the prevertebral muscles and fascia, and postero-lateral to the carotid vessels enclosed in the carotid sheath [*Plate 1*]. Along its entire cervical course, the vagus nerve (enclosed

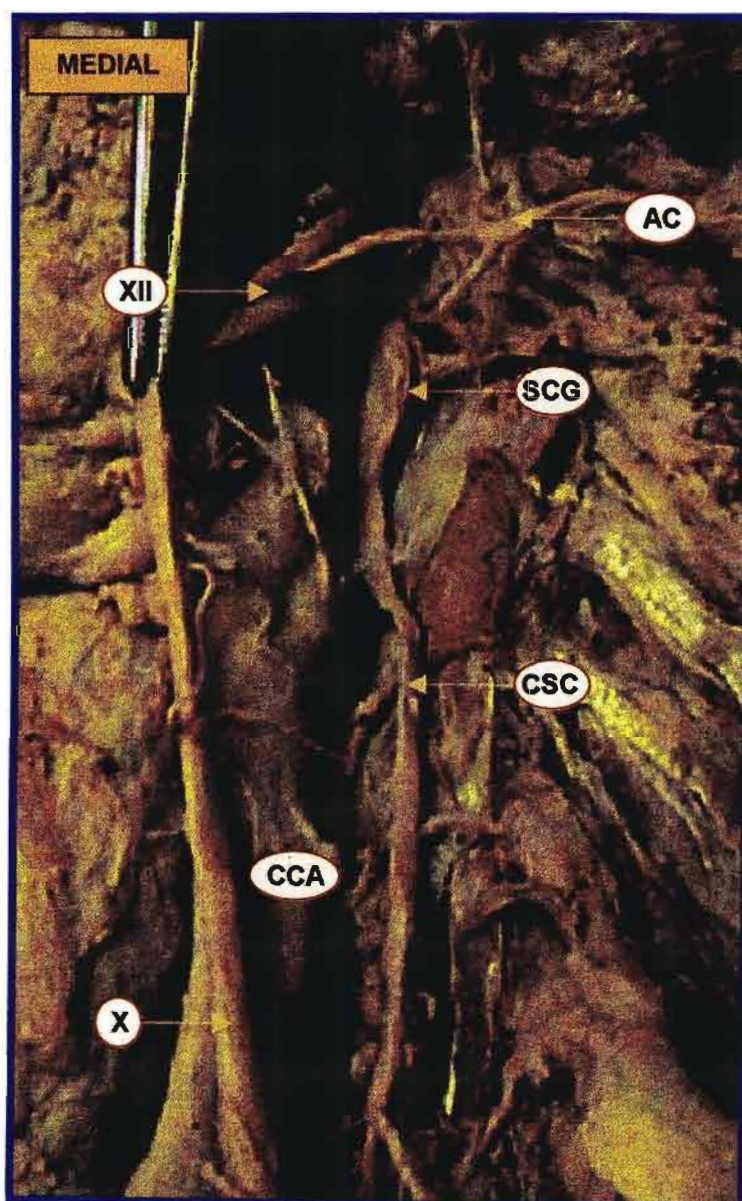


Plate 1: Antero-lateral view of left cervical sympathetic chain demonstrating its relations (adult)

KEY:

SCG	Superior Cervical Ganglion
CSC	Cervical Sympathetic Chain
CCA	Common Carotid Art.
X	Vagus Nerve (reflected)
XII	Hypoglossal Nerve
AC	Ansa Cervicalis

within the carotid sheath) was located medial to the sympathetic chain. The vertebral artery crossed the lower part of the cervical chain, from medial to lateral, at the level of its origin from the subclavian artery. The chain was observed to incline medially at the level of the thoracic inlet.

However, in one adult specimen (1.7%) the cervical sympathetic chain, on the right side, split from the inferior pole of SCG, into two cords. Each limb of this double chain terminated inferiorly in a ganglion (ICG and MCG), at the level of the seventh cervical vertebra [Plate 2]. The ansa subclavian was formed by cords passing anterior and posterior to the subclavian artery, joining these two ganglia.

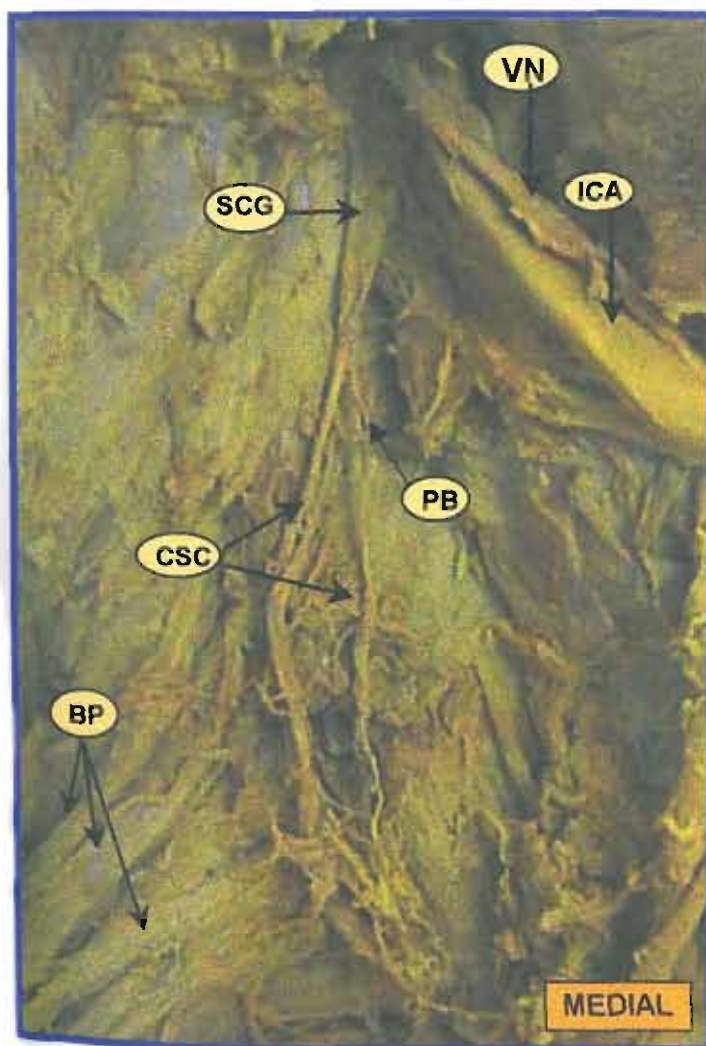


Plate 2: Antero-lateral view of right sympathetic chain demonstrating the split chain arising from the lower pole of SCG (adult)

(Note: pharyngeal branches arising from the sympathetic cord)

KEY:

SCG	Superior Cervical Ganglion
CSC	Cervical Sympathetic Chain
ICA	Internal Carotid Artery (reflected)
VN	Vagus Nerve (reflected)
BP	Brachial Plexus Roots
PB	Pharyngeal branches

The number of ganglia of the cervical sympathetic chain varied from two to four. The incidence of these was [figure 24]:

- Two ganglia: 11 sides (18.9%);
- Three ganglia: 32 sides (55.2%) and
- Four ganglia: 15 sides (25.9%).

All ganglia residing on the cervical chain between SCG (always present) and ICG/CTG (one or the other was always present) were designated MCG. MCG was the most variable of the cervical ganglia.

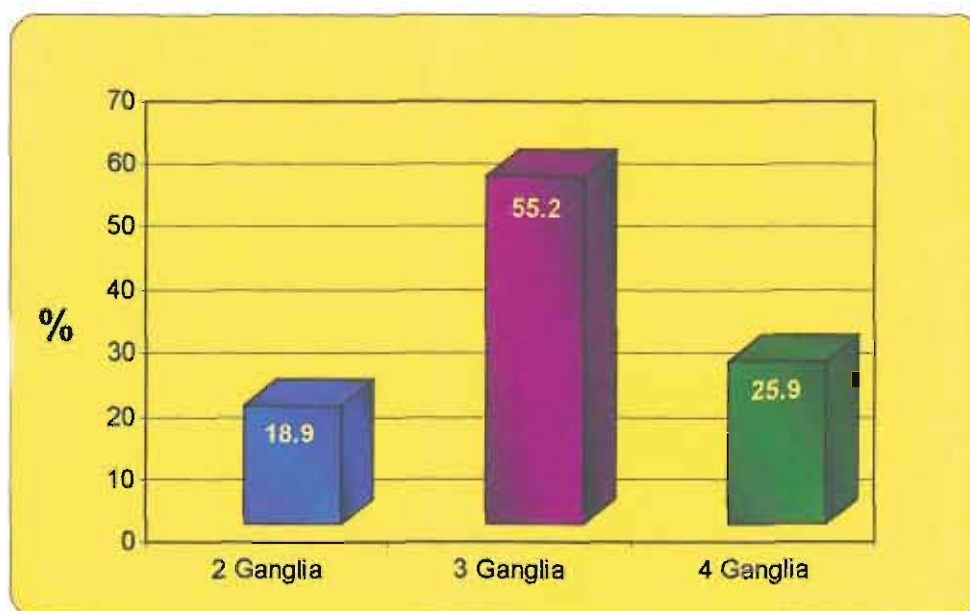


Figure 24: Number of ganglia in the cervical sympathetic chain

Table 1. Incidence of cervical ganglia

GANGLION	RIGHT			LEFT			TOTAL
	Foetal (n=21)	Adult (n=8)	Total [n=29]	Foetal (n=21)	Adult (n=8)	Total [n=29]	(n=58)
SCG	21 (100.0)	8 (100.0)	29 (100.0)	21 (100.0)	8 (100.0)	29 (100.0)	100 (58)
MCG	18 (85.7)	7 (87.5)	25 (86.2)	17 (81.0)	5 (62.5)	22 (75.9)	81.1 (47)
ICG	2 (9.5)	3 (37.5)	5 (17.2)	2 (9.5)	2 (25.0)	4 (13.8)	15.5 (9)
CTG	19 (90.5)	5 (62.5)	24 (82.8)	19 (90.5)	6 (75.0)	25 (86.2)	84.5 (49)

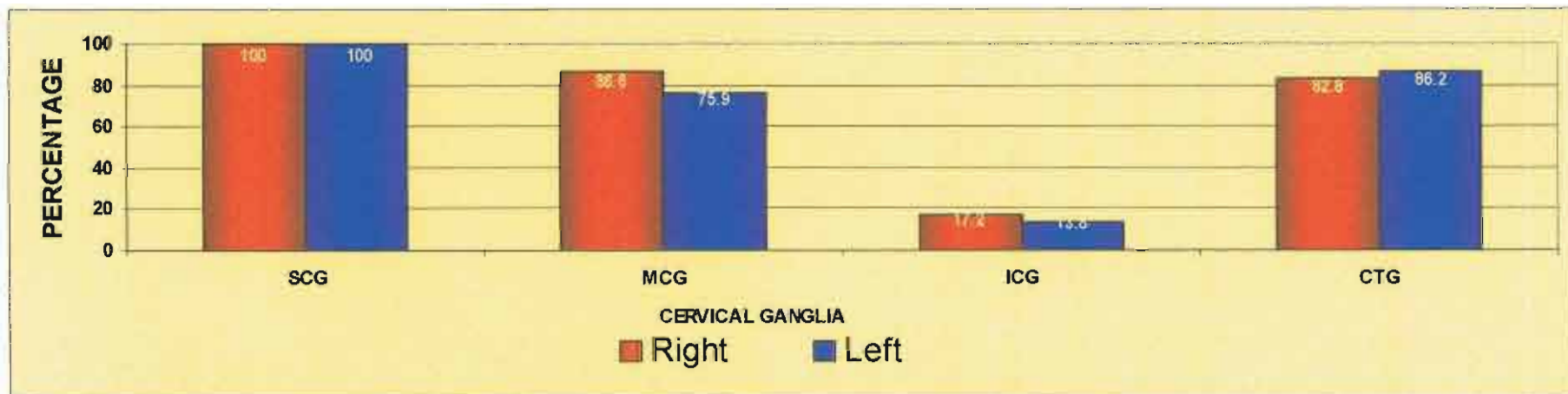


Figure 25: Incidence of cervical ganglia

4.2.2 SUPERIOR CERVICAL GANGLION

SCG was present in all specimens [Plates 1 and 2]. It was consistently spindle shaped, with a long vertical axis, lying on the longus capitis muscle.

The relation of SCG to the cervical vertebrae is indicated in Table 4. SCG was found to be located between C₁-C₄ vertebrae; with a position between C₁-C₃ being the most predominant (48.3%). However, it should be noted that the incidence of SCG above C₄ vertebra was 98.3%. In the adult specimens, SCG was always located below C₁ vertebra, primarily between C₂-C₃ in 5 sides (62.5%) and the intervertebral discs between C₁₋₂ and C₂-C₃ in 4 sides (50%)

Table 4: Vertebral location of SCG

VERTEBRAL LEVEL	VERTEBRAL SPAN	RIGHT (n=29)			LEFT (n=29)			TOTAL (n=58)
		Foetal (n=21)	Adult (n=8)	Total	Foetal (n=21)	Adult (n=8)	Total	
C _{1↔2} -C ₃	2V, 1D	10.3 (3)	6.9 (2)	17.2 (5)	-	3.5 (1)	3.5 (1)	10.4 (6)
C ₂ -C ₃	2V, 1D	-	6.9 (2)	6.9 (2)	-	10.3 (3)	10.3 (3)	8.6 (5)
C ₂	1V	-	3.5 (1)	3.5 (1)	-	-	-	1.7 (1)
C _{1↔2} -C _{2↔3}	1V, 2D	6.9 (2)	3.5 (1)	10.3 (3)	31.0 (9)	10.3 (3)	41.4 (12)	25.9 (15)
C ₂ -C _{2↔3}	1V, 1D	-	3.5 (1)	3.5 (1)	-	3.5 (1)	3.5 (1)	3.4 (2)
C ₂ -C ₄	2V, 2D	-	3.5 (1)	3.5 (1)	-	-	-	1.7 (1)
C ₁ -C ₃	2V, 2D	55.2 (16)	-	55.2 (16)	41.4 (12)	-	41.4 (12)	48.3 (28)

Note: Actual figures given in ()

Key: V= vertebral body; D= disc; ↔= intervertebral disc; - = to

The mean length and width of SCG, in the adult specimens (Table 5) was $26.7 \pm 4.46\text{mm}$ and $7.81 \pm 0.67\text{mm}$, respectively. No significant differences were observed between right and left sides [*p value: length, 0.18; width, 0.10*]. The mean length of SCG in the foetal specimens was $9.47 \pm 1.77\text{mm}$ [range: right, $4.67\text{-}10.32 \pm 1.64\text{mm}$ (mean: 8.81mm); left, $4.88\text{-}11.28 \pm 1.93\text{mm}$ (mean: 8.73mm)]. No significant differences were observed between right and left sides [*p=0.90*].

Table 5: Range of dimensions of SCG in the adult specimens

	RIGHT		LEFT		<i>p-value</i>
	<i>Min-Max</i>	<i>Mean (SD)</i>	<i>Min-Max</i>	<i>Mean (SD)</i>	
Length(mm)	18.38-32.51	27.78 (4.16)	17.99-28.94	25.68 (4.8)	0.18
Width(mm)	6.35-8.80	8.03 (0.81)	6.89-7.94	7.58 (0.45)	0.10

SCG was found posterior to the carotid sheath and anterior to the pre-vertebral fascia on longus capitis muscle [*Plates 1 and 2*]. In the foetal specimens, the lower pole of SCG was located immediately above the bifurcation of the common carotid artery [*Plate 3*]. In the adult specimens the SCG was found posterior to the internal carotid artery. The

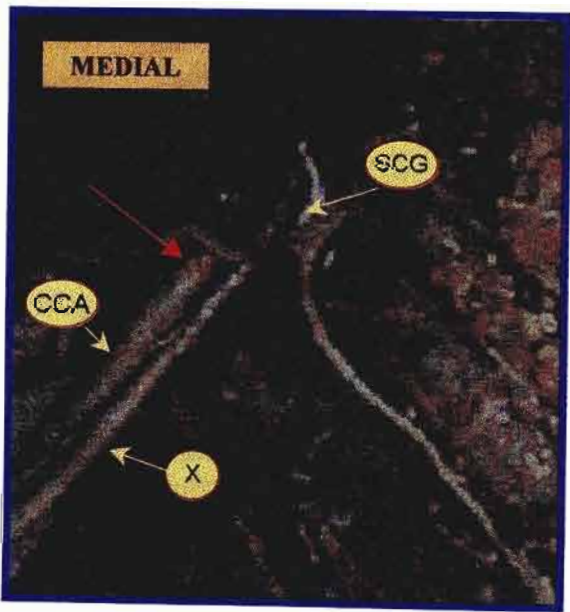


Plate 3: Antero-lateral view of left sympathetic chain demonstrating the relationship of SCG to the bifurcation of the common carotid artery (foetus)

KEY:
SCG Superior Cervical Ganglion
CSC Cervical Sympathetic Chain
CCA Common Carotid Artery
X Vagus Nerve
→ Bifurcation of CCA

internal carotid nerve, the direct upward continuation of the SCG, consistently arose from its superior pole of the ganglion.

Lateral somatic branches from SCG were observed to spinal nerves C₁-C₄. Communicating rami from SCG to the last four cranial nerves (glossopharyngeal, vagus, spinal accessory and hypoglossal nerves) were also found. The incidence of these were: glossopharyngeal nerve: 34.5% (right, 27.6%; left, 41.4%); vagus nerve: 39.7% (right, 44.8%; left, 34.5%) [Plate 4]; spinal accessory nerve: 22.4% (right, 17.2%; left, 27.6%) and hypoglossal nerve: 63.8% (right, 65.5%; left, 62.1%).

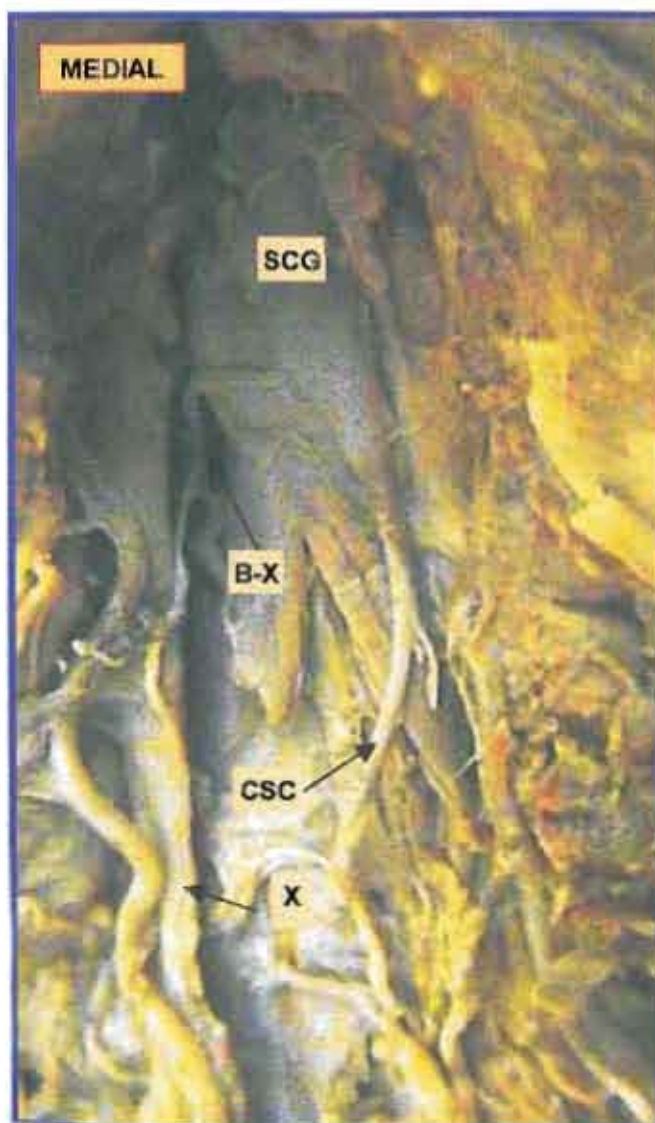


Plate 4: Antero-lateral view of the left cervical sympathetic chain demonstrating the communicating ramus between SCG and the vagus nerve in a fetus.

KEY:
 SCG Superior Cervical Ganglion
 CSC Cervical Sympathetic Chain
 X Vagus Nerve
 B-X Ramus connecting Vagus Nerve and SCG

4.2.3 MIDDLE CERVICAL GANGLION (MCG)

In the 58 cervical chains investigated, the incidence of MCG was 81.1% ($^{47}/_{58}$ sides) as indicated in Tables 3 and 7 [Plate 5, figures 25 and 26]. Of the 47 chains in which MCG was present, a single MCG was found on 32 sides (55.2%) while a double MCG was present in of 15 sides (25.9%) [Figure 26].

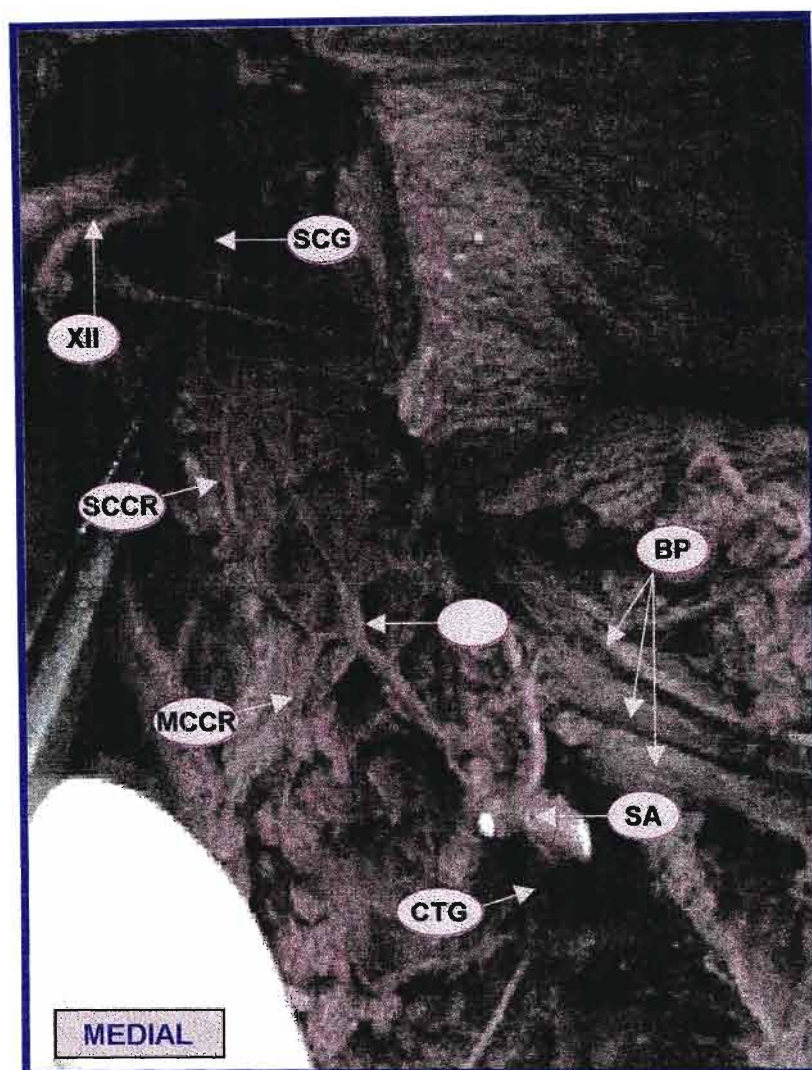


Plate 5: Antero-lateral view of left sympathetic chain demonstrating Type II MCG (foetus) (Note: the origin of SCCR and MCCR)

KEY:

SCG	Superior Cervical Ganglion	MCG	Middle Cervical Ganglion
CTG	Cervico-thoracic Ganglion	SCCR	Superior Cervical Cardiac Ramus
MCCR	Middle Cervical Cardiac Ramus	XII	Hypoglossal Nerve
BP	Brachial Plexus Trunks	Carotid Artery	

Table 6: Vertebral location of MCG

VERTEBRAL LEVEL	RIGHT (n=29)			LEFT (n=29)			TOTAL (n=58)
	Foetal	Adult	Total	Foetal	Adult	Total	
Above C ₆	9 (31.0)	2 (6.9)	11 (37.9)	4 (13.8)	1 (3.4)	5 (17.3)	16 (27.6)
At C ₆	10 (34.5)	5 (17.3)	15 (51.7)	11 (37.9)	1 (3.4)	12 (41.4)	27 (46.6)
C _{6↔7}	2 (6.9)	2 (6.9)	4 (13.8)	1 (3.4)	4 (13.8)	5 (17.3)	9 (15.5)
C ₇	3 (10.3)	0	3 (10.3)	6 (20.7)	1 (3.4)	7 (24.1)	10 (17.2)

Note: Percentage given in (). Key: C=cervical vertebra; ↔ = intervertebral disc

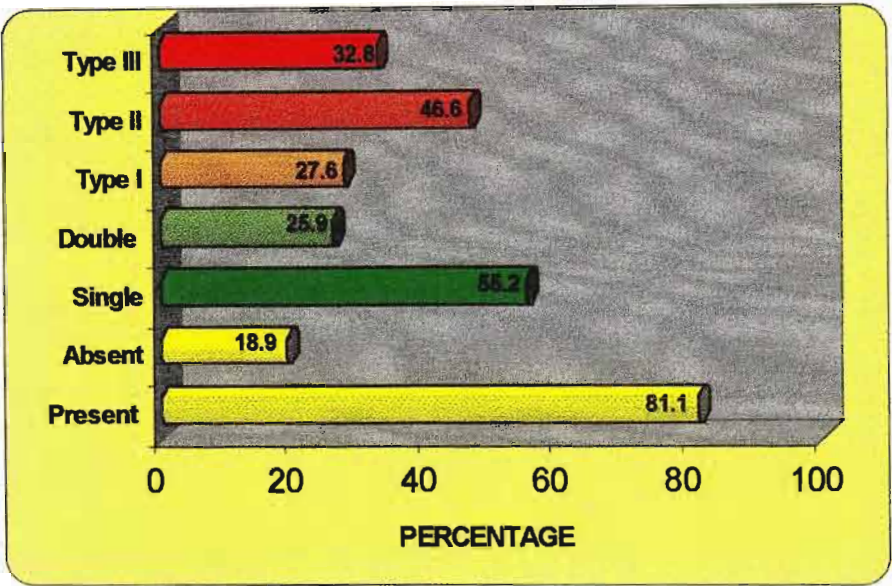


Figure 26: Incidence and variations of MCG

Based on the vertebral locations of MCG [Table 6], the classical textbook definition (Williams *et al.*, 1995) and the studies of Axford (1928) and Jamieson *et al.* (1952), three types of MCG were differentiated [Table 7]:

Type I: an MCG lying above the superior border of the 6th cervical vertebra (above C₆) – ‘high’ MCG;

Type II: a MCG lying on the body/transverse process of the 6th cervical vertebra (at C₆) – ‘typical/normal’ MCG;

Type III: a MCG lying below the inferior border of the 6th cervical vertebra (at C₆₋₇ and C₇) – ‘low’ MCG.

When present, *Type III* MCG was found below the lower border of C₆ and on C₇ vertebral bodies, with the vertebral artery passing postero-laterally, before entering foramen transversarium of C₆ vertebra. Ansa subclavian formed a loop between this ganglion and CTG/ICG. The inferior thyroid artery was closely related to *Type II* MCG and passed anterior to it [*Plate 6*]. Ansa subclavian formed a loop between this ganglion and CTG/ICG. In 2 cases, the posterior limb of the ansa subclavian formed a loop through which the inferior thyroid artery passed (ansa thyroidea). The *Type I* MCG was found between the levels of C₅ and the superior border of C₆ vertebrae. Both *Type I* and *Type II* MCG distributed rami communicantes to C₅ and C₆ spinal nerves. *Type II* and *Type III* MCG also distributed rami to C₇ and C₈ spinal nerves.

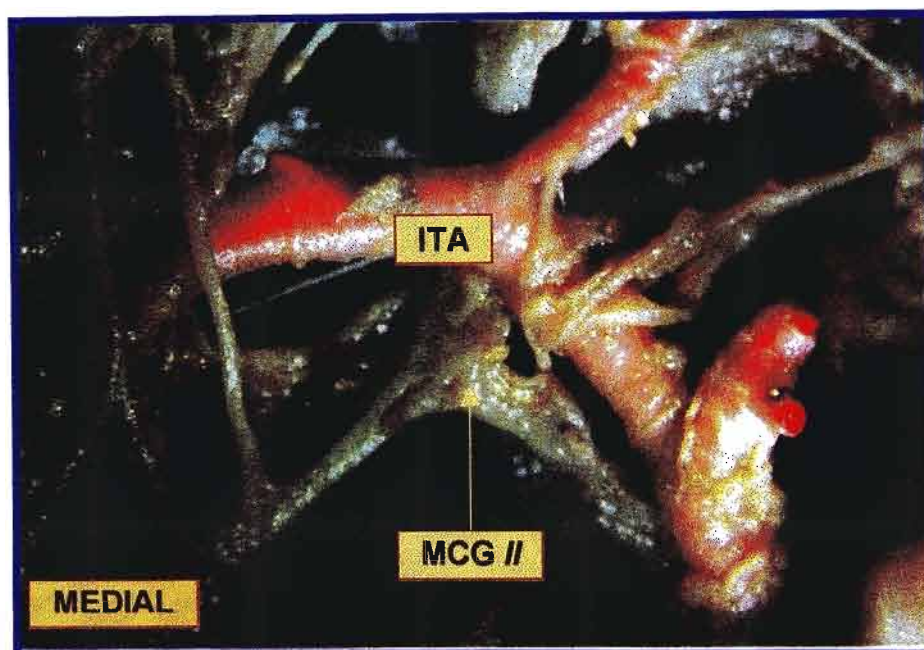


Plate 6: Anterior view of the left cervical sympathetic chain in a foetus demonstrating the relationship of the inferior thyroid artery to type II MCG

Key: ITA Inferior Thyroid Artery MCG II Type II MCG

Table 7: Incidence of MCG in foetal and adult specimens

MCG	RIGHT (n=29)			LEFT (n=29)			TOTAL (n=58)
	Foetal	Adult	Total	Foetal	Adult	Total	
Present	18 (62.1)	7 (24.1)	25 (86.2)	17 (58.6)	5 (17.2)	22 (75.9)	47 (81.1)
Absent	3 (10.3)	1 (3.4)	4 (13.8)	4 (13.8)	3 (10.3)	7 (24.1)	11 (18.9)
Single	11 (37.9)	5 (17.2)	16 (55.2)	12 (41.4)	4 (13.8)	16 (55.2)	32 (55.2)
Double	7 (24.1)	2 (6.9)	9 (31.0)	5 (17.2)	1 (3.4)	6 (24.1)	15 (25.9)
Type I	9 (31.0)	2 (6.9)	11 (37.9)	4 (13.8)	1 (3.4)	5 (17.2)	16 (27.6)
Type II	10 (34.5)	5 (17.3)	15 (51.7)	11 (37.9)	1 (3.4)	12 (41.4)	27 (46.6)
Type III	5 (17.3)	2 (6.9)	7 (24.1)	7 (24.1)	5 (17.3)	12 (41.4)	19 (32.8)

The *Type II* MCG was found to have a higher incidence (46.6%) than the *Type I* MCG (27.6%) and *Type III* (32.8%), as indicated in Table 7. Of the 15 chains in which a double MCG was found, in 8 sides [13.8%: right, 5 (8.6%); left, 3 (5.2%)] *Types I* and *II* MCG were present; in 4 sides [6.9%: right, 2 (3.5%); left, 2 (3.5%)] *Types I* and *III* MCG were present; while in 3 sides [5.2%: right 1(1.7%); left 2 (3.5%)] *Types II* and *III* were present. Therefore, a total of 62 MCG was found [right, 33; left, 29] [figures 27 and 28].

Due to the variations of MCG, different patterns of cervical chains were observed in the 58 chains studied:

- I. **Two ganglia:** 11 sides (18.9%): These comprised 11 cervical chains with ICG or CTG only [figures 24 and 27];

II. **Three ganglia:** 32 sides (55.2%): These comprised 32 cervical chains with SCG and ICG/CTG and only one of the following:

- a. *MCG Type I:* 4 chains [6.9%: right, 4 (6.9%); left, 0] [*figures 24 and 27*]
- b. *MCG Type II:* 16 chains [27.6%: right, 9 (15.5%); left, 7 (12.1%)] [*figures 24 and 27*]
- c. *MCG Type III:* 12 chains [20.7%: right, 4 (6.9%); left, 8 (13.8%)] [*figures 24 and 28*]

III. **Four ganglia:** 15 sides (25.9%). These comprised 12 cervical chains with SCG and ICG/CTG and only one of the following combinations:

- a. *MCG Types I and II:* 8 chains [13.8%: right, 5 (8.6%); left, 3 (5.2%)] [*Figures 24 and 28*]
- b. *MCG Types III and I:* 4 chains [6.9%: right, 2 (3.5%); left, 2 (3.5%)] [*figures 24 and 28*]
- c. *MCG Types II and III:* 3 chains [right, 1 (1.7%) and left, 2 (3.5%)] [*figures 24 and 28*]

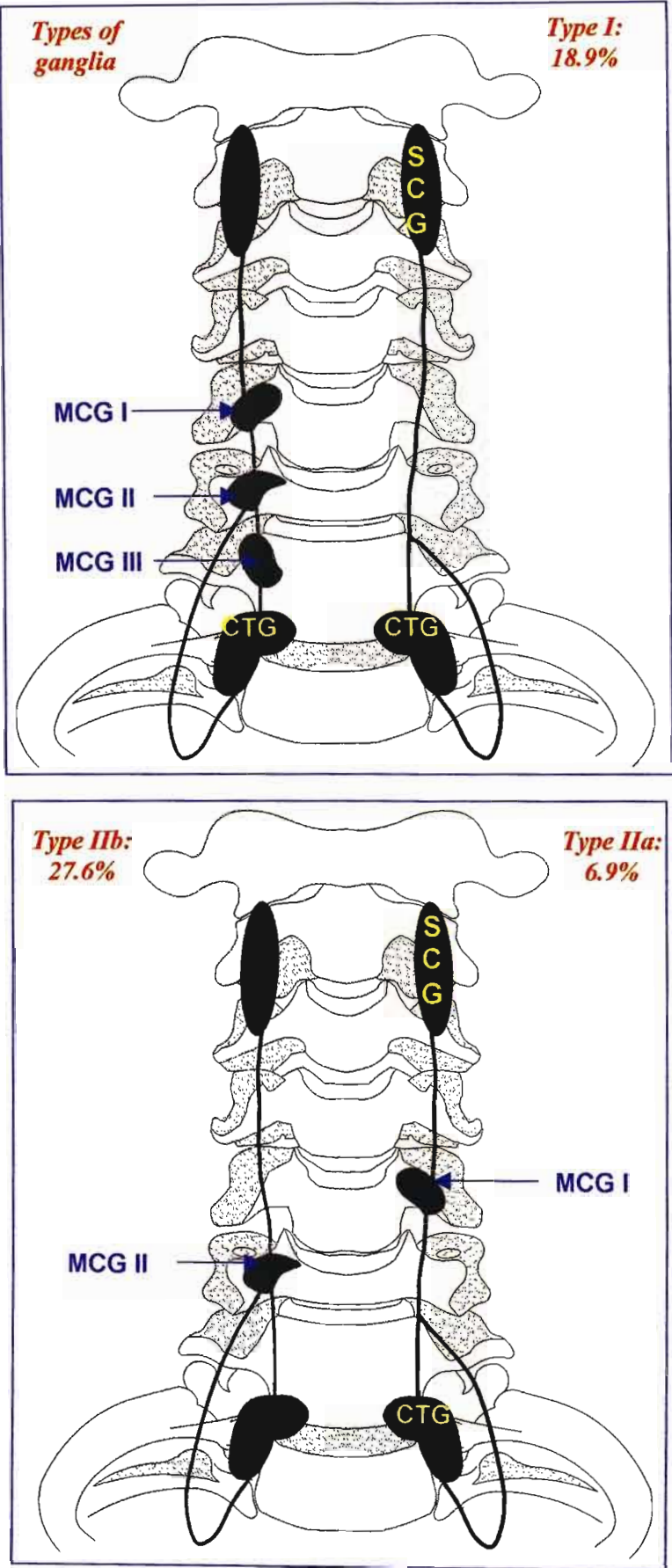


Figure 27: Diagrammatic illustration cervical chain Types I, IIa and IIb

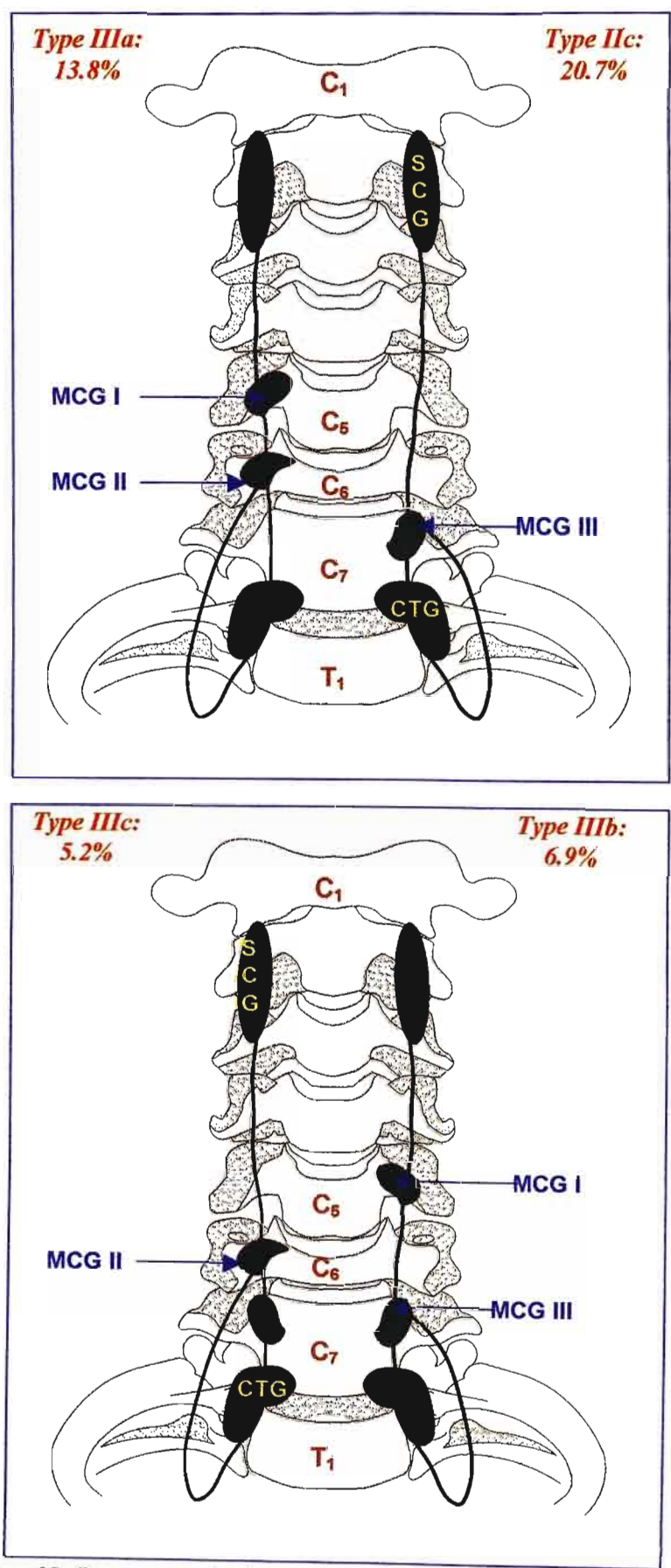


Figure 28: Diagrammatic illustration cervical chain Types IIIc, IIIa, IIIb and IIIc

Two shapes for MCG were documented:

- *Crescentric*: $\frac{47}{62}$ (75.8%); [*Type I*: $\frac{10}{62}$ MCG (16.1%): right, $\frac{7}{33}$ (21.2%); left $\frac{3}{29}$ (10.3%); *Type II*: $\frac{18}{62}$ (29.0%): right, $\frac{10}{33}$ (30.3%); left $\frac{8}{29}$ (27.6%); *Type III*: $\frac{13}{62}$ (20.8%): right, $\frac{4}{33}$ (12.1%); left $\frac{9}{29}$)].
- *Ovoid*: $\frac{15}{62}$ (24.2%); [*Type I*: $\frac{6}{62}$, 9.7%: right, $\frac{4}{33}$ (12.1%); left $\frac{2}{29}$ (6.9%); *Type II*: $\frac{9}{62}$, 14.5%: right $\frac{5}{33}$ (15.2%); left $\frac{4}{29}$ (13.8%); *Type III*: $\frac{6}{62}$, 9.7%: right, $\frac{2}{33}$ (6.1%); left $\frac{4}{29}$ (13.8%)].

In the adult specimens, the mean distance from the lower pole of SCG to the upper pole of the *Type I* MCG, *Type II* MCG and *Type II* MCG was 22.4mm, 55.2mm and 64.4mm, respectively [figure 29].

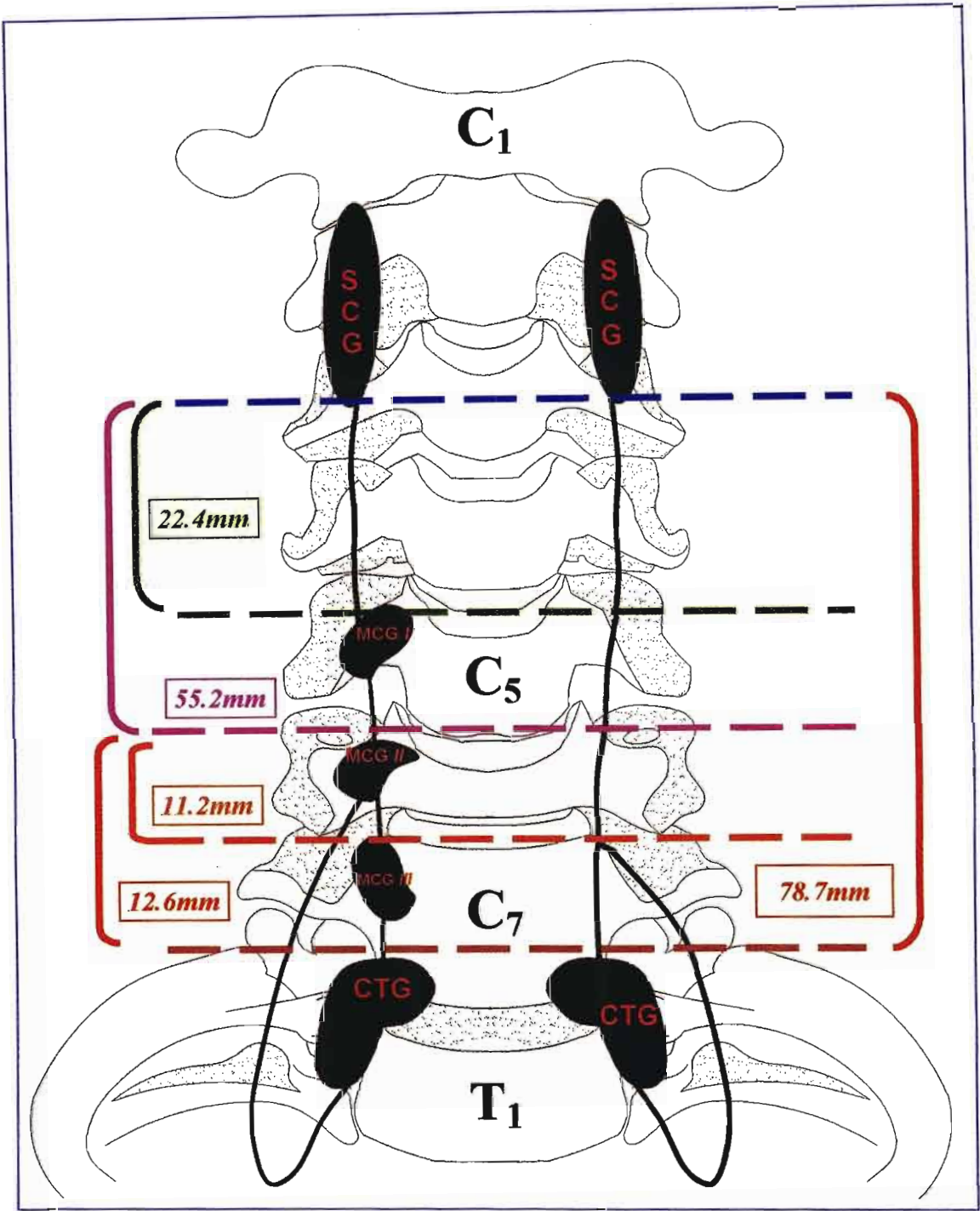


Figure 29: Illustration of mean distance of MCG (Types I & II) and CTG from SCG (adult)
Key: SCG: Superior Cervical Ganglion; MCGI: Type I MCG; MCGII: Type II MCG; CTG: Cervico-thoracic ganglion; C: Cervical vertebral; T: Thoracic vertebra

Table 8: Range of dimensions of Types I, II and III MCG in the adult specimens

MCG	Type I		Type II		Type III	
	<i>Min-Max</i>	<i>Mean (SD)</i>	<i>Min-Max</i>	<i>Mean (SD)</i>	<i>Min-Max</i>	<i>Mean (SD)</i>
Length (mm)	1.91-9.81	6.75 (4.24)	2.27-9.97	7.87(2.8)	3.54-9.86	8.54(2.24)
Width (mm)	2.21-3.67	3.17(0.83)	2.29-5.44	3.73(1.01)	2.53-5.76	3.84(1.10)

Note: The mean lengths and widths are indicated in ().

The adult dimensions of *Type I*, *II* and *III* MCG are recorded in Table 8. The mean for the length and width of MCG were, respectively: Type I MCG: 6.75±4.24mm, 3.17±0.83mm; Type II: 7.87±2.81mm, 3.73±1.01mm and Type III MCG: 8.54±2.24mm, 3.84±1.10mm. There was no significant difference in the size of the different types of MCG in the adult [*p-values*: Length: Type I vs. Type II, 0.65; Type I vs. Type III, 0.39; Type II vs. Type III, 0.64; Width: Type I vs. Type II, 0.46; Type I vs. Type III, 0.38; Type II vs. Type III, 0.86]

The range for the length of MCG in the foetal specimens were: Type I: 1.0-4.37 ± 0.88mm (mean, 3.92mm); Type II: 1.17-4.53 ± 0.78mm (mean, 3.83mm); Type III: 1.09-4.46 ± 0.99mm (mean, 3.84mm). There was no significant difference in length of the different types of MCG in the foetal specimens [*p-values*: Type I vs. Type II, 0.77; Type I vs. Type III, 0.85; Type II vs. Type III, 0.98].

4.2.4 INFERIOR CERVICAL GANGLION (ICG)

In the 58 cervical chains investigated, an unfused ICG was present in 9 chains (15.5%) [*Table 3, Figure 22*]. ICG was unilaterally present in 7 cadaveric specimens [24.1%: right, 4 (13.8 %) and left, 3 (10.5%) and in only one foetal cadaver was the ICG present bilaterally (3.5%).

ICG, typically ovoid in shape, was located at the level of the lower border of C₇ vertebra or on the disc between C₇ and T₁ vertebrae. The origin of the vertebral artery, from the subclavian artery, was located immediately posterior to ICG. [*Plate 7*]

The range of the length and width of the adult ICG was, respectively: 6.37-14.11 ± 3.38mm (mean, 9.86mm); 2.13-5.16 ± 3.66mm (mean, 3.66mm).

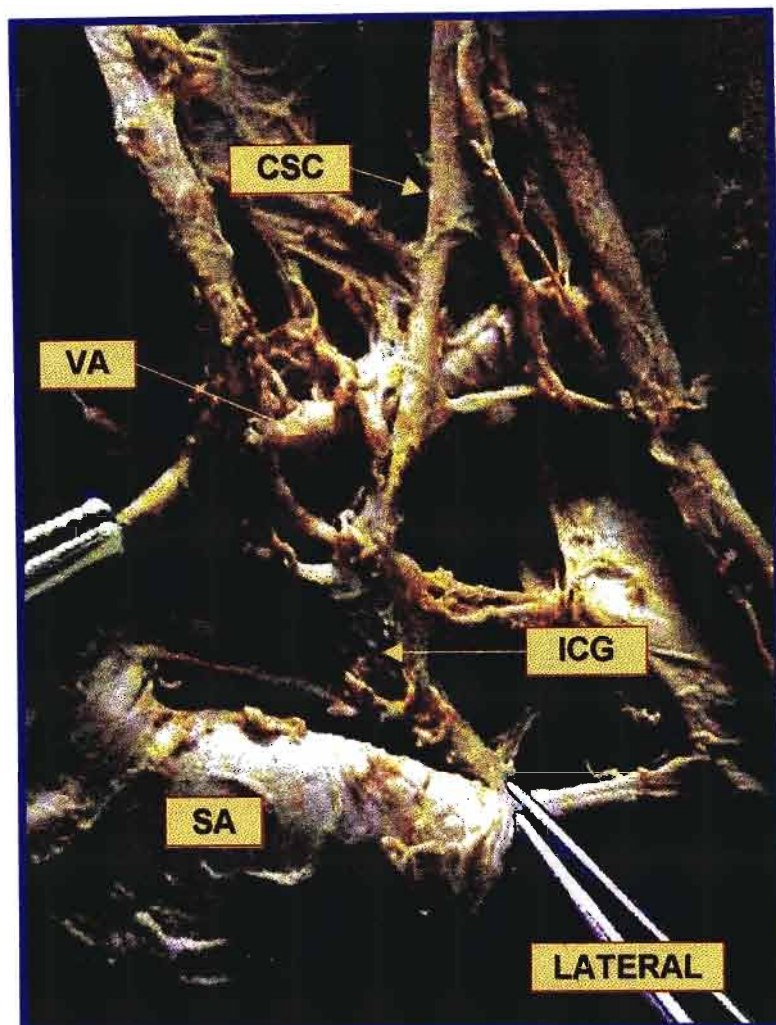


Plate 7: Antero-lateral view of the left cervical sympathetic chain demonstrating the ICG in an adult specimen (Note: The vertebral artery crossing, from medial to lateral, posterior to the chain)

Key:

ICG	Inferior Cervical Ganglion	SA	Subclavian Artery
VA	Vertebral Artery	CSC	Cervical Sympathetic Chain

4.2.5 CERVICO-THORACIC GANGLION (CTG)

In the 58 cervical chains investigated, the ICG and 1st thoracic ganglion was fused in 49 cases (84.5%) to form the CTG, as indicated in Table 3 [figure 25]. It was present bilaterally in 19 specimens (65.5%).

CTG was, typically, located on the infero-lateral border of C₇ vertebra, the supero-lateral border of T₁ vertebra, the neck of the 1st rib and the adjacent part of the 1st intercostal space [figure 30]. However, in 17 of the 38 foetal specimens in which CTG was identified, it was located only on the neck of the 1st rib, the lateral surface of the body of the 1st thoracic vertebra and the adjacent part of the 1st intercostal space. Parietal pleural covered the anterior surface of the ganglion.

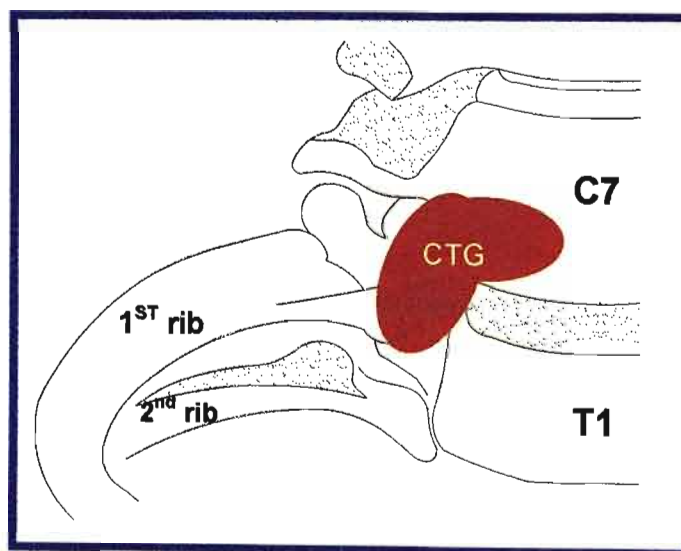


Figure 30: Illustration of location of CTG

The lateral relations of CTG were, from medial to lateral: the supreme intercostal vein, the superior intercostal artery and the T₁ root of the brachial plexus [Plate 8]. The

subclavian artery arched over the superior border of CTG immediately deep to the upper pole of CTG was the C₈ root of the brachial plexus.

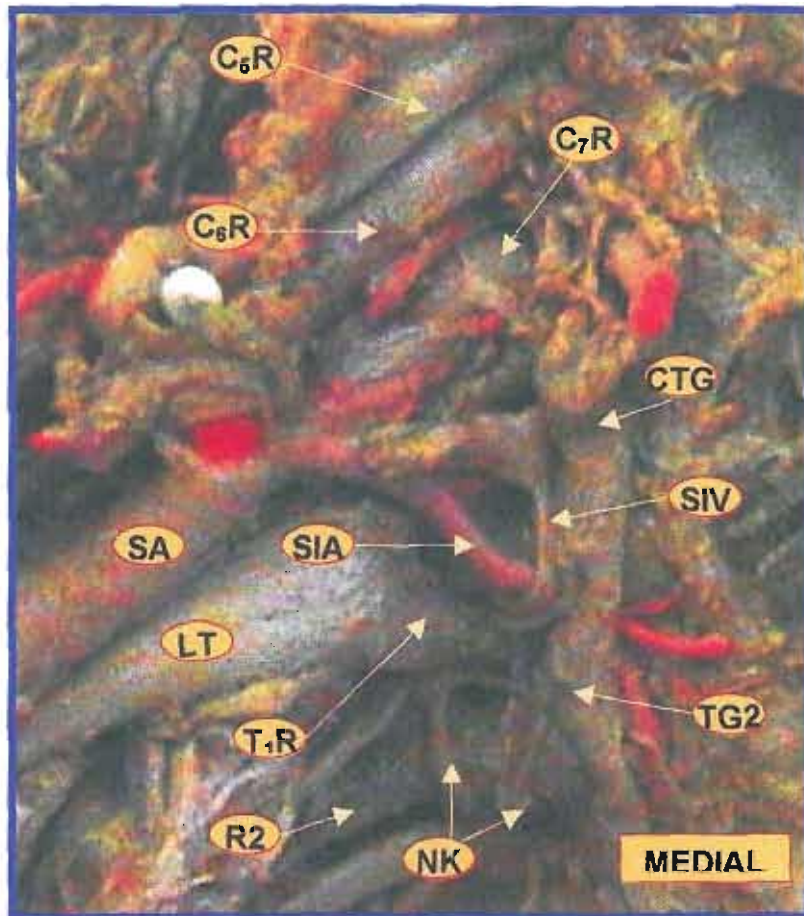


Plate 8: Antero-lateral view of right cervical sympathetic chain demonstrating the relations of CTG in a foetus. (Note: origin of the superior intercostal artery)

KEY:

CTG	Cervicothoracic Ganglion	SIA	Superior Intercostal Artery
SA	Subclavian Artery	SIV	Supreme Intercostal Vein
C _{5,6,7} R	C _{5,6,7} Brachial Plexus Roots	T ₁ R	T ₁ Brachial Plexus Root
TG2	2 nd Thoracic Ganglion	R2	2 nd Rib
NK	Nerves of Kuntz	LT	Lower Trunk of Brachial Plexus

The cervical sympathetic chain continued into the cervical region from the superior pole of CTG. The mean distance of CTG from the lower pole of SCG, *Type I* MCG, *Type II* MCG and *Type III* MCG respectively, was: 78.7mm, 53.2mm, 11.6mm and 4.1mm [figure 29].

Three different shapes of CTG were differentiated, viz. spindle, dumbbell and an inverted 'L' shape, as indicated in Table 9. The dumbbell and inverted 'L' shapes demonstrated a definite 'waist' (i.e. a macroscopically visible union of the ICG and T1 components of the CTG). This definite waist was, therefore, present in ³⁵/₄₉ CTG (71.4%).

Table 9: Incidence of different shapes of CTG




SHAPE	SKETCH	RIGHT (24)		LEFT (n=25)		TOTAL (n=49)
		Foetal (n=19)	Adult (n=5)	Foetal (n=19)	Adult (n=6)	
Spindle		5 (26.3%)	2 (40.0%)	4 (21.1%)	3 (50.0%)	14 (28.6%)
Dumbbell		6 (31.6%)	1 (20.0%)	6 (31.6%)	1 (16.7%)	14 (28.6%)
Inverted 'L'		8 (42.1%)	2 (40.0%)	9 (42.9%)	2 (33.3%)	21 (42.8%)

Table 10: Range of dimensions of CTG in the adult specimens

	RIGHT		LEFT	
	Min-Max	Mean (SD)	Min-Max	Mean (SD)
Length (mm)	15.08-21.25	17.92 (2.59)	9.48-20.95	15.10 (3.95)
Width (mm)	3.35-10.18	6.84 (2.90)	4.66-9.03	6.45 (1.98)

Note: Length, $p=0.26$; Width, $p=0.98$

The mean length and width of CTG in the adult specimens (Table 10) was 16.51mm and 6.65mm, respectively. There was no statistically significant difference in the length and width of the right and left sides of the adult CTG [*p* value: *length*, 0.26; *width*, 0.98].

The length of the foetal CTG ranged between: right, 4.67-10.32 \pm 1.97mm (mean, 7.22mm) and left, 4.88-11.28 \pm 2.06mm (mean, 7.50mm). There was no statistically significant difference between the right and left sides (*p*=0.65).

Numerous branches radiated out from CTG. Of the lateral somatic branches to the brachial plexus, rami communicantes to the ventral rami of C₈ and T₁ spinal nerves were consistent while rami communicantes to C₆ and C₇ spinal nerves varied [Plate 9].

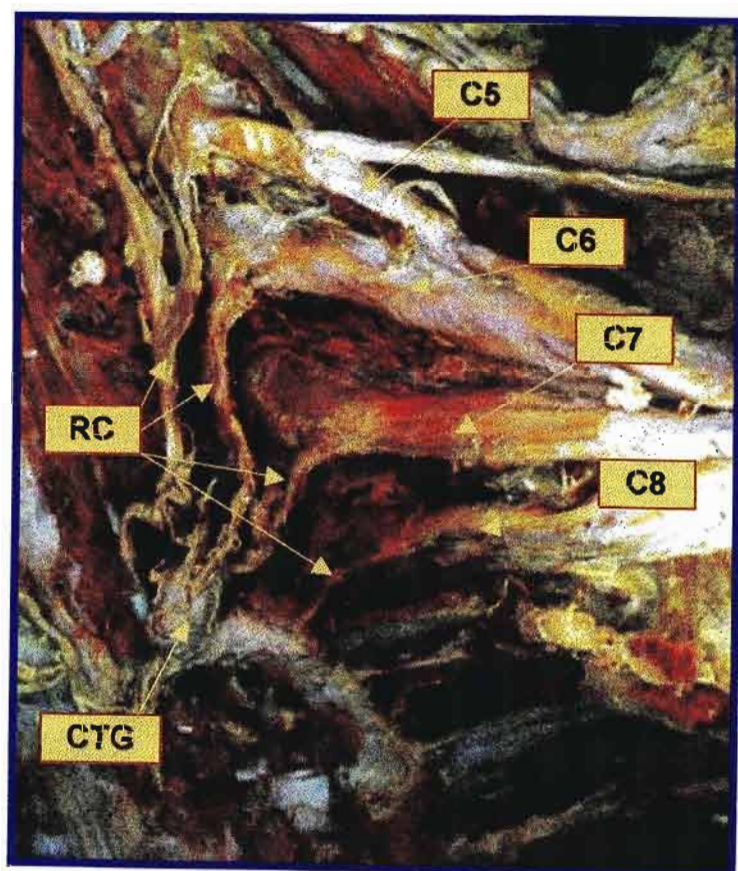


Plate 9: Antero-lateral view of left cervical chain demonstrating the rami communicantes to the brachial plexus in an adult

Key:

CTG Cervico-thoracic Ganglion
RC Rami Communicantes
C5,6,7,8 Cervical Ventral Rami

The ansa subclavian (AS)

The AS was constantly present in all specimens [Plates 10 and 11]. It comprised anterior and posterior limbs that joined the CTG/ICG to the Type II MCG, when present. When Type II MCG was absent AS attached superiorly to the Type III MCG. When both Type II and III MCG were present AS always attached to the Type II MCG and when both were absent it attached directly to the cord of the cervical sympathetic chain. The ansa contributed to the plexus on the subclavian artery.

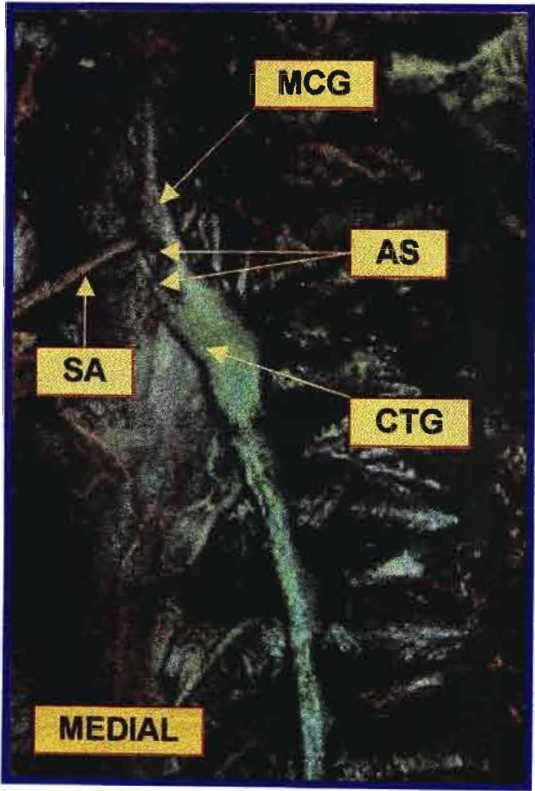


Plate 10: Antero-lateral view of left sympathetic chain in a foetus, demonstrating the formation of the ansa subclavian (Note: Type III MCG)

Key:

MCG	Middle Cervical Ganglion
CTG	Cervicothoracic Ganglion
SA	Subclavian Artery
AS	Ansa Subclavian

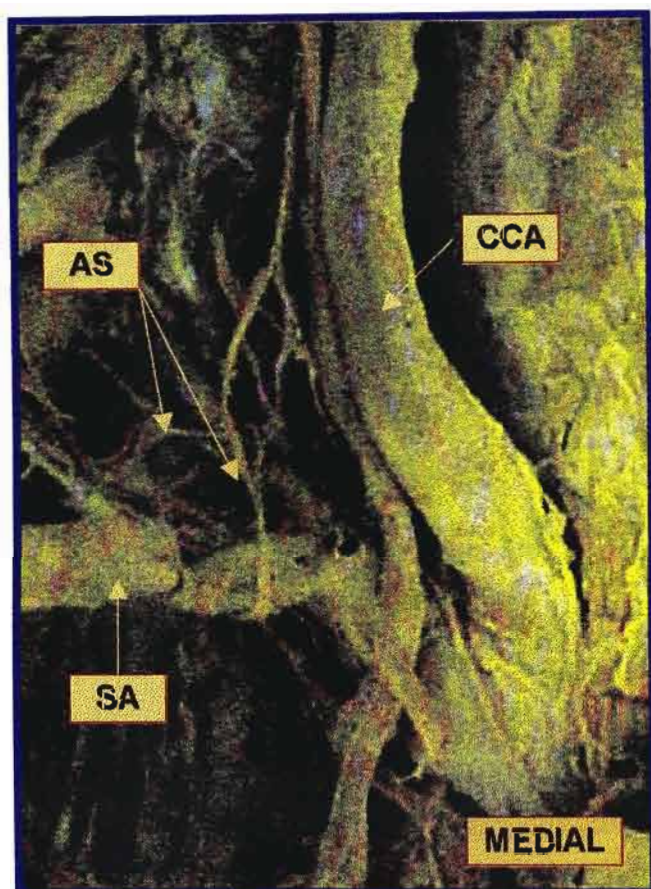


Plate 11: Antero-lateral view of Cervical Sympathetic Chain in an adult demonstrating the formation of the ansa subclavian

Key:

CCA Common Carotid Artery
SA Subclavian Artery
AS Ansa Subclavian

4.3 THORACIC SYMPATHETIC CHAIN

The thoracic sympathetic chains in 17 adult [right, 13 sides; left, 16 sides (4 right and 1 left side were excluded due to pleural adhesions)] and 28 fetuses (right, 28 sides; left, 28 sides) were examined [n=85: right, 41; left, 44].

4.3.1 COURSE AND RELATIONS

The thoracic sympathetic chain commences at the CTG or ICG and is continuous with the cervical sympathetic chain posterior to the subclavian arteries. Medial to the chain on the right side is the azygos vein and on the left side, the hemiazygos. The thoracic sympathetic chain lies posterior to parietal costal pleura. The lateral branches consisted of the rami communicantes to the intercostal nerves (ventral rami) while the medial branches comprised of numerous visceral rami, including the cardiac rami, splanchnic nerves and vascular branches [*Plate 12*].

The upper part of the chain (up to T6 vertebra) is located on the neck of the ribs, against the lateral surface of the vertebral bodies and the intervening intercostal space. The lower part of the chain lies on the vertebral bodies and the intervening intercostal space. At the level of the diaphragm, the chain deviates medially, to lie on the bodies of T₁₁-T₁₂ vertebra as it pierces the diaphragm.



Plate 12: Antero lateral view of right thoracic sympathetic chain demonstrating the medial deviation of the chain inferiorly.

Key:
 CTG Cervicothoracic Ganglion
 TSC Thoracic Sympathetic Chain
 GSN Greater Splanchnic Nerve
 TG Thoracic Ganglion

4.3.2 THORACIC GANGLIA (TG)

The upper thoracic ganglia were, typically triangular, when unfused, with the apices directed laterally [*Plate 12*]. Macroscopically, WRC and GRC connecting to the ganglia could not be differentiated.

The ganglia of the proximal part of the sympathetic chain were located slightly below the level of the intercostal nerve, so that the rami coursed upwards to the intercostal nerve. The ganglia of the lower part of the thoracic sympathetic chain were located just above the level of the spinal nerve so that the rami coursed downwards to the intercostal nerve.

The T₁ ganglion (T₁G) was unfused in $\frac{9}{85}$ cases (10.6%) in which the thoracic sympathetic chain was investigated. In the remaining $\frac{76}{85}$ cases (89.4%), T₁G was found fused with the ICG. T₁G was located against the body of T₁ vertebra in 5 cases and on the intervertebral disc between T₁ and T₂ vertebrae in 4 cases.

The second thoracic ganglion (T₂G) was the only TG that was never fused in this series and was located:

- a.) Opposite the lower border of T₂ vertebra (i.e. below the below neck of second rib) in $\frac{66}{85}$ sides [77.6%: right, $\frac{36}{41}$ sides (87.8%); left, $\frac{30}{44}$ sides (68.2%)];
- b.) On the neck of second rib in $\frac{19}{85}$ sides [22.4%: right $\frac{5}{41}$ sides (12.3%); left, $\frac{14}{44}$ sides (31.8%)].

T₃G-T₉G showed a regular pattern, being located at the neck of the rib below and the adjacent part of the intercostal space. Fusion of ganglia was noted at varying levels.

Fusion of ganglia

Three types of ganglia were observed:

- a.) *A ganglion connecting to only one spinal nerve*
- b.) *A ganglion with connections to two spinal nerves*
- c.) *A ganglion with connections to three or more spinal nerves*

In accordance with the studies of Pick (1957; 1970), types *a.* and *c.* are regarded as fused ganglia. The number of ganglia present in the thoracic sympathetic chain ranged from 8 to 11, as indicated in Table 11. The decrease in the number of ganglia was due to fusion. The incidence of fused ganglia at each level is indicated in Table 12 [figure 28] [Plate 13].

Table 11: Number of thoracic ganglia

No.	RIGHT (n=41)			LEFT (n=44)			TOTAL
	TG	Foetal	Adult	TOTAL	Foetal	Adult	TOTAL
8		3 (7.3)	0	3 (7.3)	5 (11.4)	5 (11.4)	10(22.8)
9		4 (9.8)	4 (9.8)	8 (19.5)	9 (20.5)	5 (11.4)	14 (31.9)
10		21 (51.2)	8 (19.5)	29 (70.7)	12 (27.3)	6 (13.6)	18 (40.9)
11		0	1 (2.4)	1 (2.4)	1 (2.3)	1 (2.3)	2 (4.6)
12		0	0	0	0	0	0

Note: % in (); n=85 (right, 41: foetal 28, adult 13; left, 44: foetal 28, adult 16)

851010

Table 12: Prevalence of fused ganglia

Fused	RIGHT (n=41)			LEFT (n=44)			TOTAL (n=85)
TG	Foetal	Adult	TOTAL	Foetal	Adult	TOTAL	
3-4	9 (21.9)	4 (9.8)	13(31.7)	3 (6.8)	0	3 (6.8)	16 (18.8)
4-5	5 (12.2)	2 (4.9)	7(17.1)	8 (18.2)	4 (9.1)	12 (27.3)	19(22.4)
5-6	16 (39.0)	4 (9.8)	20(48.8)	4 (9.1)	1 (2.3)	5(11.4)	25(29.4)
6-7	4 (9.8)	3 (7.3)	7 (17.1)	14 (31.8)	4 (9.1)	18 (40.9)	25(29.4)
7-8	5 (12.2)	3 (7.3)	8 (19.5)	9 (20.5)	3 (6.8)	12 (27.3)	20(23.5)
8-9	1 (2.4)	0	1(2.4)	4 (9.1)	1 (9.1)	5(11.4)	6(7.1)
9-10	12 (29.3)	8 (19.5)	20 (48.8)	16 (36.4)	9 (20.5)	25 (56.8)	45(52.9)
10-11	5 (12.2)	6 (14.6)	11 (26.8)	8 (18.2)	10 (22.7)	18(40.9)	29(34.1)
11-12	10 (24.4)	9 (22.0)	19(46.3)	12 (27.3)	6 (13.6)	18 (40.9)	37(43.5)

Note: % in (); n=85 (right, 41: foetal 28, adult 13; left, 44: foetal 28, adult 16) Key: -: fused ganglia

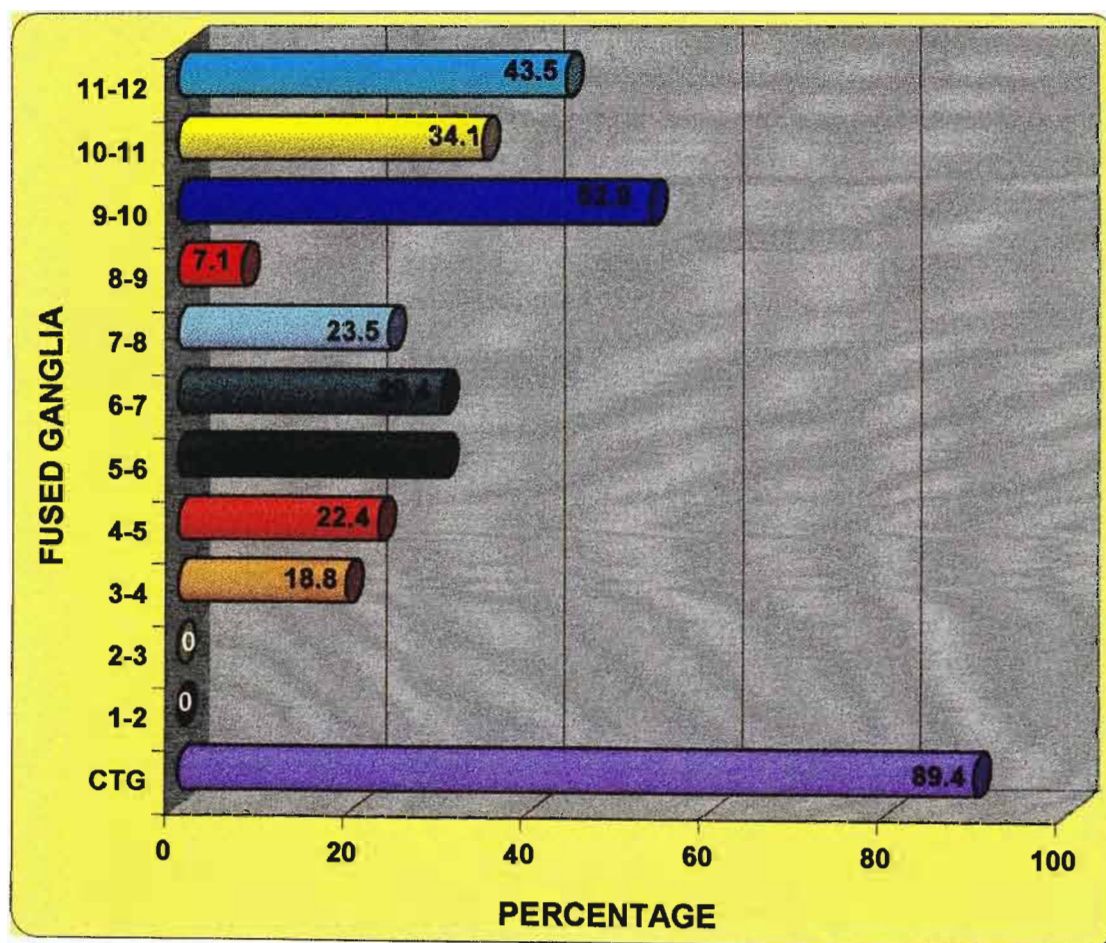


Figure 31: Summary of incidence of fused ganglia

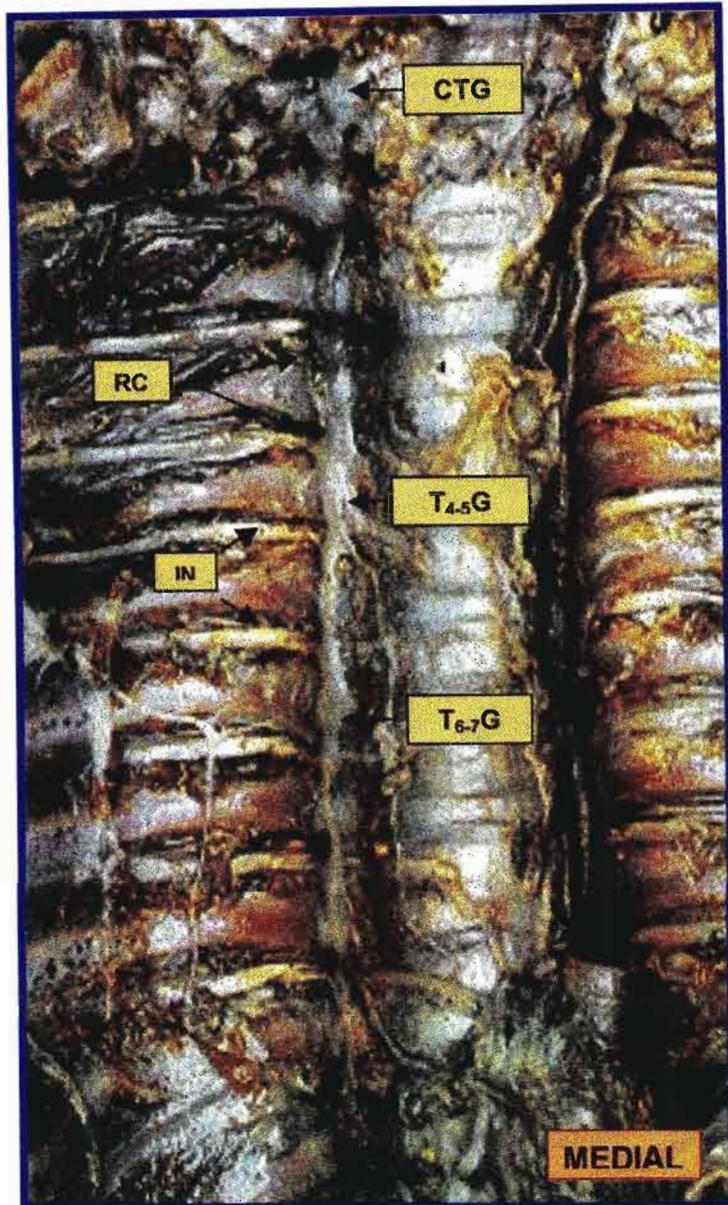


Plate 13: Antero-lateral view of right thoracic sympathetic chain demonstrating fused ganglia

Key:

CTG	Cervicothoracic Ganglion
RC	Rami Communicantes
IN	Intercostal Nerve
T4-5G	Fused T4 and T5 Ganglia
T6-7G	Fused T6 and T7 Ganglia

T₁₀G to T₁₂G showed the most variation in incidence. Here the fusion of ganglia was frequent, with all 3 ganglia being seldom present. These ganglia also inclined medially and so were located on the vertebral body of T₁₁ and T₁₂.

Rami arose from the anterior, lateral and posterior surfaces of the ganglia and either ascended or descended to reach the intercostal nerve. Rami were also distributed to the antero-lateral aspect of the vertebral bodies and intervertebral disc [Plate 14].

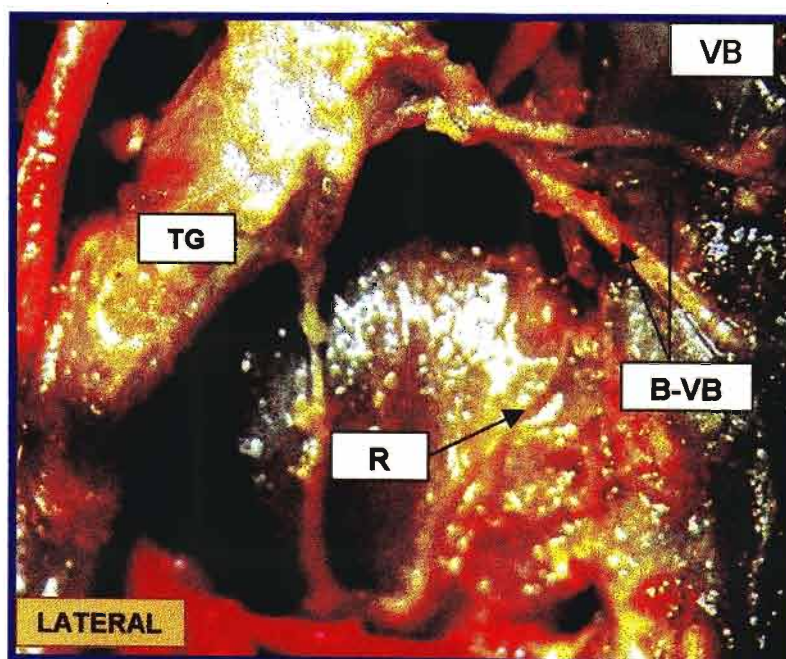


Plate 14: Anterior view of thoracic ganglion demonstrating the rami to the intervertebral disc and vertebral body

Key:

TG	Thoracic Ganglion
VB	Vertebral Body
B-VB	Rami to Vertebral Body & Intervertebral Disc
R	Rib

4.4 CARDIAC SYMPATHETIC NERVES

The cervical and thoracic cardiac rami were recorded bilaterally in 58 sides [right, 29 (foetal, 21; adult, 8); left, 29 (foetal, 21; adult, 8)].

Cardiac sympathetic rami were differentiated according to their origins from the cervical and thoracic parts of the sympathetic chain into three groups: cervical cardiac sympathetic rami (CCR), cervicothoracic cardiac rami (CTCR) and thoracic cardiac rami (TCR). The origin of the cardiac rami from the sympathetic chain was found to be highly variable and asymmetrical. These results are summarized in Table 13 and Figure 32.

Table 13: Summary of the origin and incidence of cardiac sympathetic nerves

RAMUS	INDICENCE (%)	ORIGIN (%)	
		GANGLIONIC	INTERGANGLIONIC
<i>SCCR</i>	100	53.4	46.6
<i>MCCR</i>	87.9	70.7	17.2
<i>ICCR</i>	77.8	44.5	22.3
<i>CTCR</i>	100	83.7	16.3
<i>TCR₁</i>	88.8	66.6	22.2
<i>TCR₂</i>	84.5	50.0	34.5
<i>TCR₃</i>	70.7	43.1	27.6
<i>TCR₄</i>	82.9	53.5	29.3
<i>TCR₅</i>	60.4	34.5	25.9

Key: SCCR: Superior Cervical Cardiac Ramus, MCCR: Middle Cervical Cardiac Ramus, CTCR: Cervico-thoracic Cardiac Ramus, TCR: Thoracic cardiac Ramus

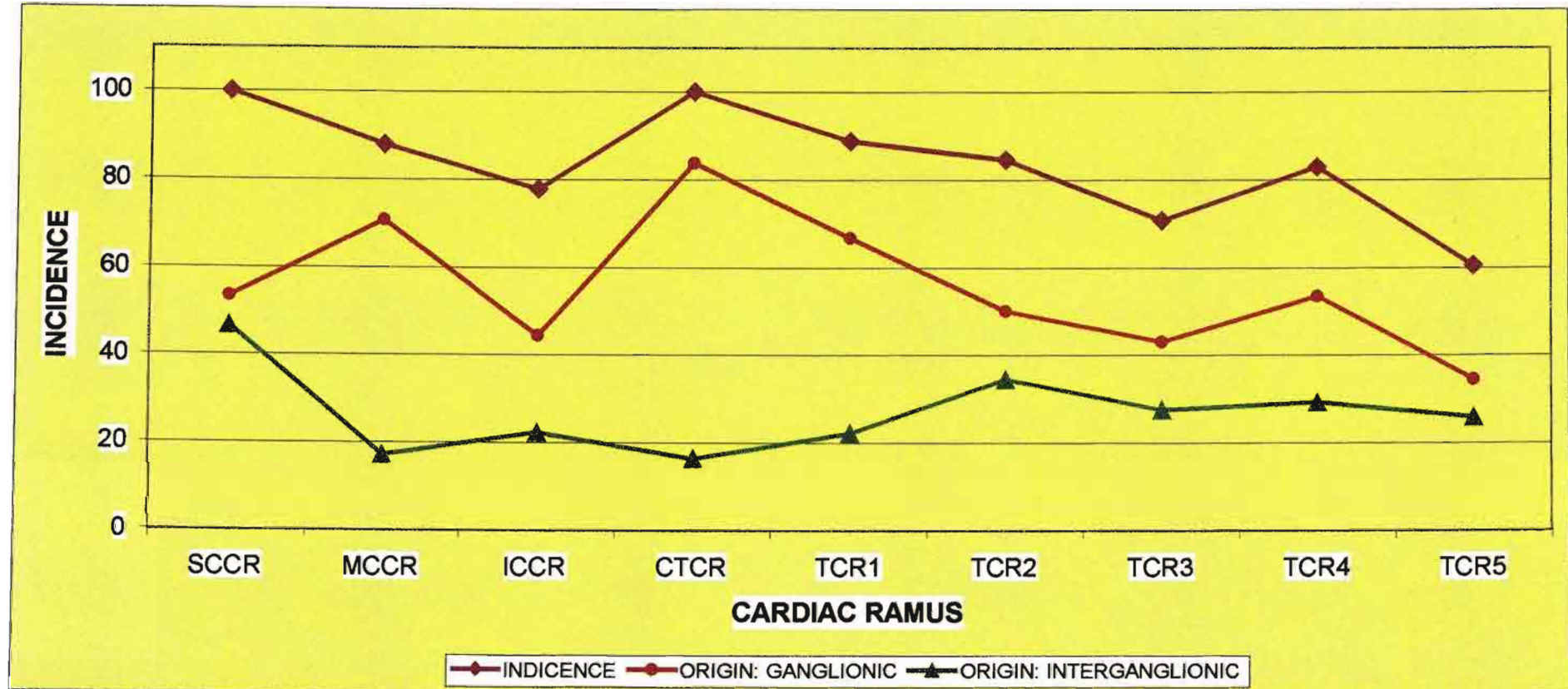


Figure 32: Summary of the incidence and origin of cardiac sympathetic nerves

4.4.1 CERVICAL CARDIAC SYMPATHETIC RAMI (CCR)

The 3 cervical cardiac rami were recorded from the cervical sympathetic chain: superior cervical cardiac ramus (SCCR), middle cervical cardiac ramus (MCCR) and inferior cervical cardiac ramus (ICCR).

i. Superior Cervical Cardiac Ramus

The incidence of SCCR was 100%, as indicated in Table 14. SCCR arose from the SCG [Plate 15] in $^{31}/_{58}$ sides [53.5%: right, 55.2% ($^{16}/_{29}$ sides); left, 51.7% ($^{15}/_{29}$ sides)]. The origin from the interganglionic segment of the chain, below the ganglion, was observed in $^{27}/_{58}$ sides [46.6%: right 44.8% ($^{13}/_{29}$ sides); left 48.3% ($^{14}/_{29}$ sides)] [figure 33]. In these, the distance from the lower pole of SCG to the origin of SCCR ranged from 4.8mm-19.3mm (mean distance: 17.3mm).

Table 14: Incidence and origin of SCCR

Origin	RIGHT (n=29)			LEFT (n=29)			TOTAL
	G	IG	Total	G	IG	Total	(n=58)
Foetal	13	8	21	11	10	21	42
(%)	(44.8)	(27.6)	(72.4)	(37.9)	(34.5)	(72.4)	(72.4)
Adult	3	5	8	4	4	8	16
(%)	(10.5)	(17.2)	(27.6)	(13.8)	(13.8)	(27.6)	(27.6)
TOTAL	16	13	29	15	14	29	58
	(55.2)	(44.8)	(100)	(51.7)	(48.3)	(100)	(100)

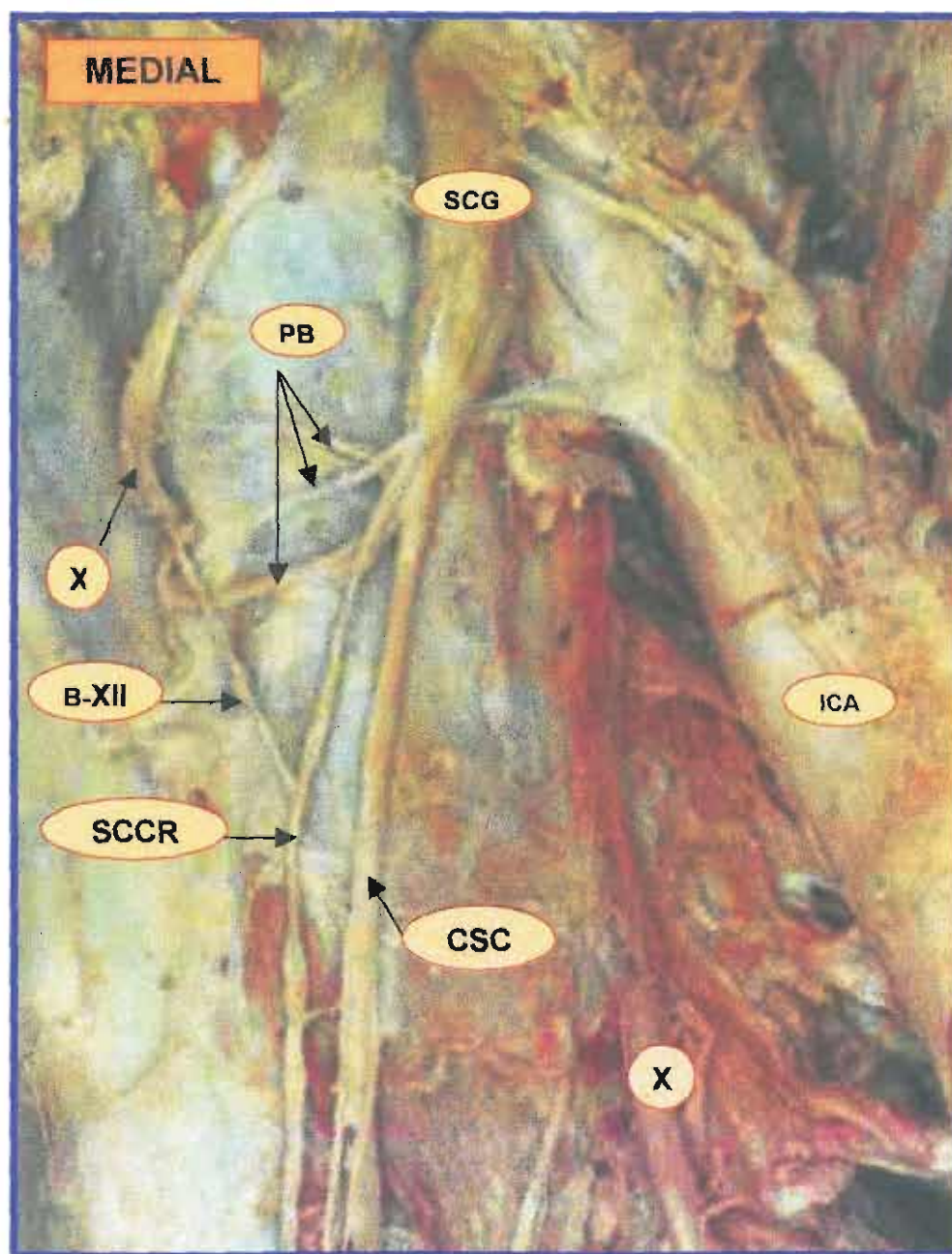


Plate 15: Antero-lateral view of left cervical sympathetic chain demonstrating the ganglionic origin of SCCR in an adult. (Note: a communicating ramus between SCCR and the Hypoglossal Nerve)

KEY:

SCG	Superior Cervical Ganglion
SCCR	Superior Cervical Cardiac Ramus
XII	Hypoglossal Nerve
B-XII	Ramus to Hypoglossal Nerve
X	Vagus Nerve
ICA	Internal Carotid Artery (reflected)
CSC	Cervical Sympathetic Chain

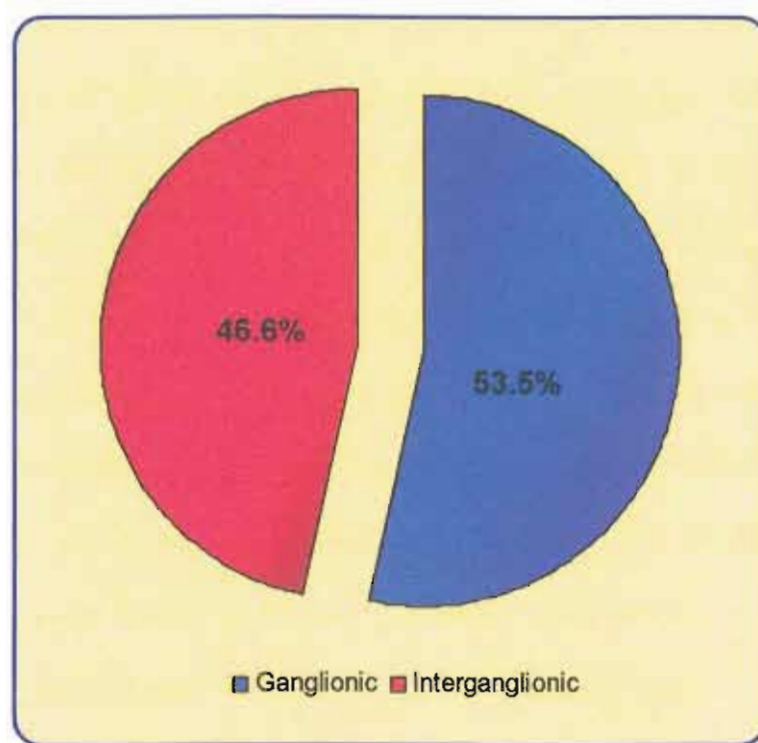


Figure 33: Incidence of origin of SCCR (n=58)

The SCCR courses down towards the heart and deviated medially. It then passes deep to the common carotid trunk. It then passes deep to the brachiocephalic trunk, on the right and the common carotid artery, on the left, and joins the cardiac plexus deep to the arch of the aorta. In $\frac{36}{58}$ sides (62.1%) the SCCR communicated with the MCCR.

ii. *Middle Cervical Cardiac Ramus*

The incidence of MCCR was $\frac{51}{58}$ sides (87.9%), as indicated in Table 13. In 41 (70.7%) sides the MCCR arose from the MCG [Table 15]. In all cases of ganglionic origin, the MCCR arose from Types II and III MCG: *Type II* MCG in $\frac{24}{58}$ sides [41.4%: right, 44.8% ($\frac{13}{29}$ sides); left, 37.9% ($\frac{11}{29}$ sides)] and *Type III* MCG [Plate 16] in $\frac{17}{58}$ sides [29.3%: right, 24.1% ($\frac{7}{29}$ sides); left, 34.5% ($\frac{10}{29}$ sides)] in [figure 34]. *Type I* MCG (present in 16 sides) did not give rise to any MCCR. *Type II* MCG (present in 27 sides) gave rise to a MCCR in 24 cases. *Type III* MCG (present in 19 sides) gave rise to MCCR in 17 cases. In only 2 cases (left) in which *Type III* MCG was present, did not give rise to a MCCR. In 3 sides in which a *Type II* MCG was present, the MCCR arose from the interganglionic segment of the chain below the ganglion. The position of this origin ranged from 3.8-4.2mm (mean distance, 3.96mm) below the lower pole of the ganglion.

The origin from the interganglionic segment of the chain, below the ganglion, was observed in $\frac{10}{58}$ sides [17.2%: right 13.8% ($\frac{4}{29}$ sides); left 20.7% ($\frac{6}{29}$ sides)] [figure 34].

The MCCR was the thickest of all the cervical cardiac rami. It passed posterior to the common carotid artery and descended behind the subclavian artery to enter the cardiac plexus on the arch of the aorta.

Table 15: Origin and incidence of MCCR

Origin	RIGHT (n=29)			LEFT (n=29)			TOTAL (n=58)
	Ganglionic	Interganglionic	Total	Ganglionic	Interganglionic	Total	
Foetal	12	3	15	17	4	21	36
(%)	(41.4)	(10.3)	(51.7)	(58.6)	(13.8)	(72.4)	(62.1)
Adult	7	1	8	5	2	7	15
(%)	(24.1)	(3.5)	(27.6)	(17.2)	(6.9)	(24.1)	(25.9)
TOTAL	19	4	23	22	6	28	51
(%)	(65.5)	(13.8)	(79.3)	(75.9)	(20.7)	(96.6)	(87.9)

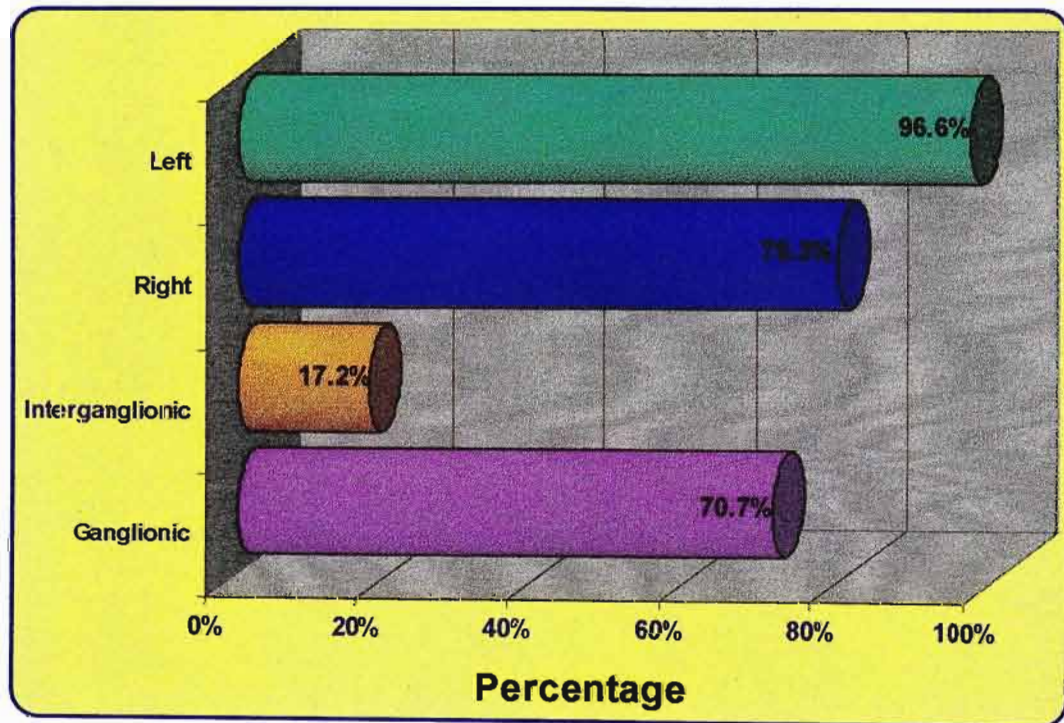


Figure 34: Incidence and origin of MCCR (n=58)

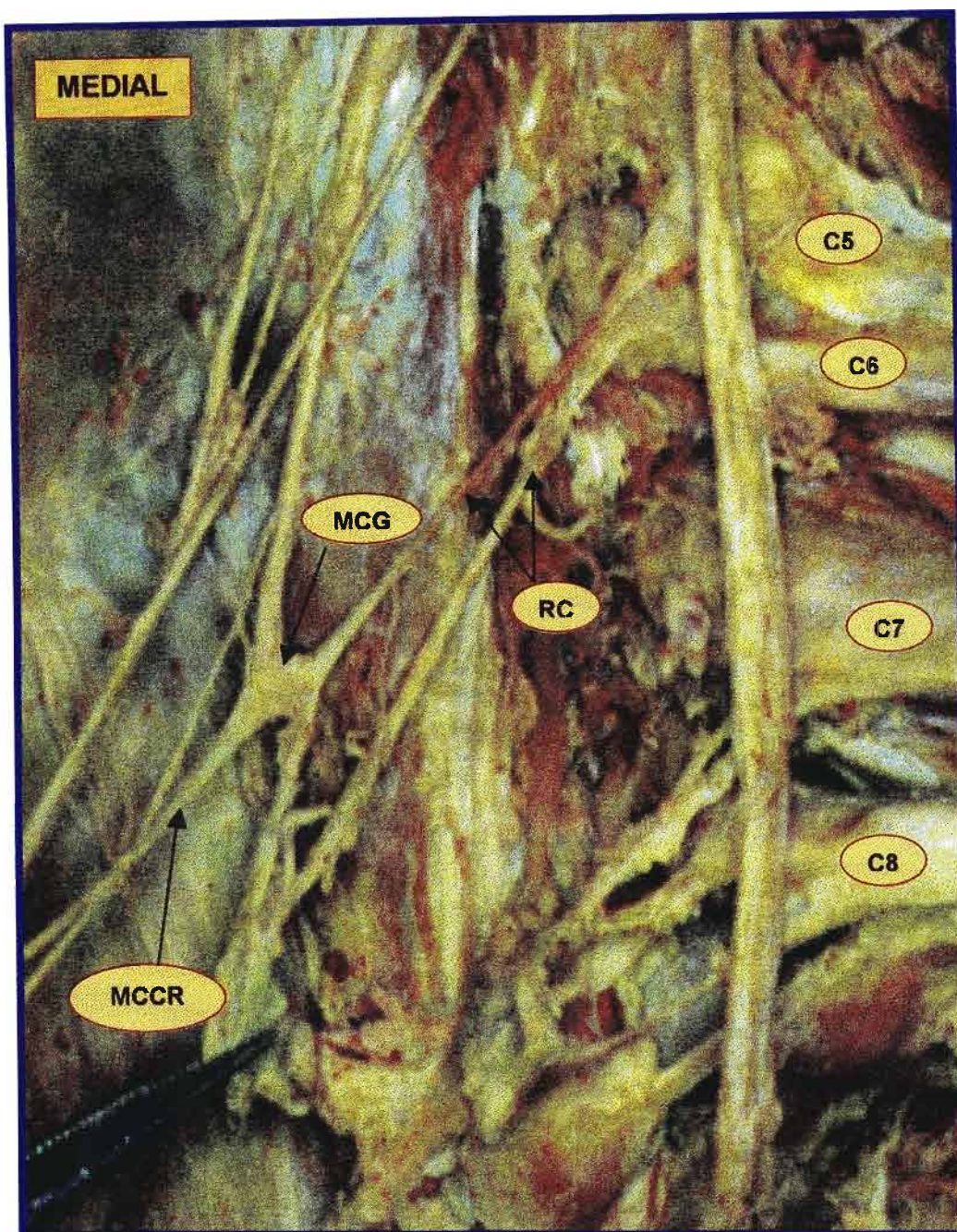


Plate 16: Antero-lateral view of left cervical sympathetic chain demonstrating the ganglionic origin of MCCR in an adult.

KEY:

MCG	Middle Cervical Ganglion Type III
MCCR	Middle Cervical Cardiac Ramus
RC	Rami Communicantes
B-XII	Ramus to Hypoglossal Nerve
C5, 6,7,8	Cervical Spinal Nerves (ventral rami)

4.4.2 CERVICO-THORACIC CARDIAC RAMUS (CTCR)

Due to the low incidence of an unfused ICG (⁹/₅₈ sides: 15.5%), the ICCR and CTCR will be considered together. The cardiac rami arising from the ICG are referred to as the ICCR and the CTG are regarded as the CTCR. ICCR ‘proper’ (i.e. ICCR arising from an unfused ICG) could only be investigated in 9 sides (5 right and 4 left) due the low incidence of ICG documented in this study.

Table 16: Origin and incidence of ICCR

Origin	RIGHT (n=5)			LEFT (n=4)			TOTAL (n=9)
	G	IG	Total	G	IG	Total	
Foetal (%)	1 (20)	1 (20)	2 (40)	1 (25)	0 (0)	1 (25)	3 (33.3)
Adult (%)	2 (40)	0 (0)	2 (40)	1 (25)	1 (25)	2 (50)	4 (44.5)
TOTAL (%)	3 (60)	1 (20)	4 (80)	1 (25)	1 (25)	3 (75)	7 (77.8)

Key: G= ganglionic origin; IG=interganglionic origin

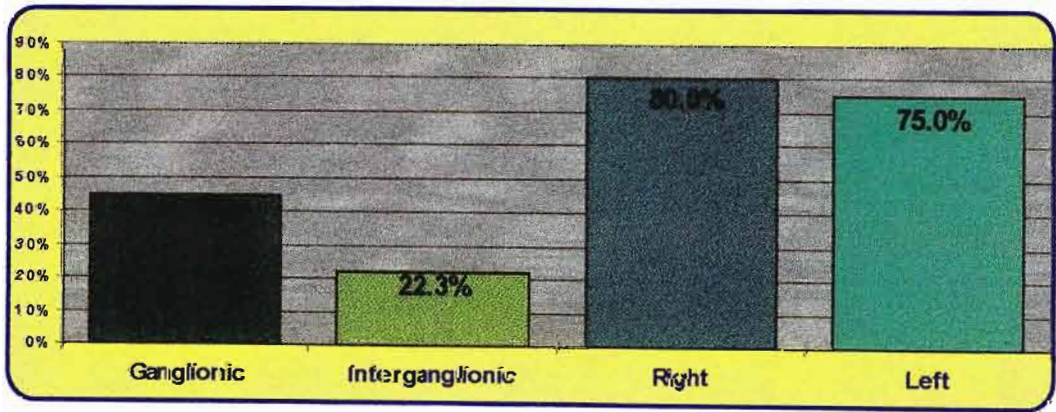


Figure 35: Incidence and origin of ICCR (n=9)

The incidence of ICCR was 77.8%, as indicated in Table 16. ICCR arose from the ICG in $\frac{4}{9}$ sides [44.5%: right, 60% ($\frac{3}{5}$ sides); left, 25% ($\frac{1}{4}$ sides)] [figure 35].

CTCR 'proper' were investigated in all sides that had a CTG [$\frac{49}{58}$ sides (84.5%): right, $\frac{24}{29}$ sides (82.8%); left, $\frac{25}{29}$ sides (86.2%)].

Table 17: Origin and incidence of CTCR

Origin	RIGHT (n=24)			LEFT (n=25)			TOTAL
	G	IG	Total	G	IG	Total	(n=49)
Foetal	17	2	19	16	3	19	38
(%)	(70.8)	(8.33)	(79.2)	(64.0)	(12.0)	(76.0)	(77.6)
Adult	4	1	5	4	2	6	11
(%)	(16.7)	(4.2)	(20.8)	(16.0)	(8.0)	(24.0)	(22.5)
TOTAL	21	3	24	20	5	25	49
(%)	(87.5)	(12.5)	(100)	(80.0)	(20.0)	(100)	(100)

Key: G= ganglionic origin; IG=interganglionic origin

The incidence of CTCR was 100%, as indicated in Table 15. CTCR arose from the CTG [Plates 17 and 18] in $\frac{41}{49}$ sides [83.7%: right, 87.5% ($\frac{21}{24}$ sides); left, 80.0% ($\frac{20}{25}$ sides)] [figure 36]. In 37 cases (90.2%) of this ganglionic origin two CTCR arose from the ganglion, while in the 4 cases (9.8%) only one ramus was noted. In 3 of these cases a second ramus was found arising from the chain below CTG. In $\frac{8}{49}$ sides (16.3%) CTCR arose from the interganglionic segment of the chain below the ganglion. The position of this origin ranged from 1.2-2.6mm (mean distance, 2.1mm) below the lower pole of the ganglion.

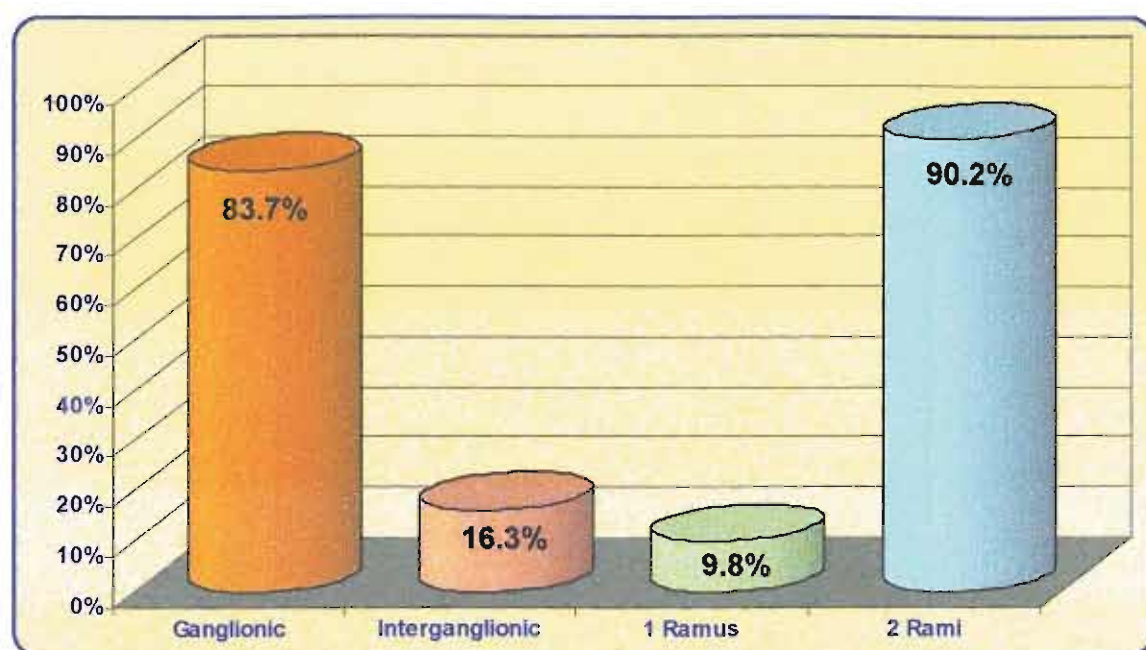


Figure 36: Incidence and origin of CTCR

CTCR and ICCR passed posterior to the subclavian artery and arch of the aorta and contributed to the plexus located posterior to the arch of the aorta.

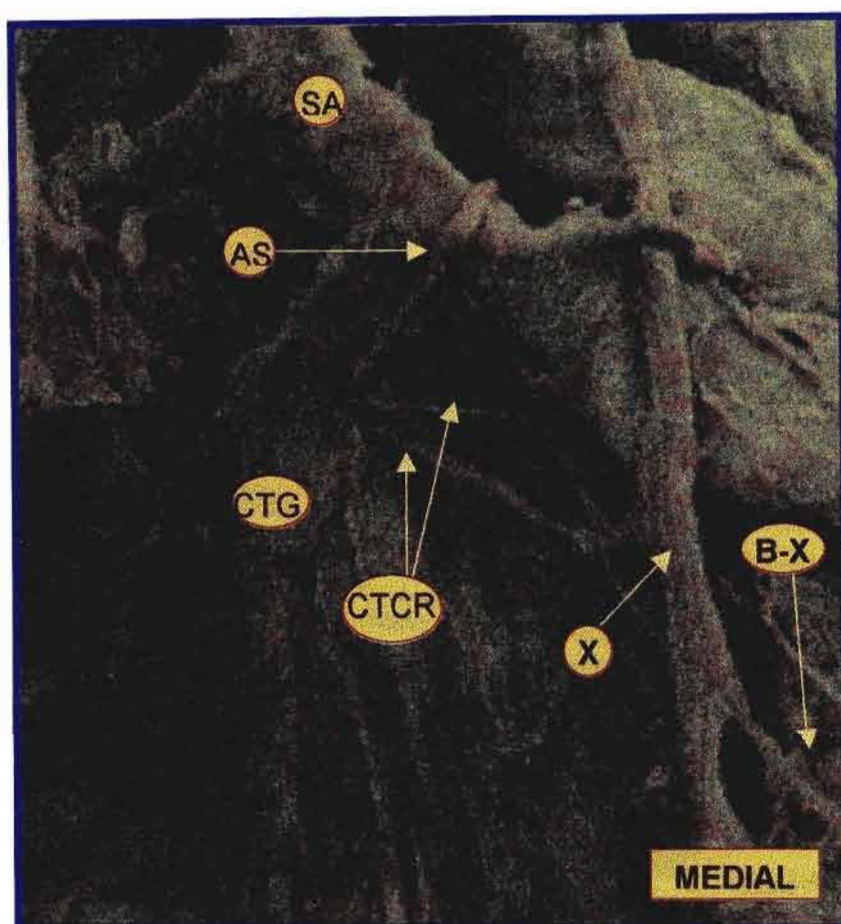


Plate 17: Antero-lateral view of adult cervical sympathetic chain demonstrating the ganglionic origin of CTCR in an adult.

KEY:

CTG	Cervicothoracic Ganglion
CTCR	Cervicothoracic Cardiac Ramus
SA	Subclavian Artery
AS	Ansa Subclavian
X	Vagus Nerve
B-X	Vagal Branch to Cardiac Plexus

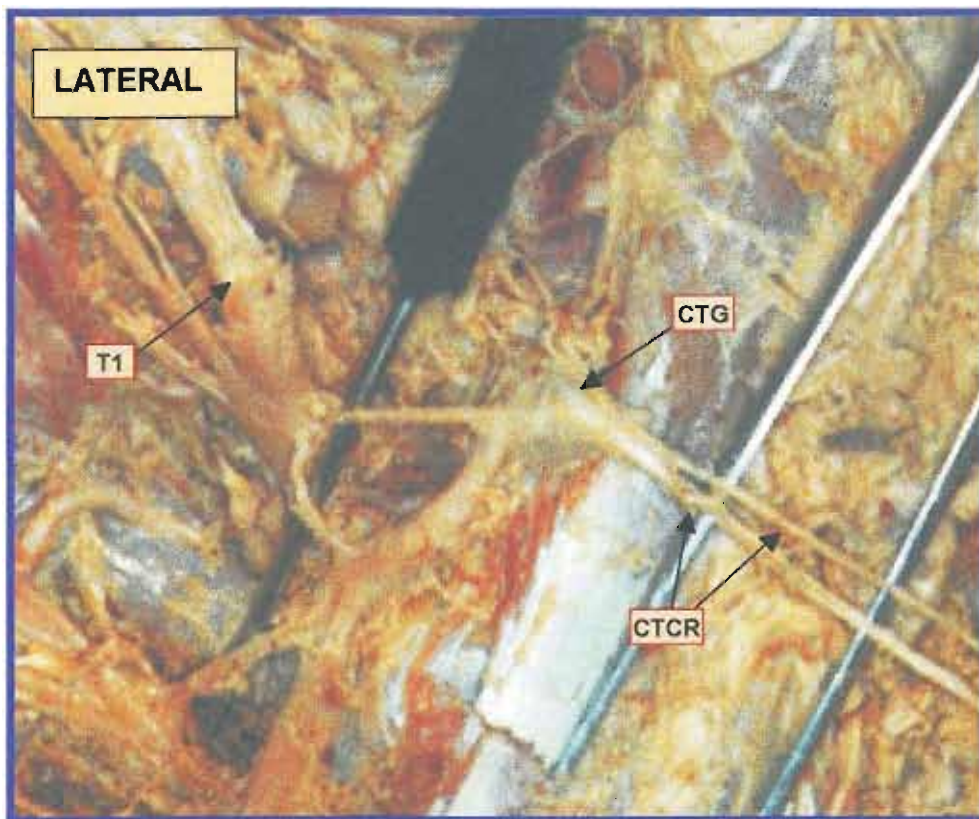


Plate 18: Antero-lateral view of right sympathetic chain demonstrating the origin of the CTCR in an adult

Key:

CTG	Cervicothoracic Ganglion
CTCR	Cervicothoracic Cardiac Ramus
T1	T1 ventral ramus

4.4.3 THORACIC CARDIAC SYMPATHETIC RAMI

In the thoracic region, cardiac rami (TCR) arose from T₁G-T₅G.

Four TCR arose from thoracic sympathetic chain below the CTG [Figure 37]. The origin of these cardiac rami was from both the ganglion and from the interganglionic segment. TCR were named sequentially after identifying CTCR or TCR₁.

Due to the low incidence of an unfused 1st thoracic ganglion (T₁G) ($\frac{9}{58}$ sides: 15.5%), the TCR₁ 'proper' (i.e. cardiac ramus arising from an unfused T₁G) could, therefore, only be investigated in 9 sides (5 right and 4 left).

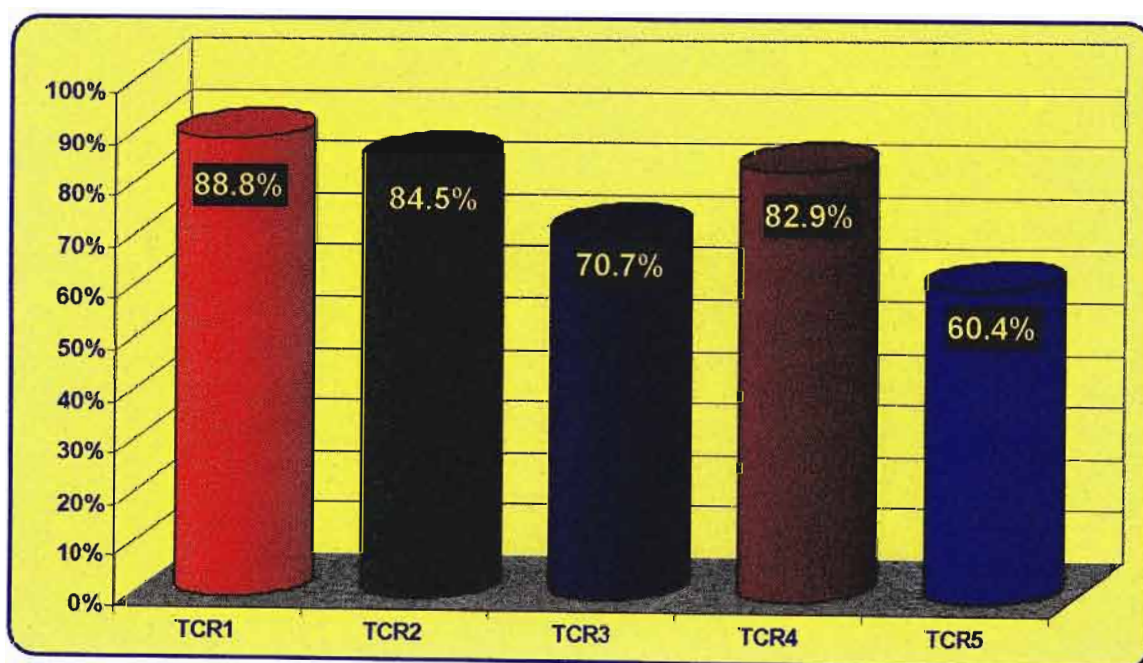


Figure 37: Incidence of TCR

Table 18: The origin and incidence of TCR₁

Origin	RIGHT (n=5)			LEFT (n=4)			TOTAL (n=9)
	G	IG	Total	G	IG	Total	
Foetal	2	0	2	2	0	2	4
(%)	(40)	(0)	(40)	(50)	(0)	(50)	(44.4)
Adult	2	1	3	0	1	1	4
(%)	(40)	(20)	(60)	(0)	(25)	(25)	(44.4)
TOTAL	4	1	5	2	1	3	8
(%)	(80)	(20)	(100)	(50)	(25)	(75)	(88.8)

Key: G= ganglionic origin; IG=interganglionic origin

The incidence of TCR₁ was 88.8%, as indicated in Table 18. TCR₁ displayed a ganglionic origin in ⁶/₉ sides [66.6%: right, 80.0% (⁴/₅ sides); left, 50.0% (²/₄ sides)] [figure 38]. In ²/₉ sides (22.2%) TCR₁ arose from the upper half of the interganglionic segment of the chain below T₁G.

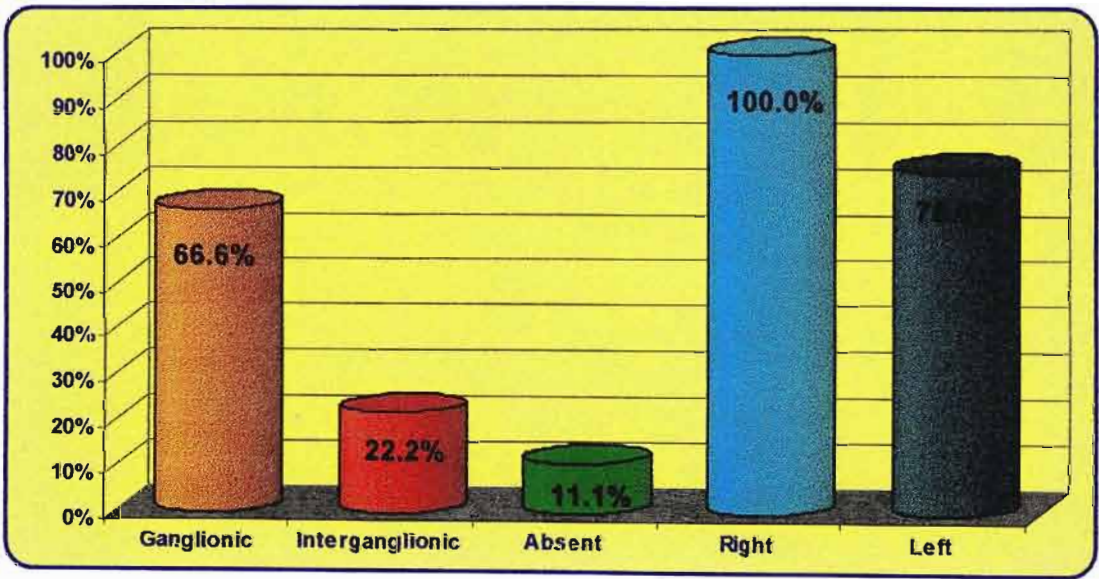


Figure 38: Origin and incidence of TCR₁

The incidence of TCR_2 was 84.5%, as indicated in Table 19. TCR_2 displayed a ganglionic origin in $^{29}/_{58}$ sides [50.0%: right, 51.7% ($^{15}/_{29}$ sides); left, 48.3% ($^{14}/_{53}$ sides)] [*figure 39*].

In $^{20}/_{58}$ sides (34.5%) TCR_2 arose from either the lower half of the interganglionic segment of the chain above or the upper half of the chain below the ganglion. The origin of the ramus from the interganglionic segment was as follows: between T_2G and T_3G , $^{13}/_{20}$ sides [65%: right, $^5/_8$ sides (62.5%); left $^8/_12$ sides (66.6%)]; between CTG and T_2G , $^5/_20$ sides [25%: right, $^3/_8$ sides (37.5%); left $^2/_12$ sides (16.6%)]; between T_2G and fused T_{3-4}G , $^2/_20$ sides [10%: right, $^0/_8$ sides; left $^2/_12$ sides (16.6%)].

Table 19: Origin and incidence of TCR₂

Origin	RIGHT (n=29)			LEFT (n=29)			TOTAL (n=58)
	G	IG	Total	G	IG	Total	
Foetal	13	8	21	11	10	21	42
(%)	(44.8)	(27.6)	(72.4)	(37.9)	(34.5)	(72.4)	(72.4)
Adult	2	0	2	3	2	5	7
(%)	(6.9)	(0)	(6.9)	(10.3)	(6.9)	(17.2)	(12.1)
TOTAL	15	8	23	14	12	26	49
(%)	(51.7)	(27.6)	(79.3)	(48.3)	(34.5)	(89.7)	(84.5)

Key: G= ganglionic origin; IG=interganglionic origin

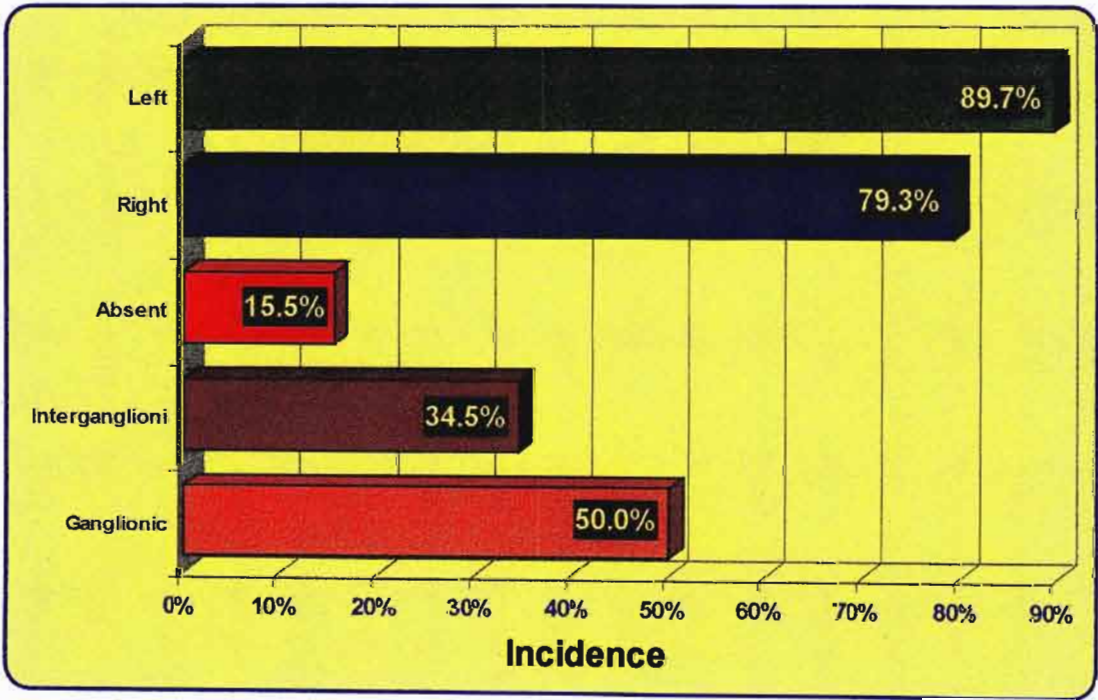


Figure 39: Incidence and origin of TCR₂

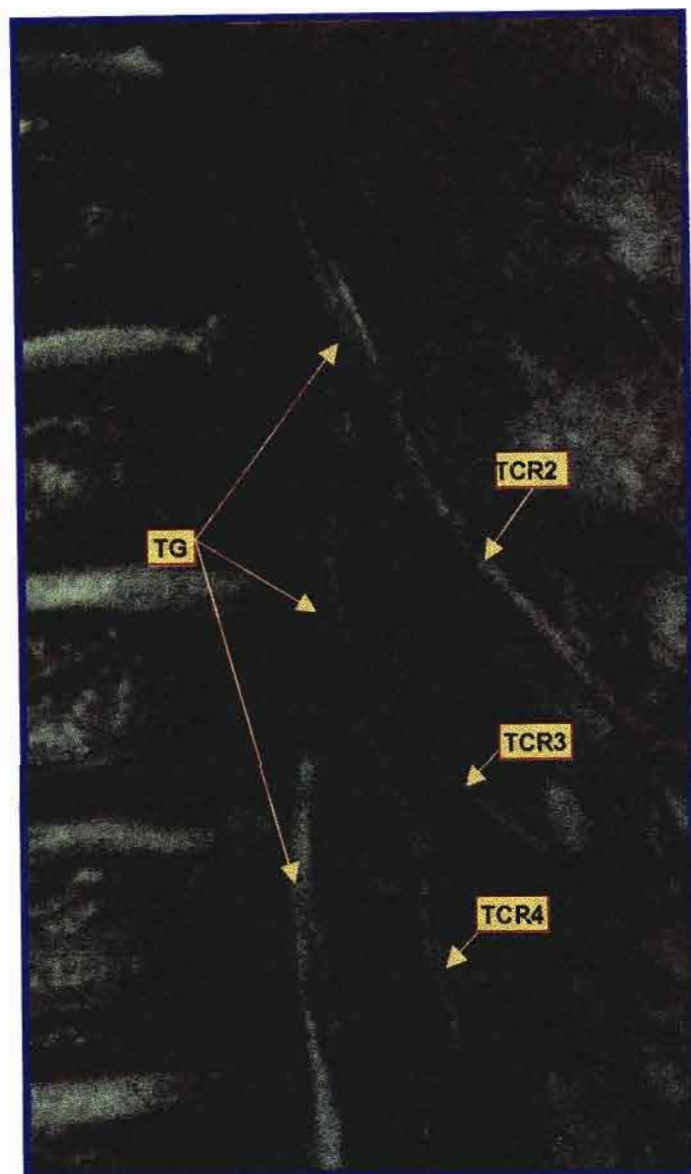


Plate 19: Anterolateral view of right thoracic sympathetic chain demonstrating the origin of thoracic cardiac rami in a foetus.

Key:

TG Thoracic Ganglia
TCR Thoracic Cardiac Rami

The incidence of TCR₃ was 70.7%, as indicated in Table 20. TCR₃ displayed a ganglionic origin in $\frac{25}{58}$ sides [43.1%: right, 37.9% ($\frac{11}{29}$ sides); left, 48.3% ($\frac{14}{29}$ sides)] [figure 40].

In $\frac{16}{58}$ sides (27.6%) TCR₃ arose from either the lower half of the interganglionic segment of the chain above or the upper half of the chain below the ganglion. The origin of the ramus from the interganglionic segment was as follows: between T₂G and T₃G, $\frac{10}{16}$ sides [62.5%: right, $\frac{4}{7}$ sides (57.1%); left $\frac{6}{9}$ sides (66.6%)]]; between T₃G and T₄G, $\frac{6}{16}$ sides [37.5%: right, $\frac{3}{7}$ sides (42.9%); left $\frac{3}{9}$ sides (33.3%)].

Table 20: Origin and incidence of TCR₃

Origin	RIGHT (n=29)			LEFT (n=29)			TOTAL (n=58)
	G	IG	Total	G	IG	Total	
Foetal	9	6	15	11	8	19	34
(%)	(31.0)	(20.7)	(51.7)	(37.9)	(27.6)	(65.5)	(58.6)
Adult	2	1	3	3	1	4	7
(%)	(6.9)	(3.5)	(10.3)	(10.3)	(3.5)	(13.8)	(12.1)
TOTAL	11	7	18	14	9	23	41
(%)	(37.9)	(24.1)	(62.1)	(48.3)	(31.0)	(79.3)	(70.7)

Key: G= ganglionic origin; IG=interganglionic origin

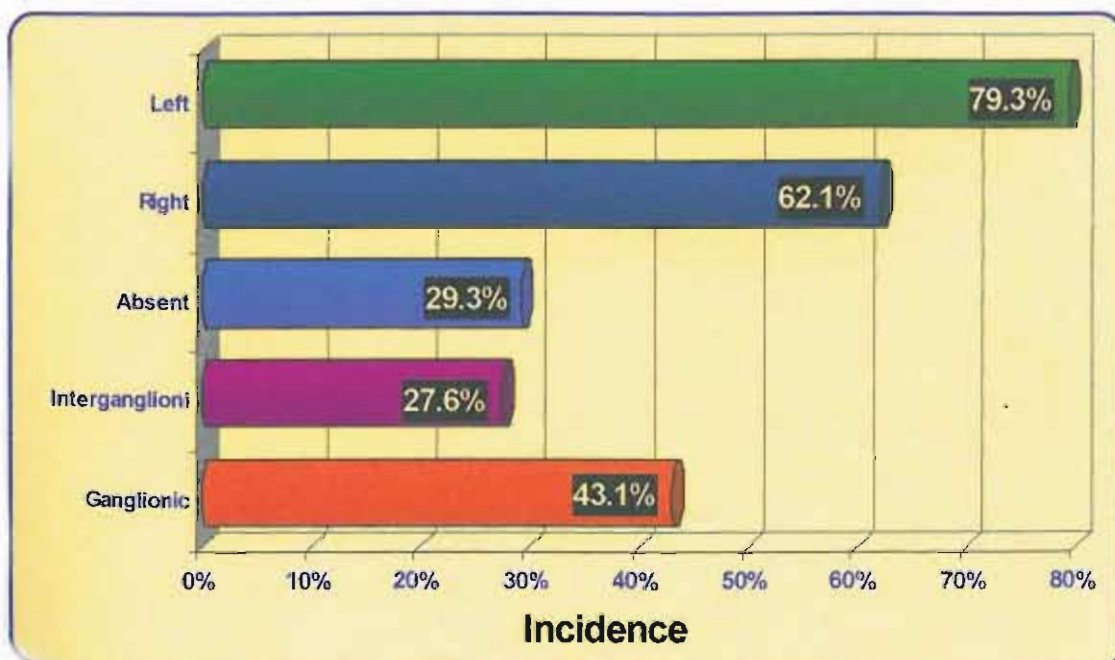


Figure 40: Incidence and origin of TCR₃

The incidence of TCR₄ was 82.9%, as indicated in Table 21. TCR₄ displayed a ganglionic origin in $^{31}_{58}$ sides [53.5%: right, 48.3% ($^{14}_{29}$ sides); left, 58.6% ($^{17}_{29}$ sides)] [figure 41].

In $^{17}_{58}$ sides (29.3 %) TCR₄ arose from, either the lower half of the interganglionic segment of the chain above or the upper half of the chain below the ganglion. The origin of the ramus from the interganglionic segment was as follows: between T₃G and T₄G, $^3_{17}$ sides [17.7%: right, 2_8 sides (25%); left 1_9 sides (11.1%)]; between T₄G and T₅G, $^{11}_{17}$ sides [64.7%: right, 5_8 sides (62.5%); left 6_9 sides (66.6%)]; between T₄G and fused T₅₋₆G ganglia, $^2_{17}$ sides [11.8%: right, 1_8 sides (12.5); left 1_9 sides (11.1%)].

Table 21: Origin and incidence of TCR₄

Origin	RIGHT (n=29)			LEFT (n=29)			TOTAL (n=58)
	G	IG	Total	G	IG	Total	
Foetal	12	6	18	13	8	21	39
(%)	(41.4)	(20.7)	(62.1)	(44.8)	(27.6)	(72.4)	(67.2)
Adult	2	2	4	4	1	5	9
(%)	(6.9)	(6.9)	(13.8)	(13.8)	(3.5)	(17.2)	(15.5)
TOTAL	14	8	22	17	9	26	48
(%)	(48.3)	(27.6)	(75.9)	(58.6)	(31.0)	(89.7)	(82.9)

Key: G= ganglionic origin; IG=interganglionic origin

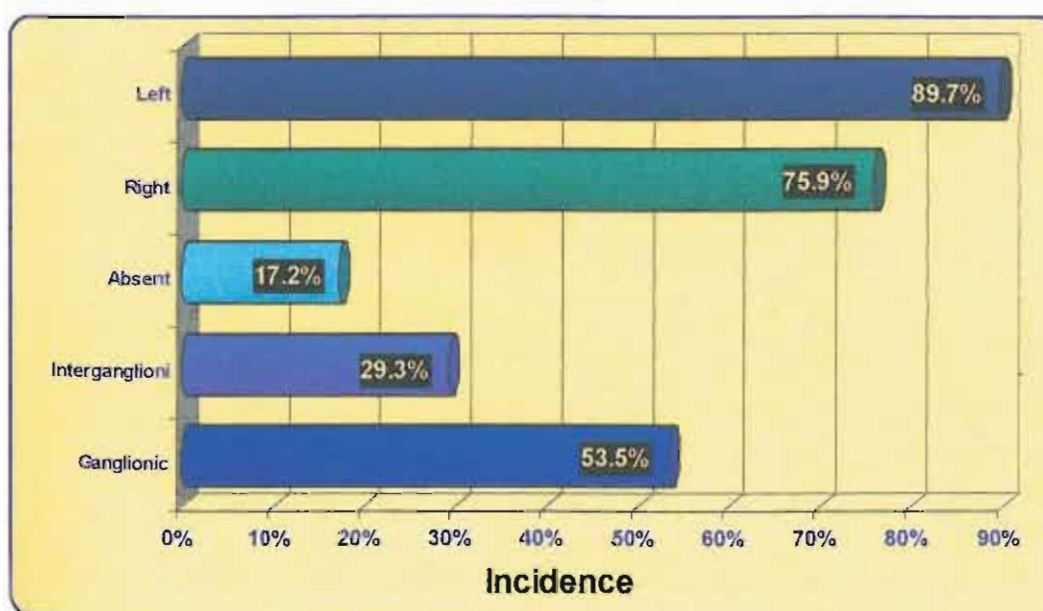


Figure 41: Incidence and origin of TCR₄

The incidence of TCR₅ was 60.4%, as indicated in Table 22. TCR₅ displayed a ganglionic origin in $^{20}_{58}$ sides [34.5%: right, 31.0% ($^9_{29}$ sides); left, 37.9% ($^{11}_{29}$ sides)] [figure 42].

In $^{15}_{58}$ sides (25.9 %) TCR₅ arose from, either the lower half of the interganglionic segment of the chain above or the upper half of the chain below the ganglion. The origin of the ramus from the interganglionic segment was as follows: between T₅G and T₆G, $^{14}_{15}$ sides [93.3%: right, 7_7 sides (100%); left 7_8 sides (87.5%)]; between T₅G and fused T₆₋₇G ganglia, $^1_{15}$ sides [6.7%: right, 0_7 sides; left 1_8 sides (12.5%)].

Table 22: Incidence and origin of TCR₅

Origin	RIGHT (n=29)			LEFT (n=29)			TOTAL (n=58)
	G	IG	Total	G	IG	Total	
Foetal	8	7	15	11	8	19	34
(%)	(27.6)	(25.0)	(51.7)	(37.9)	(27.6)	(65.5)	(58.6)
Adult	1	0	1	0	0	0	1
(%)	(3.5)	0	(3.5)	0	0	0	(1.7)
TOTAL	9	7	16	11	8	19	35
(%)	(31.0)	(24.1)	(55.2)	(37.9)	(27.6)	(65.5)	(60.4)

Key: G= ganglionic origin; IG=interganglionic origin

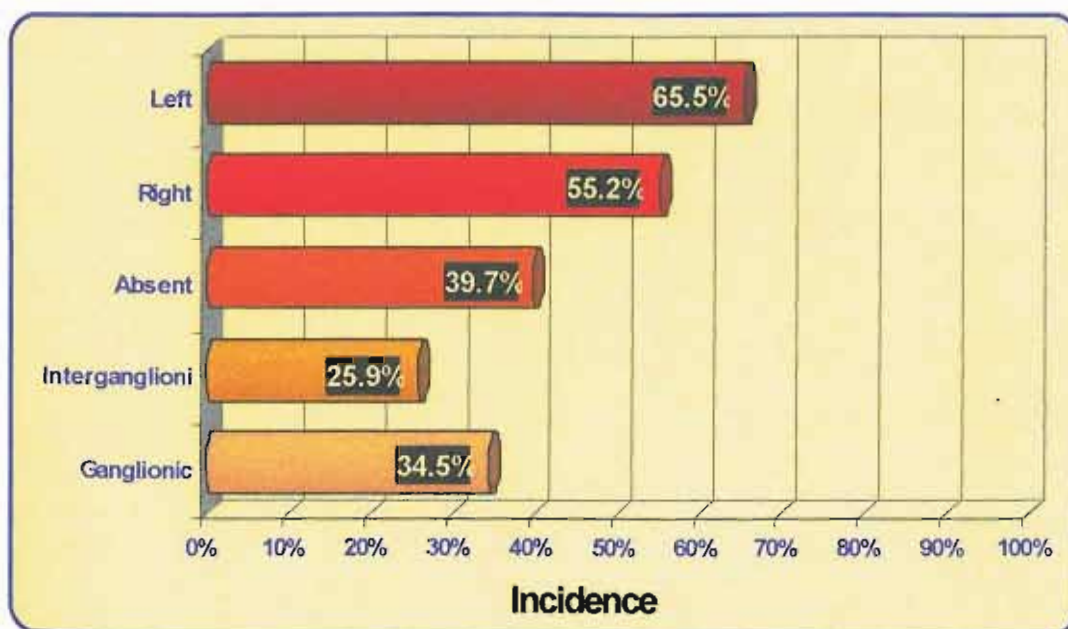


Figure 42: Incidence and origin of TCR₅

4.4.5 CARDIAC PLEXUS

The cardiac plexus received both sympathetic and parasympathetic fibres. All sympathetic contributions from the cervical and thoracic sympathetic chains were found to arborize directly in the deep cardiac plexus. This plexus is located posterior to the arch of the aorta and anterior to the left bronchus at the bifurcation of the pulmonary trunk. Fibres from this cardiac plexus were seen to pass forwards onto the anterior surface of the arch of the aorta and postero-laterally to the bronchi. Thus, the 'superficial' cardiac plexus and the pulmonary plexus received indirect branches from the sympathetic chain via the 'deep' plexus.

4.5 OTHER MEDIAL BRANCHES

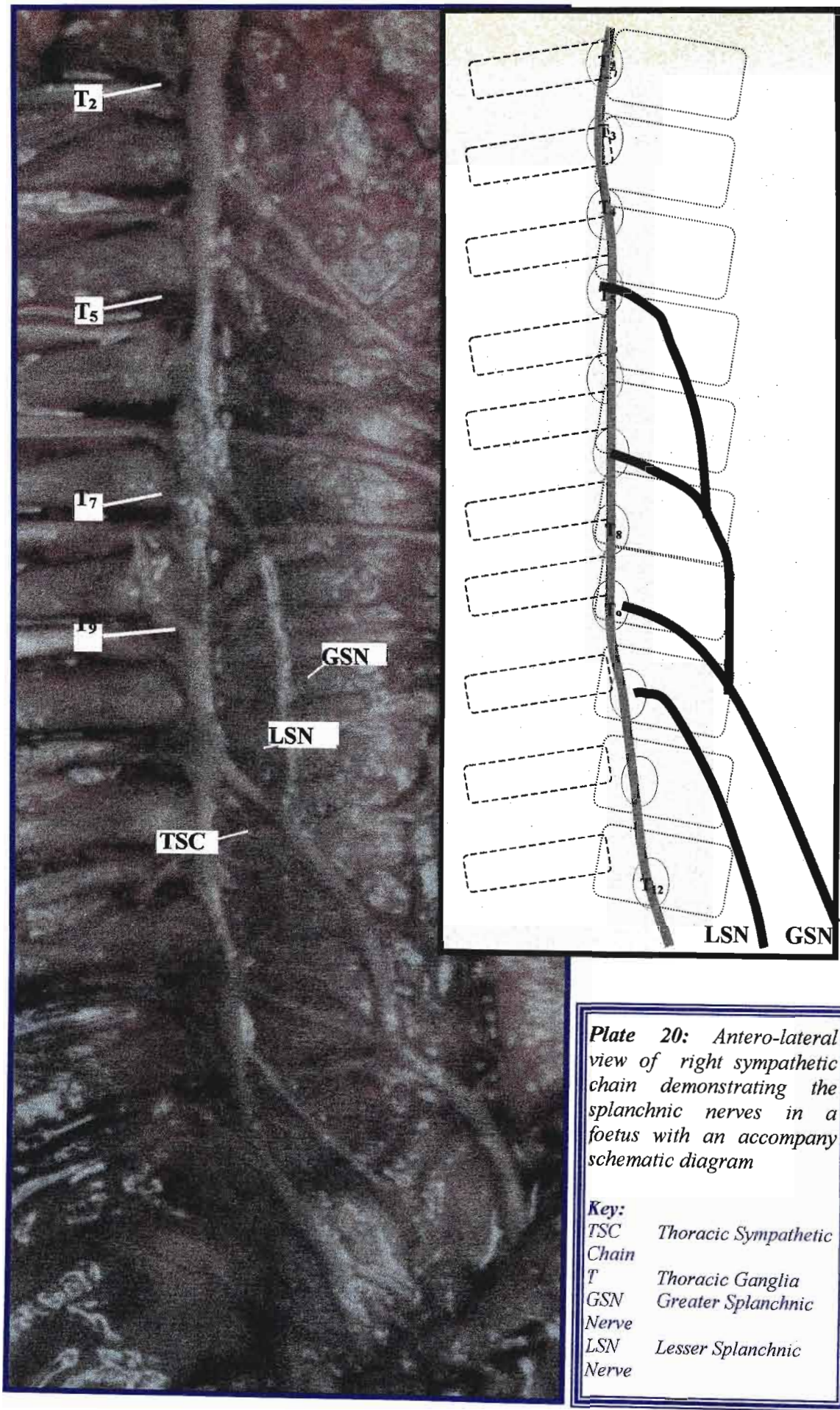
4.5.1 SPLANCHNIC NERVES

The splanchnic nerve patterns were investigated in 16 foetal and 8 adult specimens [n=48 sides: right, 24 and left, 24].

As indicated in Table 23, the GSN was always present whereas the LSN and lsn were inconsistent: LSN, 87.5% [right, 91.2%; left, 83.3%]; lsn, 45.8 [right, 41.7%; left, 50.0%] [Plates 20 and 21].

Table 23: Incidence of splanchnic nerves

	RIGHT (n=24)			LEFT (n=24)			TOTAL
	Foetal	Adult	Total	Foetal	Adult	Total	(n=48)
GSN	16	8	24	16	8	24	48
(%)	(66.6)	(33.4)	(100)	(66.6)	(33.4)	(100)	(100)
LSN	15	7	22	14	6	20	42
(%)	(62.5)	(29.2)	(91.2)	(58.3)	(25.0)	(83.3)	(87.5)
lsn	6	4	10	8	4	12	22
(%)	(25.0)	(16.7)	(41.7)	(33.4)	(16.7)	(50.0)	(45.8)



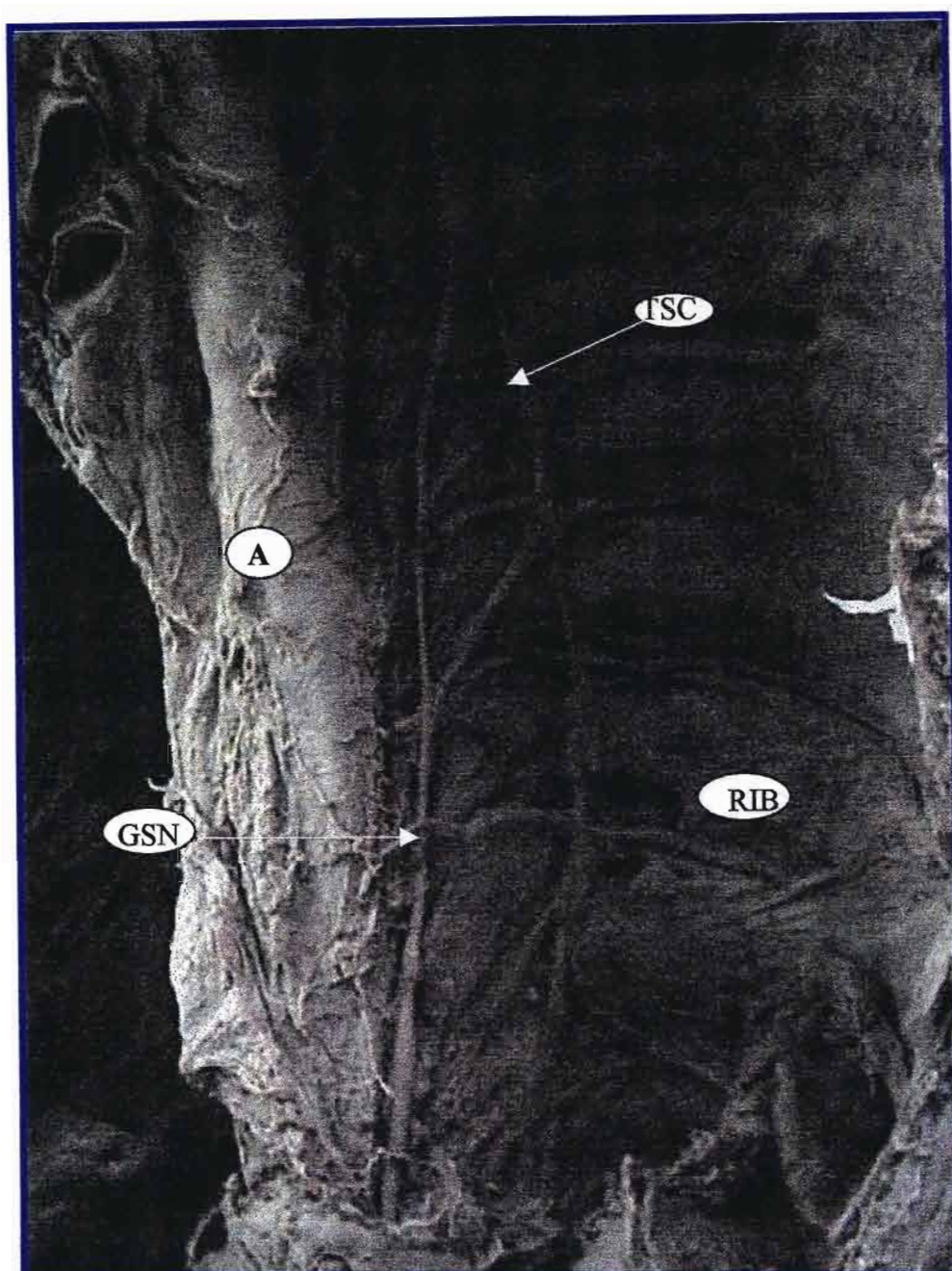


Plate 21: Antero-lateral view of left sympathetic chain demonstrating the splanchnic nerves in a adult with an accompany schematic diagram

Key:

TSC	Thoracic Sympathetic Chain
T	Thoracic Ganglia
GSN	Greater Splanchnic Nerve
LSN	Lesser Splanchnic Nerve
A	Aorta

The number of roots of GSN varied from 2-8, as indicated in Table 24, with a range of 3-5 being most common [$^{39}/_{48}$ sides (81.3%): right, $^{19}/_{24}$ sides (79.2%); left, $^{20}/_{24}$ sides (83.4%)]. There was no correlation between number of roots of GSN with the absence of the LSN and lsn [Plate 22].

Table 24: Incidence of the number of roots of GSN

No of Roots	RIGHT (n=24)			LEFT (n=24)			TOTAL (n=48)
	Foetal	Adult	Total	Foetal	Adult	Total	
2	2 (8.3)	1 (4.2)	3 (12.5)	3 (12.5)	1 (4.2)	4 (16.7)	7 (14.6)
3	2 (8.3)	2 (8.3)	4 (16.7)	7 (29.2)	3 (12.5)	10 (41.7)	14 (29.2)
4	6 (16.7)	2 (8.3)	8 (33.3)	4 (16.7)	3 (12.5)	7 (29.2)	15 (31.3)
5	6 (16.7)	1 (4.2)	7 (29.2)	2 (8.3)	1 (4.2)	3 (12.5)	10 (20.8)
6	-	1 (4.2)	1 (4.2)	-	-	-	1 (2.1)
7	-	-	-	-	-	-	-
8	-	1 (4.2)	1 (4.2)	-	-	-	1 (2.1)

The range of roots values [Table 25] was: GSN, T3-T11; LSN, T8-T12; lsn, T10-12.

Table 25: Range of root values for GSN, LSN, lsn

	GSN		LSN		lsn	
	<i>Right</i>	<i>Left</i>	<i>Right</i>	<i>Left</i>	<i>Right</i>	<i>Left</i>
Adult	T ₃₋₄ -T ₁₀	T ₃ -T ₁₁	T ₉ -T ₁₁	T ₉ -T ₁₂	T ₁₁ -T ₁₂	T ₁₁ -T ₁₂
Foetus	T ₄ -T ₁₁	T ₄ -T ₁₀	T ₈ -T ₁₂	T ₈ -T ₁₂	T ₁₀ -T ₁₂	T ₁₁ -T ₁₂
Combined	T ₃₋₄ -T ₁₁	T ₃ -T ₁₁	T ₈ -T ₁₂	T ₈ -T ₁₂	T ₁₀ -T ₁₂	T ₁₁ -T ₁₂

The incidences of the highest and lowest roots of GSN are indicated in Tables 26 and 27.

Table 26: Incidence of highest root of GSN

Root Value	RIGHT (n=24)			LEFT (n=24)			TOTAL (n=48)
	Foetal	Adult	Total	Foetal	Adult	Total	
3	-	-	-	1 (4.2)		1 (4.2)	1 (2.1)
3-4	-	1 (4.2)	1 (4.2)			-	1 (2.1)
4	2 (8.3)	1 (4.2)	3 (12.5)	2 (8.3)		2 (8.3)	5 (10.4)
4/5	-	-	-	1 (4.2)		1 (4.2)	1 (2.1)
5	3 (12.5)	2 (8.3)	5 (20.8)	5 (20.8)	1 (4.2)	6 (25.0)	11 (22.9)
5/6	1 (4.2)	-	1 (4.2)	1 (4.2)		1 (4.2)	2 (4.2)
6	4 (16.7)	3 (12.5)	7 (29.2)	5 (20.8)	3 (12.5)	8 (33.3)	15 (31.3)
6/7	1 (4.2)	-	1 (4.2)			-	1 (2.1)
7	4 (16.7)	-	4 (16.7)	2 (8.3)	2 (8.3)	4 (16.7)	8 (33.3)
8	1 (4.2)	-	1 (4.2)			-	1 (2.1)
9	-	1 (4.2)	1 (4.2)	1 (4.2)		1 (4.2)	2 (4.2)

Table 27: Incidence of lowest root of GSN

Root Value	RIGHT (n=24)			LEFT (n=24)			TOTAL (n=48)
	Foetal	Adult	Total	Foetal	Adult	Total	
5	-	-	-	-	1 (4.2)	1 (4.2)	1 (2.1)
6	-	1 (4.2)	1 (4.2)	-	-	-	1 (2.1)
7	-	-	-	2 (8.3)	-	2 (8.3)	2 (4.2)
7/8	1 (4.2)	-	1 (4.2)	1 (4.2)	-	1 (4.2)	2 (2.1)
8	4 (16.7)	-	4 (16.7)	4 (16.7)	1 (4.2)	5 (20.8)	9 (18.8)
8/9	1 (4.2)	2 (4.2)	3 (12.5)	-	-	-	3 (6.3)
8-9	1 (4.2)	-	1 (4.2)	1 (4.2)	1 (4.2)	2 (8.3)	3 (6.3)
9	5 (20.8)	2 (8.3)	7 (29.2)	5 (20.8)	2 (8.3)	7 (29.2)	14 (29.2)
9/10				1			
10	3 (12.5)	3 (12.5)	6 (25.0)	1 (4.2)	3 (12.5)	4 (16.7)	10 (20.8)
11	1 (4.2)	-	1 (4.2)	-	1 (4.2)	1 (4.2)	2 (4.2)

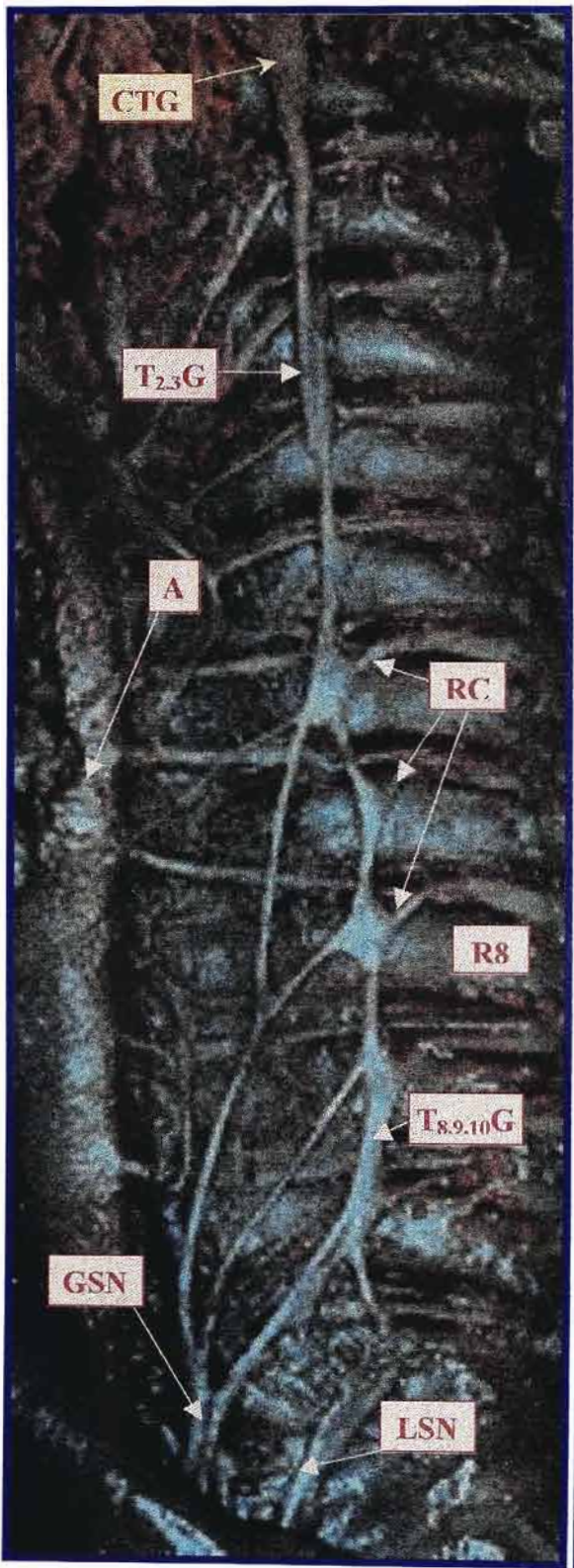


Plate 22: Antero-lateral view of left thoracic sympathetic chain demonstrating the origin of GSN and LSN in a foetus.

KEY:	
CTG	Cervicothoracic Ganglion
T2,3G	Fused T2 & T3 Ganglion
T8,9,10	Fused T8, T9 & T10
Ganglion	
A	Aorta
GSN	Greater Splanchnic Nerve
LSN	Lesser Splanchnic Nerve
R8	Eight Rib
RC	Rami Communicantes

4.5.2 VASCULAR BRANCHES

The vascular branches of the cervical and upper thoracic parts of the sympathetic chain were examined in ten fetuses and four adult specimens [n=28].

4.5.1 Vertebral Artery

CTG contributed a consistent lateral branch to the vertebral artery, which ran upwards to enter foramen transversarium, together with the vertebral artery [*Plate 23*]. In 2 fetuses (2 left sides), the vertebral nerve was formed by 2 rami arising from the upper pole of CTG. The ICG and T₁G, unfused on 1 foetal side (left), each contributed a ramus to form the vertebral nerve, which accompanied the vertebral artery into the vertebral foramina.

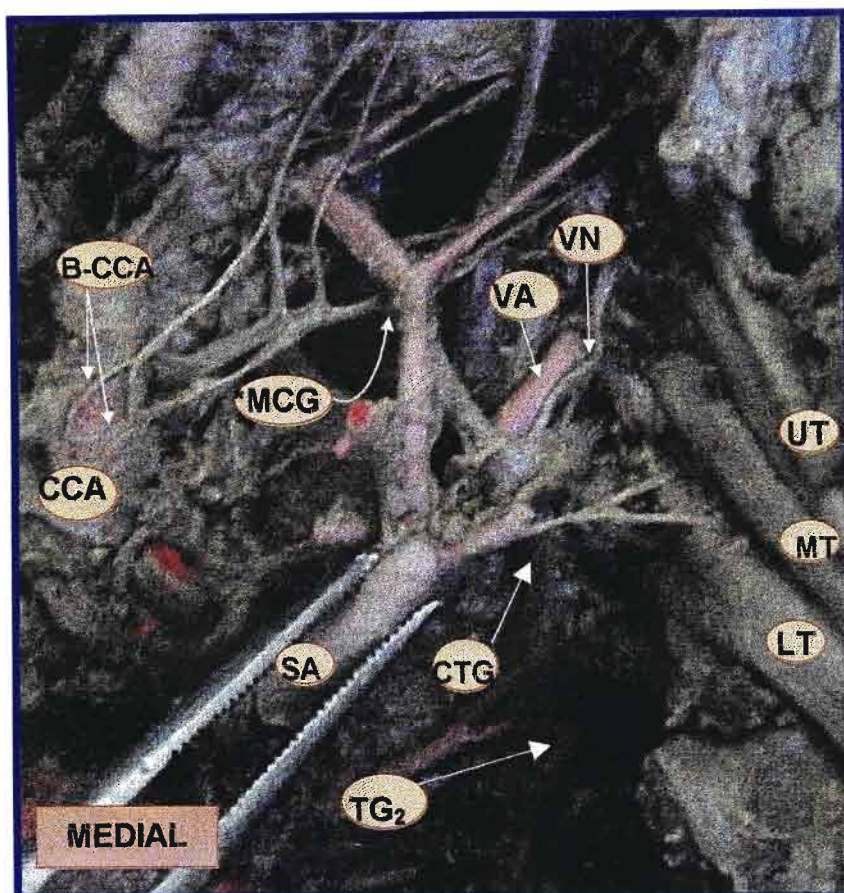


Plate 23: Antero-lateral view of a foetal left cervical sympathetic chain demonstrating the vertebral nerve and branches to the common carotid artery

KEY:

CTG	Cervicothoracic ganglion
*MCG	MCG (under inferior thyroid artery)
SA	Subclavian Artery
CCA	Common Carotid Artery
B-CCA	Branches to CCA from MCG
VA	Vertebral Artery
VN	Vertebral Nerve
UT, MT, LT	Upper, Middle and Lower Trunks of Brachial Plexus
TG ₂	2 nd Thoracic Ganglion

4.5.2 Subclavian Artery

Rami from CTG winding around the subclavian artery were recorded in $^{20}_{28}$ sides [71.4%: right, $^{12}_{24}$ sides (42.9%); left, $^8_{24}$ sides (33.3%)]. In $^7_{24}$ sides [29.2%: right, $^5_{24}$ (20.8%), left, $^2_{24}$ (8.3%)] of these 2 rami to the subclavian artery was recorded. Where the ICG and T1 ganglion were unfused, a ramus from the right T1 ganglion was recorded to the subclavian artery. No rami were recorded from the unfused ICG.

The ansa subclavian was distinctly separate from the above branches and was observed in 100% of cases and comprised anterior and posterior limbs that formed a loop around the subclavian artery. In $^{18}_{28}$ sides [64.3%: right, $^8_{28}$ (28.6%); left, $^{11}_{28}$ (39.3%)] the ansa subclavian contributed to the plexus around the subclavian artery [*Plate 24*].



Plate 24: Antero-lateral view of left sympathetic chain demonstrating the plexus around the subclavian artery.

Key:

SA	Subclavian Artery
CTG	Cervicothoracic ganglion

4.5.3 Carotid Arteries

Rami from SCG to Internal Carotid Artery (ICA) were recorded in $\frac{16}{28}$ sides [57.1%: right, $\frac{10}{28}$ (35.7%); left, $\frac{6}{28}$ (21.4%)]. Rami from CTG to ICA were recorded in $\frac{19}{28}$ sides [67.9%: right, $\frac{8}{28}$ (%); left, $\frac{11}{28}$ (%)]. In the case of the unfused ICG and T1 ganglion, no rami to the ICA were recorded at this level. The rami arose from the SCG. A ramus from the SCG in $\frac{3}{28}$ sides [10.7%: right $\frac{1}{28}$ (3.6%); left, $\frac{2}{28}$ sides (7.1%)] and from the MCG in $\frac{1}{28}$ sides [3.6%: right, 0; left, $\frac{1}{24}$ (3.6%)] to the common carotid trunk, just proximal to its bifurcation [*Plate 23*].

4.6.4 Brachiocephalic Trunk

In the adult specimens a ramus to the brachiocephalic trunk was recorded in $\frac{4}{8}$ sides (right, 3; left, 1). Each had a different origin, from the: MCG, $\frac{1}{8}$ sides (12.5%); ICG, $\frac{1}{8}$ sides (12.5%); T1 ganglion, $\frac{1}{8}$ sides (12.5%); the interganglionic chain between the SCG and MCG, $\frac{1}{8}$ sides (12.5%). This ramus was only present on one foetal side and arose from the MCG.

4.6.5 Intercostal Arteries

Branches to the superior intercostal artery were observed in all specimens. These arose directly from the CTG. The thoracic sympathetic chain supplied branches to the posterior intercostal arteries along its course in the thorax. These displayed no pattern and comprised numerous fine branches.

4.5.6 Aorta

Fine filaments were distributed to the aorta from the thoracic sympathetic chain and GSN. The direct branches from the chain were very slender rami and flimsy while the branches from the GSN were larger [Plate 25].

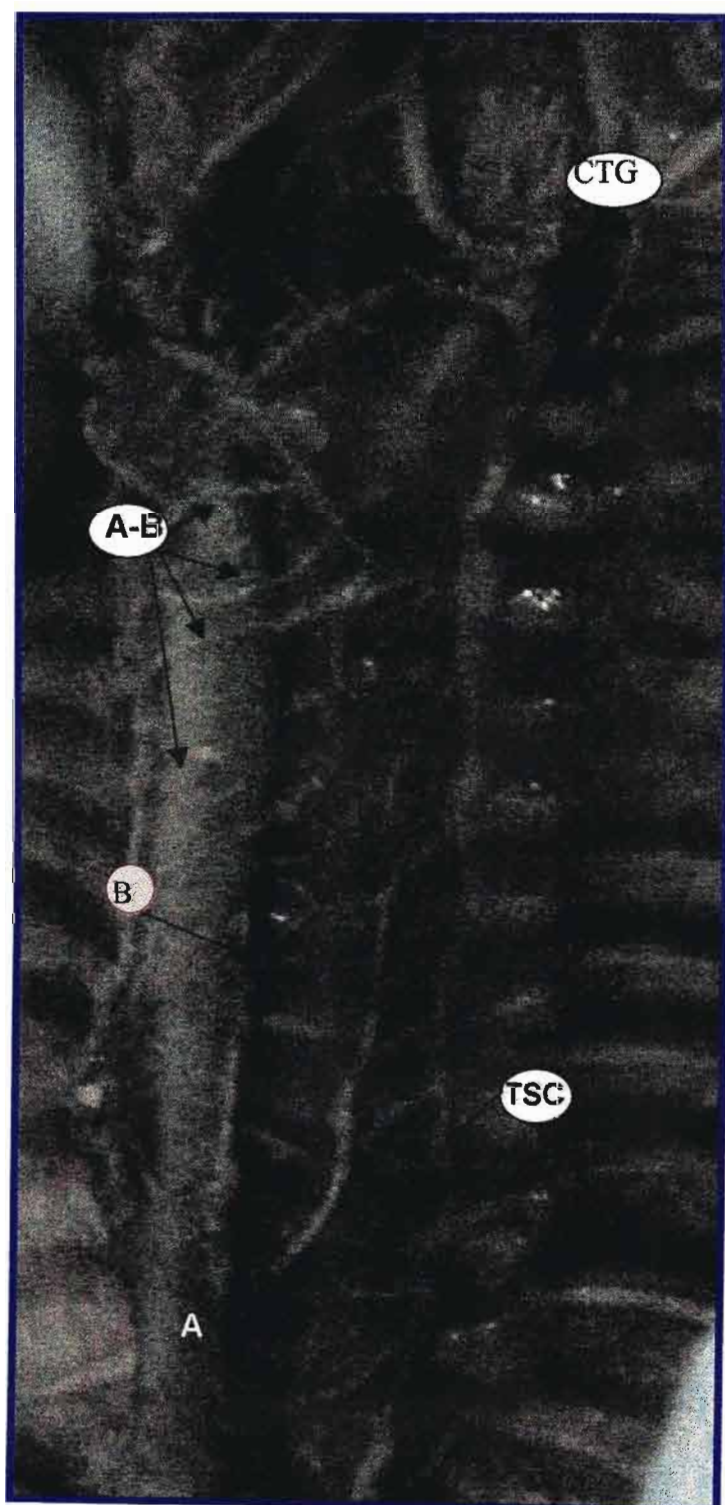


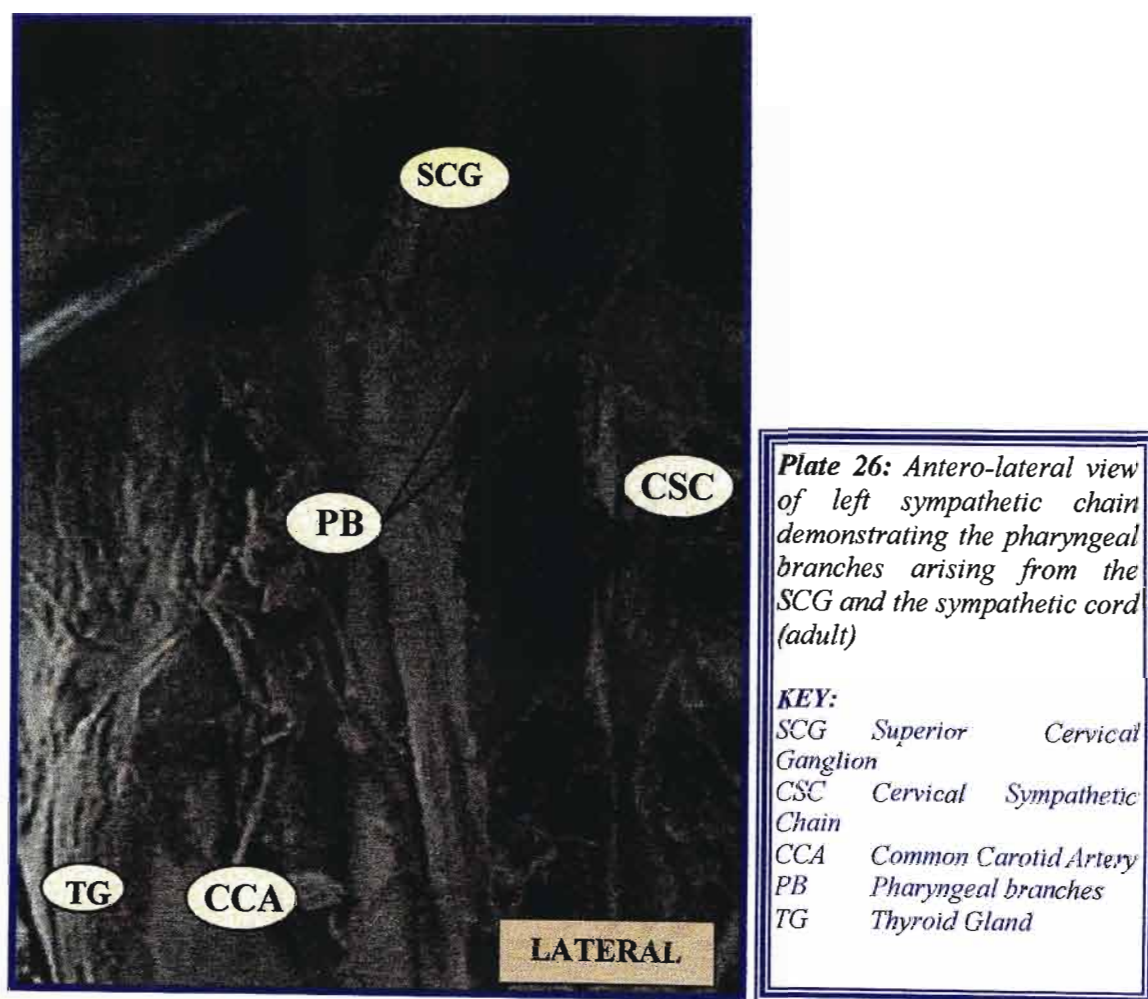
Plate 25: Antero-lateral view of the left sympathetic chain demonstrating the aortic branches from the chain.

Key:

- A* Aorta
- A-B* Aortic branches
- CTG* Cervicothoracic Ganglion
- TSC* Thoracic Sympathetic Chain
- B* Branches from GSN

4.5.7 Miscellaneous

Rami were also noted to the phrenic nerve were noted in 20.7% (right, 37.9%; left, 31.0%). In addition, the cervical part of the sympathetic chain distributed rami to the pharynx. These were numerous from the upper part of the cervical chain and arose SCG and the chain below this ganglion [Plate 26]. Pulmonary branches were noted to arise from the cardiac plexus and passed forwards onto the arch of the aorta and postero-laterally to the bronchi.



4.6 HISTOLOGICAL ANALYSIS

There is no definitive method of differentiating between sympathetic and parasympathetic ganglia. Analysis of the microstructure of the different parts of CTG and fused thoracic ganglia revealed that all parts exhibited the characteristic features of ganglia described by Stevens and Lowe (1993) and contained ganglionic tissue. There was no point which could have been an interganglionic segment of chain.

The ganglion exhibited typical characteristics: large neuron cell bodies, nisse substance, large nuclei with prominent nucleoli. Ganglion neurons are surrounded by glia called satellite cells. In between the clumps of ganglion cells are small bundles of axons. Only the myelinated axons are actually visible. The ganglion is surrounded by a capsule of dense irregular connective tissue containing many closely packed fibroblasts. This capsule is the equivalent of the perineurium of the peripheral nerve. The histology of the interganglionic segment between ICG and T₁G confirmed the absence of ganglionic cell bodies and thus the presence of unfused ganglia.

Examination of the microstructure of the cardiac rami revealed that these exhibited characteristic features of peripheral nerves as aoutlined by Stevens and Lowe (1993). It also confirmed the cardiac rami were nerve tissue [Plate 27]. Myelin is visible as long tapering profiles with granular or foamy texture. The nuclei of Schwann cells, which make the myelin are visible and are typically long and tapering.

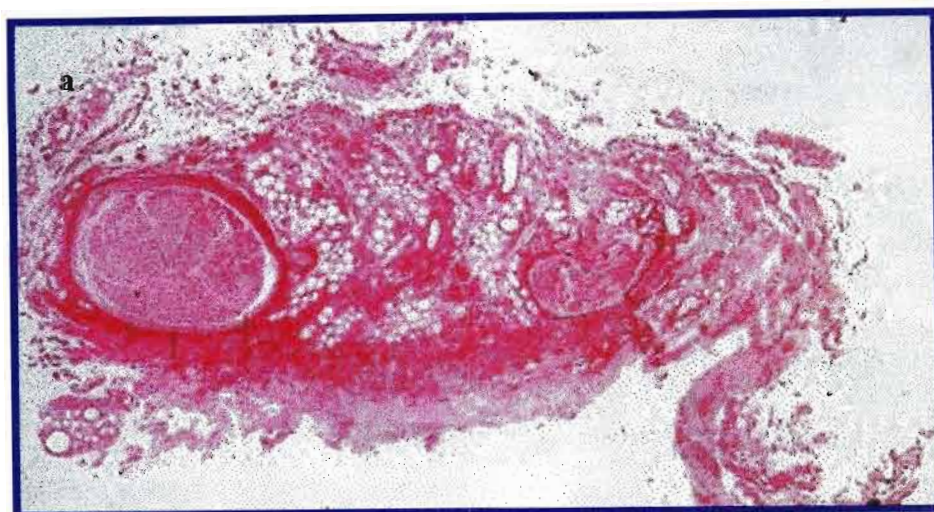


Plate 27: Histological slides demonstrating the ganglionic cells (a) and a longitudinal section of the cardiac ramus (b).

CHAPTER 5

DISCUSSION

5.1 Sample

The sample comprised a greater number of foetal specimens than adult specimens [60 sides (67.4%) vs. 29 sides (32.6%)]. The foetal study has the advantage of having, in a relatively small specimen, a unique overall view of the sympathetic nervous system from its origin in the spinal nerves to its termination (Groen *et al*, 1987). Furthermore, a comparison between the foetal stage (from 15mm) and the adult is feasible because the arrangement of the sympathetic nerves does not change in further development (Kuntz, 1953; Pick, 1957). In the human foetus the dimension of the sympathetic components are relatively large in comparison to the adult (Kuntz, 1953; Pick, 1970; Baljet and Drukker, 1981). In addition, the foetal parietal pleura is thinner and more transparent. Thus, the pleura may be stripped away without sacrificing the finer branches of the sympathetic chain. There is no pleural thickening from co-existent lung disease that is often prevalent in the adult specimens. Moreover, adult specimens are not as readily available and accessible.

The only disadvantage in the use of foetal specimens is that morphological comparisons of foetal dimensions need to be made within each developmental stage for it to be purposeful. The great difficulty with this is that such information is not available in the literature reviewed. Hence, this study records only the length of foetal cervical ganglia. The lengths and widths of adult cervical ganglia have been documented and can be compared to other studies.

5.2 CERVICAL SYMPATHETIC CHAIN

5.2.1 Course and relations

The course and relations of the left and right cervical sympathetic chains conformed to that of the descriptions in standard textbooks (Williams *et al*, 1995; McMinn, 1994). The cervical chain was found posterior to the carotid sheath and anterior to prevertebral fascia, lying on the transverse processes of the cervical vertebrae.

The literature reviewed is unclear as to the incidence of a double sympathetic chain in the cervical region. Although Mitchell (1953) observed the chain to be 'sometimes' double, no evidence of incidence is provided. Pick (1970) describes the double chain only in the formation of the ansa subclavian or the loop around the inferior thyroid artery. This study observed such a 'double chain' in the formation of the ansa subclavian in all specimens. In addition to these, this study records a double cervical chain in one adult specimen, extending from the SCG to the ICG.

This study confirms previous reports that the number of ganglia in the cervical region ranged from 2 (absent MCG) to four (double MCG) ganglia (Axford, 1928, Jamieson *et al.*, 1952; Becker and Grunt, 1957; Ellison and Williams, 1969).

Table 28: Reported incidence of cervical ganglia

AUTHOR	n=	SCG	MCG	ICG	CTG
<i>Jamieson et al. (1952)</i>	100	100	53	18	82
<i>Potts (1925)</i>	1	100			
<i>Pick & Sheehan (1946)</i>	25	100		20	80
<i>Becker & Grunt (1957)</i>	114	100	87.7	62.3	37.7
<i>Perlow & Vehe (1935)</i>	48	-	-	16.7	83.3
<i>Kimmel (1959)</i>	10	100			
<i>Groen et al. (1987)</i>	12	-	-	-	100
<i>Jit & Mukerjee (1960)</i>	100	-	-	22	76
<i>Ellison & William (1969)</i>	24	100	75	-	88
<i>Toni & Frignani (1955)</i>	80	-	-	40	48.75
<i>Weighted Mean</i>		<i>100</i>	<i>72.6</i>	<i>29.8</i>	<i>74.5</i>
<i>THIS STUDY</i>	<i>58</i>	<i>100</i>	<i>81.1</i>	<i>15.5</i>	<i>84.5</i>

5.2.2 Superior Cervical Ganglia

As indicated in Table 28, the constant, bilateral SCG documented in this series, corroborates the results of numerous authors (Mitchell, 1953; Becker and Grunt, 1957; Pick, 1970). This study further confirms the findings of Becker and Grunt (1957) that it is never seen as a multiple structure and is the most invariable of the cervical ganglia, thus refuting the claims of Laubmann (1931) who describe it as being double, or multinodular in “occasional” foetal chains.

Although various authors have reported differing ranges for SCG, literature is in agreement as to the average size of the adult SCG (28mm) (Jamieson et al, 1952; Becker and Grunt, 1957). This dissertation reports the mean length of SCG to be 25.68mm. A comparison of foetal dimensions is meaningless unless a comparison at each foetal age is made. This is not possible, as such details are not provided in literature.

The close relationship of the bifurcation of the common carotid artery to the lower pole of SCG in the foetus can probably be explained by differing foetal growth rates.

Literature reports the location of SCG to range between C₁-C₄ vertebrae. Jamieson *et al.* (1952) reported the extent of SCG between cervical vertebrae: C₁-C₃, 61%; C₁-C₂, 29%; C₂-C₃, 6%; C₁, 1%; C₂, 1% and C₁-C₄, 2%. Mitchell (1956) described SCG lying between the 2nd to 4th cervical transverse processes. Becker and Grunt (1957) describe, in a series of 100 adult sides, a variable relation of SCG to the cervical vertebrae: C₁₋₂ (29%); C₁₋₃ (61%); C₂₋₃ (6%); C₁ (1%); C₂ (1%); C₂₋₄(2%). This study records the SCG located between C₁-C₄ vertebrae (Table 3); with a position between C₁-C₃ being the most predominant (48.3%), in accordance with the findings of Becker and Grunt (1957) and Jamieson et al. (1952). In addition, it should be noted that the incidence of SCG above C₄ vertebra was 98.3%. This corroborates the findings of Jamieson *et al.* (1952) and Becker and Grunt (1957), who report a location above C₄ vertebra in 98% in both studies. In the adult specimens SCG was always located below C₁ vertebra, primarily between C₂-C₃ in 5 sides (62.5%) and the intervertebral discs between C₁₋₂ and C₂-C₃ in 4 sides (50%) (i.e. all

adult SCG, in this series was located above the 4th cervical vertebra). This study further reports SCG spanning over 2 vertebrae in 69% of cases.

In current surgical practice, resection of the SCG and its branches or of the entire cervical sympathetic trunk, from the SCG to CTG, is rarely practiced. Nevertheless, its importance as an anatomical landmark, its preference over other sympathetic ganglia in histological studies and its contributions to mediastinal and the cervical plexus, remains pivotal in understanding sympathetic pathways

5.2.3 Middle Cervical Ganglion

The nomenclature of MCG varies widely in the literature reviewed. According to the textbook definition of MCG “it is usually at the level of the 6th cervical vertebra” (Williams *et al.*, 1995). This study documented a varying location for MCG and has differentiated three types based on their vertebral location:

Type I: an MCG lying above the superior border of the 6th cervical vertebra (above C₆) – ‘high’ MCG;

Type II: a MCG lying on the body/transverse process of the 6th cervical vertebra (at C₆) – ‘typical/normal’ MCG;

Type III: a MCG lying below the inferior border of the 6th cervical vertebra (at C₆₋₇ and C₇) – ‘low’ MCG.

The 6th cervical vertebra was used as the reference point because the conventional textbook definition of MCG is that is usually found *at* the level of C₆ vertebra or may lie opposite CTG (level of C₇ vertebra) (Williams *et al.*, 1995).

This study records the overall incidence of MCG to be 81.1%. This compares favourably with the results of Becker and Grunt (1957) (81.1% vs. 87.7%). The weighted mean incidence calculated from the literature reviewed (Table 24) was 72.6%.

A double MCG was present in 25.9%. This differed widely from the results of Becker and Grunt (1957) and Jamieson *et al.* (1952) of 55.3% and 2%, respectively. This study,

however, confirms the findings of Jamieson et al.(1952) that two 'low' MCG (*Types II and III*) may be found on a single cervical chain. This study reports the bilateral incidence of MCG to be 31% ($^{18}/_{47}$ sides) comparing favourably with the result of 39% reported by Becker and Grunt (1957).

It should be noted that this study reports the higher incidence of the normal/typical MCG (as per textbook definition), *Type II* MCG (46.6%) than the *Type I* MCG (27.6%) and *Type III* (32.8%). Of the 15 chains in which a double MCG was found, in 8 sides [13.8%] *Types I and II* MCG were present; in 4 sides [6.9%] *Types I and III* MCG were present; while in 3 sides [5.2%] *Types II and III* were present. Therefore, a total of 62 MCG was found.

Type II MCG has been combined with *Type I* MCG to facilitate a comparison with the reviewed literature. A comparison of frequency of occurrence of *Types I and II* with *Type III* MCG, reported in literature and in this study is indicated in Table 29.

Table 29: Comparison of incidences of Types I & II MCG

Author	n	Type I & II (High)	Type III (Vertebral/ low/ intermediate)
Jamieson et al.(1952)	100	35	20.4
Kirgis & Kuntz (1942)	88	31.8	100
Pick & Sheehan (1946)	25	56	36
Mitchell (1953)	?	75-80	100(±)
Becker & Grunt. (1957)	114	62.3	87.7
Ellison & Williams (1969)	24	16.7	58.3
<i>Weighted Mean</i>	<i>351</i>	<i>40.4</i>	<i>67.1</i>
<i>THIS STUDY</i>	<i>58</i>	<i>74.2</i>	<i>32.8</i>

The weighted mean incidence for the 'high' MCG calculated from the literature reviewed (Table 29) differs significantly from the incidence reported in this study (40.4% vs. 74.2%). When compared to individual authors however similarities were noted in that Jamieson *et al.* (1952) and Pick and Sheehan (1946) reported a higher incidence of the 'high' MCG. It should be noted that if the normal/typical MCG was excluded from the 'high' MCG (as it should be) then this study reports the incidence of a 'high' MCG as 27.6% and a 'low' MCG as 31.8%. If this is compared to the literature reviewed then similarities were noted with the findings of Kirgis and Kuntz (1942) and Jamieson *et al.* (1952) who reported incidences for a 'high' MCG of 32% and 35%, respectively.

The results of this study show a greater frequency of MCG lying at or below the level of C6 vertebra (*Types II and III*), in keeping with the results of Kirgis and Kuntz (1942), Mitchell (1953) and Becker and Grunt (1957), who describe this MCG as occurring more frequently. Only Pick and Sheehan (1946) and Jamieson *et al.* (1952) report a greater incidence of the "high" MCG (*Type I* MCG).

Several other authors also comment on the greater frequency of the 'low'/'vertebral' ganglion but fail to provide numeric evidence (Axford, 1928, Sheehan, 1933, Woollard and Norrish, 1933, Saccomanno, 1943, Bonica, 1953). It should however be noted that various authors have used different vertebral levels to distinguish a high and a low MCG, e.g. Becker and Grunt (1957) defines a 'high' MCG as any ganglion lying at C6 vertebra or above; Jamieson *et al.* (1952) defines a 'high' MCG as any ganglion lying above the transverse process of C6 vertebra; Axford (1928) defined a 'high' MCG as occurring at the

level of the 5th or 6th cervical vertebra. Our results compared favourably with Jamieson *et al.* (1952) who reported the varying loci of MCG from C5 to C7.

The 'low' MCG is frequently referred to as the "vertebral ganglion" because of its frequent association with the vertebral artery. Some authors have suggested that the vertebral ganglion merely represents a detached portion of the MCG or ICG (Axford, 1928; Woolard and Norrish, 1933). However, Mitchell (1953) and Becker and Grunt (1957) report that this ganglion does not vary inversely in size with either the MCG or the ICG. This study corroborates this finding. The term 'vertebral ganglion' is inappropriate because the vertebral nerve arises from the CTG.

On the other hand, the term 'intermediate ganglion' purported by Jonnesco (1923) is inapt as well since this term is used to describe ganglia found on the rami communicantes and the ventral rami especially to the limb plexuses. Lazorthes and Cassans (1939) suggestion that the 'low' MCG be grouped together as CTG is badly chosen as the 'low' MCG cannot be regarded as a detached portion of CTG. Furthermore, the 'low' MCG is entirely cervical.

This study concurs with the observation of Potts (1925) that the *Types II* and *III* (low/vertebral) MCG supplies the cardiac plexus. The study also confirms the close relation of the vertebral artery to the *Type III* MCG.

The term “thyroid ganglion of Haller (or Krause)” has been applied to the ‘high’ MCG and is unsuitable because the ganglion is not closely related to the thyroid gland or to the inferior thyroid artery and furthermore there exists more than one thyroid artery.

The literature reviewed presented inconsistencies with regards to the vertebral levels of the ‘high’ and ‘low’ MCG. The cervical ganglia are recorded according to their positions relative to each other on the cervical chain viz. superior, middle and inferior ganglia. Differentiating MCG into *Type I*, *Type II* and *Type III* seems more appropriate because while it still maintains its name relative to the other cervical ganglia, *Type I*, *Type II* and *Type III* (not used previously in literature) will establish a common vertebral location for comparison. Hollinshead (1968) suggests the terms supero-middle and infero-middle.

In the adult specimens, the mean distance from the lower pole of SCG to the upper pole of the *Type I* MCG, *Type II* MCG and *Type III* MCG was 22.4mm, 55.2mm and 64.4mm, respectively [figure 29]. Jamieson reported the length of chain from the upper pole of SCG to the upper pole of MCG to be 57mm. He did not differentiate between the different types of MCG. Without differentiating between the three types of MCG, this study records a distance of 45.6mm between the lower pole of SCG and the upper pole of MCG. The distance between the lower pole of MCG (*Type II*) and the upper pole of CTG recorded in this study compares favourably with that reported by Jamieson *et al.*(1952) (12.6mm vs. 15mm).

There was no statistically significant differences in the mean length and width of adult *Types I, II* and *III* MCG [6.75mm, 3.17mm vs. 7.87mm, 3.73mm vs. 7.54mm, 3.84mm]. These concurred with the results of Becker and Grunt (1957) of 7-8mm in length but differed widely from the results of Jamieson *et al.* (1952) who reported the length of: 'low' MCG, 14mm; 'high' MCG, 3mm. Our results support the results of Becker and Grunt (1957) and Mitchell (1953) that the average size of the different types of MCG remains fairly constant regardless if one or the other is present.

This study also concurs with Axford (1928), Jamieson *et al.* (1952), Mitchell (1953) and Becker and Grunt (1952) that there is sufficient evidence to include two types of MCG as a constant entity in the cervical sympathetic chain.

5.2.4 Inferior Cervical Ganglion

Statistics on the occurrence of a separate ICG and T1 ganglion vary; Perlow and Vehe reported its presence in only 8 of 48 sides (16.7%); and Jamieson *et al.* (1952) 18 in 100 sides. Becker and Grunt (1957) described as separate ganglion in 62.3% of sides.

This study records the overall incidence of ICG to be 15.5%. Histology confirmed that no ganglion cells were present in the cord connecting this ganglion to the 1st thoracic ganglion. The weighted mean incidence calculated from the literature reviewed (Table 28) was 29.8% and differed significantly from the findings of this study. When compared to individual authors, similarities were noted in the findings of Perlow and Vehe (1935), Jamieson *et al.* (1952) and Jit and Mukerjee (1960) who reported incidences of 16.7%, 18% and 22%, respectively.

Jamieson *et al.* (1952) report a bilateral incidence of 9% while this dissertation records a bilateral incidence of 3.5%. The average length and width differed from the results of Jamieson *et al.* (1952) [9.86mm vs. 15mm and 3.66mm vs. 6mm].

It is not particularly important if one is dealing with an ICG or the upper end of a CTG-connections and relations are similar (Hollinshead, 1968).

5.2.5 Cervico-thoracic Ganglion

This study records the overall incidence of CTG to be 84.5%. The weighted mean incidence calculated from the literature reviewed (Table 28) was 74.5% and differed from the findings of this study. When compared to individual authors, similarities were noted in the findings of Jamieson *et al.* (1952), Perlow and Vehe (1935), and Ellison and Williams (1969) who reported incidences of 82%, 83.3% and 88%, respectively. Mitchell (1953) without calculating a weighted mean estimates the incidence of CTG to be between 75-80%. Only Becker and Grunt (1957) quote an incidence of 37.7% [Table 24], differing widely from this generally accepted view. The bilateral incidence of CTG reported in this study was 65.5%, confirming the result of 66% reported by Jit and Mukerjee (1960).

This dissertation records three shapes of CTG, inverted 'L' shape, spindle and dumbbell shapes with a higher incidence of the inverted 'L' shaped CTG (42.8%) as compared to the spindle and dumbbell shapes (28.6%, each). Jit and Mukerjee (1960) described extreme variability in the shape of the CTG: irregular, 26%; dumbbell, 16%; inverted 'L' shape, 16%, club shaped, 8%; quadrilateral, 5%, semilunar, 3%, spindle, 2% and rectangular, cone shaped, globular and fusiform, each 1%. Pelow and Vehe (1935) described CTG in their series as club shaped. A comparison of the reported incidence of shapes of CTG presents certain difficulties, as previous authors do not provide an illustration of their various shapes and how they distinguish between them e.g. irregular vs. club shaped; spindle vs. ovoid; quadrilateral vs. rectangular, fusiform vs. globular, etc. Furthermore, the name 'stellate ganglion', frequently attributed to CTG is inappropriate because the ganglion is never star

shaped. In addition, all other sympathetic chain ganglia are named according to their positions; either relative to each other (as in the cervical region) or according to their connection to the spinal nerves (as in the thoracic region). CTG seems a more appropriate term because it aptly describes the position of the ganglion at the junction between the cervical and thoracic regions.

The inverted 'L' and the dumbbell shapes showed a definite isthmus between the ICG and T1 ganglia components. Thus, this study records a definite constriction or 'waist' in 71.4% (³⁵/₄₉) of CTG. White et al. (1952) described a consistent, definite isthmus between the ICG and T1 components of CTG, while Becker & Grunt (1957) and Jit and Mukerjee (1960) reported the incidence of a definite isthmus to be only 37.7% (⁴³/₁₁₄) and 37.5% (³⁰/₈₀); respectively.

The mean length and width of CTG, in the adult, was found to be 16.51mm and 6.65mm, respectively. This length of CTG compares favourably with the results of Jamieson et al. (1952) and Jit and Mukerjee (1960) of 22mm, 8mm and 20.5mm; respectively while Becker and Grunt (1957) reported the length of CTG to be 28mm.

CTG lesions result in interruption of sympathetic fibres to the head, neck, arm and certain viscera. Preservation of CTG is clinically important to avoid complications of Horner's syndrome and cardiac arrhythmias. Ganglia residing superior to the 2nd rib are diligently preserved during limited sympathectomy (indicated for palmar hyperhidrosis, chronic regional pain syndromes).

The ansa subclavian

The ansa subclavia (also called the ansa Vieussens) joined the upper end of the CTG to MCG or directly to the chain and was constantly present in all specimens concurring with the findings of Jit and Mukerjee (1960). It comprised anterior and posterior limbs that joined the CTG/ICG to the Type II MCG, when present. When Type II MCG was absent AS attached superiorly to the Type III MCG. When both Type II and III MCG were present AS always attached to the Type II MCG and when both were absent it attached directly to the cord of the cervical sympathetic chain. The ansa contributed fibres to the plexus around the subclavian artery as reported previously by Jamieson *et al.* (1952).

The most common pattern of the cervical chain noted by Becker and Grunt (1957) is illustrated in figure 7 (literature review), while the variations in the chain in this series is indicated by figure 42. The most frequent chain (55.3%) documented by Becker and Grunt (1957) was only present in 13.8% of chains in this series (Type IIIa). The most frequent chain pattern documented in this series was *Type IIb* (27.6%).

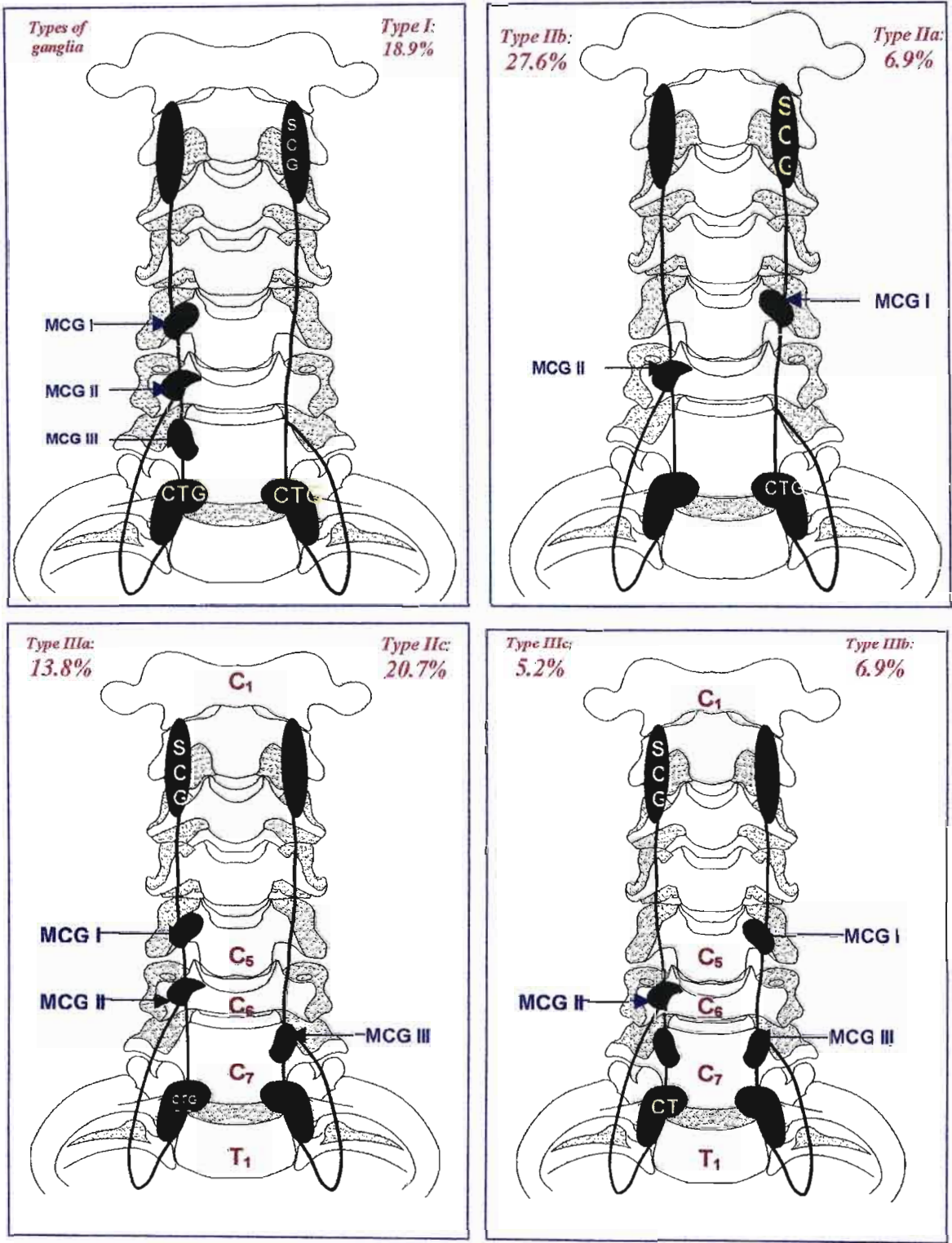


Figure 42: Diagrammatic illustration cervical chain Types

5.3 THORACIC SYMPATHETIC CHAIN

5.3.1 Course and relations

The course and relations of the thoracic sympathetic chain conformed to that described in the literature reviewed. The thoracic part of the chain is continuous at the root of the neck with the cervical sympathetic chain.

The sympathetic trunk lies lateral to the hemiazygos system of veins on the left side and the azygos vein of the right side. Both chains lie immediately against the pleura and, usually, in front of the intercostal vessels; thus facilitating the removal of the chain without injury to the vessels (Hollinshead, 1956). The venous pattern however may be variable and in the upper part of the thorax, the first intercostal vein typically passes in front of the chain.

The upper part of the chain (up to T6 vertebra) is located on the neck of the ribs, against the lateral surface of the vertebral bodies and the intervening intercostal space. The lower part of the chain lies on the vertebral bodies and the intervening intercostal space. At the level of the diaphragm, the chain deviates medially, to lie on the bodies of T₁₁-T₁₂ vertebra as it pierces the diaphragm.

Knowledge of the structure of the thoracic sympathetic trunk (ganglia and interganglionic segment), rami communicantes, and visceral (splanchnic) nerves assume great clinical importance to the surgeon performing limited sympathectomy via minimally invasive surgery. Recent literature on the physiological and clinical significance of the branches of

the sympathetic chain for such varied conditions such as hyperhydrosis, angina pectoris and pancreatitis have demanded a re-examination of the precise anatomy and topographical relations of the of the sympathetic chain.

5.3.2 Thoracic ganglia

While the cervical ganglia are given names relating to their positions on the sympathetic chain such a system of nomenclature cannot be applied to TG on account of their number and are therefore classified according to their segmental levels (Ellison and Williams, 1969). Pick and Sheehan (1946) have mentioned that in the thoracic region the segmental pattern of the trunk ganglia is often blurred by varying degrees of fusion or splitting of primordial cell masses. They found that occasionally the fourth ganglion is fused with the fifth and less often with the third ganglion.

The number of thoracic ganglia in this study is 8-11. Groen et al. (1987) reported the number of TG as varying between 8-10. Jit and Mukerjee (1960) reported the number of TG as: 11, 71%; 12 TG, 23%; 10 TG, 4%; 13 TG, 2%. Other investigators have reported (without providing incidences) 9-13 TG, in the adult (Hovalaque, 1927, White et al, 1952; Kuntz, 1953; Mitchell, 1953; Wrete, 1959; Pick, 1970). Toni and Frignani (1955) report the number of TG, in the foetus, to be 6-13. Fusion of ganglia was found to be more common in the lower thoracic chain than in the upper thoracic chain. This study records the following ganglia to be frequently fused with its neighbouring ganglion: T₉G, T₁₀G, T₁₁G and T₁₂G with an incidence of: T₉₋₁₀G, 52.9%; T₁₀₋₁₁G, 34.1% and T₁₁₋₁₂G, 43.5%.

The presence of the number of ganglia less than 12 is explained by fusion i.e. a merging of previously separated ganglia or a non-dehiscence of primordial ganglionic masses (Pick and Sheehan, 1946, Mitchell, 1953).

According to Pick's schema (figure 29), based on the embryological development of the ganglia, Types a, b and c ganglia were observed in this study. When types b and c were

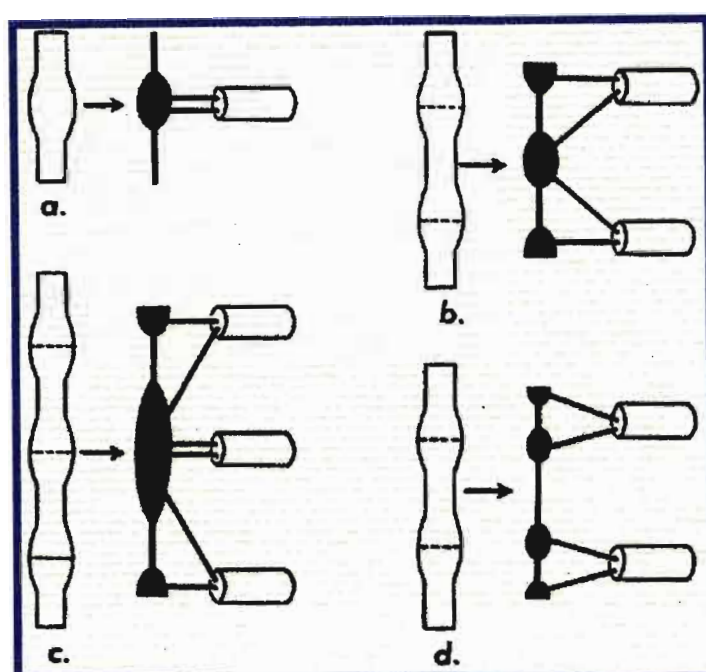


Figure 43: Schema illustrating the development of possible variations of the ganglionated chain from the primordial cell column [Adapted from Pick, 1970]

observed to be the only ganglion contributing to more than one spinal then it was considered fused and explained the occurrence of less than 12 ganglia. The Type d ganglion was not observed. The Type d ganglion represents the non-dehiscence of primordial masses and explains the observations of some authors of more than 12 ganglia.

An enumeration of ganglia in fetuses and adults is meaningless because of their fusion-related variability (Groen et al., 1987). In order to determine sympathetic segments according to Pick (1956, 1970) an extensive histological examination of all rami communicantes is necessary. This method can hardly be used in macro and microscopic dissection in view of the difficulty of differentiating grey from white rami (Wrete, 1959; Low and Dyck, 1978). Moreover rami are often mixed (Pick and Sheehan, 1946; Mitchell, 1953). Groen et al. (1987) suggests: 'a true comparison between foetal and adult stages and between specimens within each stage can be based upon a constant factor i.e. the thoracic spinal nerves and their connections with the sympathetic trunks.'

Interest in the connections of the thoracic sympathetic chain has been centered especially on those of the upper portion, because of the importance of these from the point of view of sympathectomies of the upper limb for such conditions such as hyperhidrosis, Raynaud's Disease, etc. If the fibres to the limb are to be interrupted by excision of a limited portion of the chain, or by section of the RC themselves then the anatomy of the RC becomes important (Hollinshead, 1956). Unfortunately, they vary more in the upper thoracic portion of the chain than anywhere else in the thorax. It is not possible to distinguish between white and gray rami communicantes macroscopically by their relationship to sympathetic ganglia. Wrete (1959) claimed that the distinction between white and gray rami becomes blurred in preserved tissue and is only faintly visible on fresh material. The number of rami communicantes and additional neural connections to the thoracic intercostal nerves is variable. Histological differentiation of gray and white rami remains technically difficult

and maybe inaccurate. Criteria for numbering TG require standardization for accurate identification.

The ascending course of rami described by Pick, 1970, is not in agreement with the findings of Potts (1925; Groen et al, 1987). Contrary to the findings of Kuntz (1953), Mitchell (1953), Pick (1957, 1970), Groen et al.(1987) demonstrated no preference of specific types of rami communicantes for a distinct region of the sympathetic chain. This study confirms the findings of Groen et al. (1987) that each region showed no preference for particular types of rami (i.e. posterior, antero-lateral) but did note that the rami in the upper thoracic chain ascend to meet that spinal nerve while in the lower chain the rami ascend and descend to meet its connecting spinal nerves.

The thoracic arterial pattern exhibits fewer variations. The method proposed by Wrete (1959) utilizing segmental arteries for identification appears to have merit and is worthy of re-evaluation. Wrete considers the numbering should be quite independent if communicating rami, which are highly variable in their course. He suggests each ganglion should be named after the space between the intercostal arteries. His suggestion is not free from objections since there may be 2 ganglia in a space or a space may be devoid of a ganglion. Furthermore variations in the arterial pattern exists.

5.4 CARDIAC SYMPATHETIC NERVES

Cardiac rami are generally named according to the ganglion nearest its point of origin from the sympathetic trunk (Ellison and Williams, 1969).

According to Mitchell (1956), in the classical anatomical textbooks (1772 to 1920), only the cervical cardiac nerves are shown as 3 distinct trunks arising from the corresponding ganglia descending downwards to the deep cardiac plexus: “The important anatomical discovery of the thoracic cardiac nerves which form direct connections between the upper 4 or 5 thoracic ganglia to the heart was made concurrently by Braeucker and Jonnesco and Enarchesco in 1927” (White and Smithwick, 1942). Subsequent reports on the extent of the origin of TCR vary amongst authors, from SCG: to T2 (Perman, 1924); to T3 (Kuntz and Morehouse, 1930) and to T4/5 (Mizeres, 1972). The literature reviewed is vague regarding the incidence of cardiac rami, particularly with regards to the thoracic cardiac rami.

This study reports the origin of TCR from the thoracic sympathetic chain up to the interganglionic segment between T₅ and T₆ ganglia. The incidence of TCR₅ was 60.4%. In $\frac{15}{58}$ sides (25.9 %) TCR₅ arose from the interganglionic segment of the chain, either above or below the ganglion. The origin of the ramus from the interganglionic segment was as follows: between T₅G and T₆G, $\frac{14}{15}$ sides [93.3%: right, $\frac{7}{7}$ sides (100%); left $\frac{7}{8}$ sides (87.5%)]; between T₅G and fused T₆₋₇G ganglia, $\frac{1}{15}$ sides [6.7%: right, $\frac{0}{7}$ sides; left $\frac{1}{8}$

sides (12.5%)]. It should be noted that this study records an interganglionic origin occurring between T5 ganglion and a fused T₆₋₇G ganglion (6.7%).

Cannon et al.(1926) demonstrated cardiac nerves bilaterally from the first 3 or 4 ganglia below CTG. They suggested from their physiological investigations, that some nerves, which are too small to be observed in gross dissections, might be present at still lower levels.

Ellison and Williams, 1969, reported the infrequent symmetry in the thoracic cardiac nerves and concluded that “though various features are commonly present on both sides the first dissection in the cervicothoracic sympathectomy is no reliable guide to the detailed anatomy on the second side”.

The results of this study corroborates the inter- and intra-individual variability in the origin of cardiac sympathetic nerves documented by Ellison and Williams (1969). The study confirms the great variability in the origin of CCR as demonstrated by Mizeres (1972). Variability in the origin of the cardiac nerves was also seen in the thoracic region.

Furthermore, CCR and TCR were also noted to arborize in the deep cardiac plexus. The superficial plexus was not clearly distinguishable from the deep plexus concurring with the independent studies of Mitchell (1956) and Mizeres (1972) who suggests that the superficial and deep cardiac plexuses are created by artificial dissection. No direct branches from the sympathetic chain were traced to the pulmonary plexus. The branches

traced to the bronchi from the cardiac plexus appear to support the view that these TCR should be more accurately named cardiopulmonary nerves. A detailed study of the pulmonary plexus is warranted.

The success of limited T2-4 sympathectomy in relieving pain at rest, of patients with intractable angina pectoris, appears to indicate that a significant afferent pain pathway from the heart is selectively interrupted (Khogali et al, 1999). Cardiac sympathetic denervation via video assisted thoroscopic surgery is reported to be successful with increased exercise tolerance time, ECG improvement, some degree of anti-ischaemic effect, reduction in angina symptoms, decreased incidence of tachy-arrhythmias, unaffected left ventricular function and an improved quality of life with a one year follow up (Wettersvik et al, 1995). Importantly, the patients do not lose their warning signal of an angina attack and were able take the necessary pharmacological action (Khogali et al, 1999). It is interesting to note that the variability in pattern of the cervical ganglia, CCR and cardiac plexus does not appear to impact on the outcome of limited thoracic sympathectomy for pain relief.

However, the complexity of cardiac pain pathways is not fully understood. A physiological study of the role of these nerves in cardiac pain together with a clinical series is warranted to contribute to defining the afferent and efferent cardiac pathways, particularly the contributions of the CTG and first thoracic ganglion to the cardiac plexus.

5.5 OTHER MEDIAL BRANCHES

5.5.1 Splanchnic nerves

This study records the following incidence of the splanchnic nerves: GSN; 100%; LSN, 87.5% [right, 91.2%; left, 83.3%]; Isn, 45.8% [right, 41.7%; left, 50.0%]. The constant presence of GSN concurred with the reports of previous authors (Table 30).

Table 30: Reported incidence of GSN, LSN and Isn

Author	Year	n=	Incidence (%)			
			GSN	LSN	Isn	ASN
<i>Matsui (cited Jit and Mukerjee)</i>	1925		100	100	98.3	-
<i>De Sousa Pereira (cited Jit and Mukerjee)</i>	1929		100	99	46	4
<i>Edwards & Baker</i>	1940	100	100	95.5	92.5	-
<i>Näätänen (cited Jit and Mukerjee)</i>	1947		100	94	16	-
<i>Contu & Mattioli (cited Jit and Mukerjee)</i>	1953		100	99	17	-
<i>de Sousa (cited Jit and Mukerjee)</i>	1955		100	100	80	18
<i>Jit & Mukerjee</i>	1960	100	100	86	37	0
<i>Naidoo et al. (in press)</i>	2001	38	100	92.1	55.2	0
Weighted Mean			100	95.7	55.2	0
This study			100	87.5	45.8	0

KEY: GSN = Greater Splanchnic Nerve; LSN = Lesser Splanchnic Nerve; Isn = Least Splanchnic Nerve; ASN = Accessory Splanchnic nerve

The weighted mean incidence of LSN calculated from the literature reviewed (Table 30) was 95.7%. This study reports an incidence of 87.5%. When compared to individual authors, similarities were noted in the findings of Jit and Mukerjee (1960) and Naidoo *et al.* (*in press*) who reported incidences of 86% and 92.1%; respectively.

The weighted mean incidence of Isn calculated from the literature reviewed (Table 30) was 55.2% and differed significantly from the result of this study (45.8%). When compared to individual authors, similarities were noted in the findings of Jit and Mukerjee (1960) and De Sousa Pereira (1926) who reported incidences of 37% and 46%; respectively.

The number of roots of GSN varied from 2-8, with the number of roots ranging from 3-5 being most common [$^{39}/_{48}$ sides (81.3%); right, $^{19}/_{24}$ sides (79.2%); left, $^{20}/_{24}$ sides (83.4%)]. Jit and Mukerjee (1960) found the origin of the GSN to vary from 1-8 roots with 4 being the most common (31%). There was no correlation between number of roots of GSN with the absence of the LSN and Isn. A comparison between the incidence of the number of roots between this series and the series documented by Jit and Mukerjee is given in Table 31.

Table 31: Comparison of number of roots of GSN

<i>No of Roots</i>	Jit & Mukerjee (1960)	<i>This study</i>
2	9	14.6
3	29	29.2
4	31	31.3
5	15	20.8
6	7	2.1
7	2	-
8	2	2.1

In the foetus, Groen et al. (1987) found the GSN to arise from 1-4 large branches most frequently from T8-9 ganglia with highest origin being T6 and the lowest being T11

ganglion. Intra-individual differences in the origin and number of the splanchnic nerve rami were frequently observed.

Edwards and Baker (1940) employed more flexible criteria in the classification of splanchnic nerve origin, allowing for the absence of a single root of origin from one ganglion e.g. T5, 6, 8, 9,10. On the other hand, if the GSN arose from ganglia T5, 8, 9,10 or T4, 5, 7, 8, 10 with the absence of two or more ganglionic roots, it was not classified as normal. They found in 100 cases that the GSN conformed to the so-called “normal pattern” in 23% and that the nerves were rarely bilaterally symmetrical, originating most frequently from T7-9 ganglia.

In 16.7% the highest root of GSN was above the T5 ganglion. This has clinical implications, given the widely discussed technique of undertaking splanchnicectomy from the T5 ganglion distally, as employed by Stone and Chauvin, 1990 (Naidoo et al, *in press*). This approach overlooks important nerve contributions and thereby may compromise clinical outcome.

Jit and Mukerjee (1960) found the LSN in 86% of cases with the number of roots varying from 1-4. The most common roots were from T10 and T11 ganglia. Wittmoser (1995) and Reber (1987) recorded that the branches formed by thoracic ganglia found in the 9th-11th intercostal spaces were destined for the upper abdomen in general and the pancreas in particular. In the foetus, Groen et al. (1987) observed the LSN originating via 1-2 rami from thoracic segments T10 and T11 (range T10-T12).

The advent of minimally invasive and video assisted surgery has rekindled interest in the variable patterns of the splanchnic nerves. It is postulated that the inconsistent results of splanchnicectomies for the palliation of abdominal pain for conditions such as chronic pancreatitis and pancreatic carcinoma may be due to anatomical variations in the splanchnic neural pattern (Naidoo *et al.*, *in press*).

In the light of the described GSN variations, it is suggested that the procedure to effect splanchnicectomy be undertaken from the level of the T3 ganglion (Naidoo *et al.*, *in press*). In patients where recurrence of pain occurs following splanchnicectomy, it may be postulated that the medial collateral branches – often under appreciated by the surgeon – provide an alternate neural pathway via the aortic and oesophageal plexuses to the upper sympathetic chain. The reported early results following the discussed technique attests to the value of the thoracoscopic procedure as well as the completeness of denervation afforded by this method (Moodley *et al.*, 1999).

5.5.2 Vascular branches

CTG contributed a consistent lateral branch to the vertebral artery, which ran upwards to enter foramen transversarium, together with the vertebral artery. This is in keeping with the results of Mitchell (1953) and Pick (1970). The vertebral nerve contributes fibres around the vertebral artery. The plexus thus formed however does not follow the vertebral artery into the skull but is replaced in the upper part of the neck by another plexus whose sensory fibres are derived from the SCG via the 2nd and 3rd spinal nerves (Hollinshead, 1968).

Rami from CTG winding around the subclavian artery were recorded in 71.4% with 2 rami existing in 29.2% of these. Where the ICG and T1 ganglion were unfused, a ramus from the right T1 ganglion was recorded to the subclavian artery. No rami were recorded from the unfused ICG.

The ansa subclavia was distinctly separate from the above branches and was observed in 100% of cases and comprised anterior and posterior limbs that formed a loop around the subclavian artery. In 18/28 sides [64.3%: right, 8/28 (28.6%); left, 11/28 (39.3%)] the ansa subclavia contributed to the plexus around the subclavian artery thus confirming the results of Jamieson *et al.* (1952) that it passed to the subclavian artery, and form a sympathetic plexus around this artery.

This study corroborates the findings of Mitchell (1956) and Pick (1970) that the SCG, MCG and CTG contribute rami to the common carotid artery, the internal and external carotid artery and its branches.

This study further records branches from the chain between MCG and T1 ganglion, inclusive, to the brachiocephalic trunk in 17% of specimens. These rami were present in half of all the adults dissected in this series.

The removal of the CTG was for many years the operation of choice in attempts to alleviate the symptoms of Raynaud's disease. 'Stellectomy' and removal of the upper segments of the thoracic chain resulted in postganglionic or anatomical denervation of the blood vessels to the upper limb and in view of the ensuing selectivity to epinephrine, which has been said to occur after postganglionic denervation, was for some time abandoned by many surgeons. In recent years, however, a number of clinicians have reverted to the postganglionic denervation as the one giving most favourable and long-term results (Hollinshead, 1968).

The peri-vascular sympathetic contributions issued proximally to the subclavian artery and the brachiocephalic trunk may represent alternate neural pathways to the upper limb and account for the inconsistent and unpredictable results obtained at surgery. Moreover, the close relationship of the sympathetic nerves with blood vessels needs to be considered in the management of conditions such as axillary hyperhidrosis and high sympathetic dystrophy. These relations may be important landmarks for easier identification of these

nerves, especially in this millennium of minimally invasive surgery and a further investigation is essential.

5.5.3 Miscellaneous

Communications to the phrenic nerve were not noted. This study concurs with the inference of Jit and Mukerjee (1960) that “it is doubtful if Mitchell’s (1953) statement that the ‘ganglion (CTG) or the ansa subclavia invariably communicates with the phrenic nerve’ is true.”

During the course of this investigation, branches to the pharynx were noted. In view of the sympathetic contributions to the pharynx that was noted it is suggested that the innervation of the pharynx and larynx be investigated.

Direct contributions to the pulmonary plexus were not noted. However, this study records contribution from the cardiac plexus to the pulmonary plexus. In light of the observations in this study and the studies by Mitchell (1956) suggesting that the pulmonary plexus is a continuation of the cardiac plexus an investigation of the innervation of the lungs is warranted.

CHAPTER 6

CONCLUSION

The course and relations of the cervical and thoracic sympathetic chain were confirmed to be similar to currently accepted norms. This study records a double cervical sympathetic chain extending from the lower pole of SCG to the upper pole of ICG in one adult side. The incidence of this occurrence is unclear in the literature reviewed.

This study confirms the constant presence of SCG, located between C₁-C₄ vertebrae; with a position between C₁-C₃ being most predominant (48.3%). However, it should be noted that the incidence of SCG above C₄ vertebra was 98.3%. In the adult specimens, SCG was always located below C₁ vertebra, primarily between C₂-C₃ (62.5%) and the intervertebral discs between C₁₋₂ and C₂-C₃ (50%).

This study also concurs with Axford (1928), Jamieson et al.(1952), Mitchell (1953) and Becker and Grunt (1952) in that there is sufficient evidence to include 4 ganglia as a constant entity in the cervical sympathetic chain.

A total of 62 MCG was found. A double MCG was present 25.9%. This study differentiates between three types of MCG (Types I, II & III). It should be noted that this study reports the higher incidence of the normal/typical MCG (as per textbook definition), i.e. *Type II* MCG (46.6%) than the *Type I* MCG (27.6%) and *Type III* (32.8%). Of the 15 chains in which a double MCG was found, in 13.8% *Types I* and *II* MCG were present; in 6.9% *Types I* and *III* MCG were present; while in 5.2% *Types II* and *III* were present.

It is proposed that previous terminology used to distinguish the two types of MCG, viz. 'high' and 'low', intermediate, thyroid or vertebral, be disregarded in view of their inaptness and inconsistencies amongst authors.

This dissertation records the overall incidence of ICG to be 15.5%, in keeping with the reported incidence in literature.

The incidence of CTG was 84.5%. Three shapes of CTG were recorded: inverted 'L' shape, spindle and dumbbell shapes. The inverted 'L' shaped CTG had a higher incidence (42.8%) than the spindle and dumbbell shapes (28.6%, each). A definite isthmus ('waist') between the ICG and T1 ganglia components of CTG was demonstrated in the inverted 'L' and the dumbbell shapes (71.4%). The term 'stellate ganglion', frequently attributed to CTG is inappropriate because the ganglion is never star shaped. CTG seems a more appropriate term because it aptly describes the position of the ganglion at the junction between the cervical and thoracic regions.

The number of thoracic ganglia in this study is 8-11. This study records a frequent fusion of T₉G and T₁₀G and T₁₁G and T₁₂G. Fusion of ganglia was found to be more common in the lower thoracic chain than in the upper thoracic chain.

The incidence of CCR and TCR are documented. This study further reports the origin of TCR from the thoracic sympathetic chain up to the interganglionic segment between T₅G and T₆₋₇G ganglia.

The incidence of the splanchnic nerves were: GSN; 100%; LSN, 87.5% and lsn, 45.8%.

Vascular branches from the cervical sympathetic chain were documented to the subclavian, vertebral , common carotid, internal carotid and external carotid arteries. This study further records branches from the chain between MCG and T1 ganglion, inclusive, to the brachiocephalic trunk in 17% of specimens.

An accurate knowledge of the anatomy of the sympathetic nervous system and the adjacent structures is, inescapably a definite asset to the procedures used in interrupting the neural mechanism (Jamieson *et al.*, 1952). Successful sympathetic denervation of the heart, a field often beset with failure, is dependant on adequate morphological knowledge. It is hoped that this study using human fetuses as well as adult cadaveric specimens will draw the attention to important variations that are relevant to the surgeon.

The intricate anatomical relations presented in this study attests the complex anatomy of the sympathetic nervous system

REFERENCES

JOURNALS

1. ACKERKNECHT E H (1974) The history of the discovery of the autonomic nervous system. *Medical History* **18**, 1-8
2. ADAMS D C R, WOOD S J, TULLOH B R, BAIRD R N, POSKITT K R (1992) Endoscopic transthoracic sympathectomy : experience in the South West of England. *European Journal of Vascular Surgery* **6**, 558-562
3. ADAR R (1994) Surgical treatment of palmar hyperhidrosis before thoracoscopy : experience with 475 patients. *European Journal of Surgery Suppl.* **572**, 9-11
4. ADAR R, KURCHIN A, ZWEIG A, MOZES M (1977) Palmar hyperhidrosis and its surgical treatment. *Annals of Surgery* **186**, 34-41
5. ALEXANDER HL (1933) The autonomic control of the heart, lungs and bronchi. *Annals of internal medicine: American college of surgeons and physicians*, **Jul 1**, 1033-1043
6. ALEXANDER W F, KUNTZ A, HENDERSON W P, EHLICH E (1949) Sympathetic conduction pathways independent of sympathetic trunks – their surgical implications. *Journal of the International College of Surgeons* **12**, 111-119

-
7. ALLAN F D (1958) An analysis of the cervicothoracic visceral branches of the vagus and the sympathetic trunk in the presence of an anomolus right subclavian artery. *Anatomical Record* **132**, 71-80
 8. AXFORD M (1928) Some observations on the cervical sympathetic in man. *Journal of Anatomy* **62**: 301-318
 9. AZAKIE A, MCELHINNEY D B, THOMPSON R W, RAVEN R B, MESSINA L M, STONEY R J (1998) Surgical management of the subclavian vein effort thrombosis as a result of thoracic outlet compression. *Journal of Vascular Surgery*, **28(5)**, 777-786
 10. BALJET B, DRUKKER J (1975) An acetylcholinesterase method for in toto staining of peripheral nerves. *Stain Technology* **50(1)**, 31-36
 11. BALJET B, DRUKKER J (1981) Some aspects of the innervation of the abdominal and pelvic organs in the human fetal fetus. *Acta Anatomica* **111**, 222-280
 12. BALJET B, DRUKKER J (1979) The extrinsic innervation of the abdominal organs in the female rat. *Acta Anatomica* **104**, 243-267
 13. BECKER R F, GRUNT J A (Jan. 1957) The cervical sympathetic ganglia. *Anatomical Record*, 127 (1), 1-14

-
14. BONICA J J (July-Aug, 1968) Autonomic innervation of the viscera in relation to nerve block. *Anaesthesiology* **29**(4), 293-813
 15. BOYD J D (1957) Intermediate sympathetic ganglia. *British Medical Bulletin* 207-212
 16. BROOKER R M (1940) Anatomic studies of the sympathetic nervous system. *Archives of Surgery*, 799-806
 17. CANNON WB, ROSENBLUETH A (1933) Studies on conditions of activity in endocrine organs: XXIX Sympathin E and Sympathin I. *American Journal of Physiology* **104**:557-574
 18. CLAES G, GOTHBERG G, DROTT C (1993) Endoscopic electrocautery of the thoracic sympathetic chain: a minimally invasive method to treat hyperhidrosis. *Scandinavian journal of plastic and reconstructive hand surgery* **27**, 29-33
 19. CUSCHIERI A, SHIMI SM, CROSTHWAITE G, JOYPAUL V (1994) Bilateral endoscopic splanchnicectomy through a posterior thoracoscopic approach. *Journal of the Royal College of Surgeons (Edinburgh)* **39**, 44-47.
 20. DROTT C (1994) The history of cervicothoracic sympathectomy. *European Journal of Surgery Supplement* **572**, 5-7
-

21. EDWARDS LF, BAKER RC (1940) Variations in the formation of the splanchnic nerves in man. *Anatomical Record* **77**, 335-342.
22. EHRLICH E, ALEXANDER W F (1951) Surgical implications of upper thoracic independent sympathetic pathways. *AMA Archives of Surgery* **62(5)**, 609-614
23. ELLISON JP, WILLIAMS TP (1969) Sympathetic nerve pathways to the human heart, and their variations. *American Journal of Anatomy* **124**, 149-162
24. GROEN GJ, BALJET B, BOEKELAAR AB, DRUKKER J (1987) Branches of the sympathetic trunk in the human foetus. *Anatomical Embrologie* **176**, 401-411.
25. HASHMONAI M, KOPPELMAN D, SCHEIN M (1994) Thoracoscopic versus open suparclavicular upper dorsal sympathectomy : a prospective randomised trial -. *European Journal of Surgery Suppl.* **572**, 13-16
26. HAUGEN F P (1968) The autonomic nervous system and pain. *Anaesthesiology* **29(9)**, 785-792
27. HOLLINSHEAD WH (1956) *Anatomy for Surgeons*. Volume 2. Cassell and Company Limited: New York, USA, 197-214
28. HOVALAQUE A (1927) *Anatomie des nerfs craniens et rachidiens et du systeme grand sympathique chez l'homme*. G Dion et Cie: Paris

29. JAMIESON RW, SMITH DB, ANSON BJ (1952) The cervical sympathetic ganglia-an anatomical study of 100 cervicothoracic dissections *Quart Bull, Northwestern University Medical School* **26**:219-227
30. JIT I, MUKERJEE RN (1960) Observations on the anatomy of the human thoracic sympathetic chain and its branches; with an anatomical assessment of operations for hypertension. *Journal of Anatomical Society of India* **9**, 55-82.
31. KHOGALI SS, MILLER M, RAJESH PB, MURRAY RG, BEATTIE JM (1999) Video-assisted thoracoscopic sympathectomy for severe intractable angina. *European Journal of Cardiovascular Surgery* **16** (1), 595-598
32. KIMMEL DL (1959) The cervical sympathetic rami and the vertebral plexus in the human fetus. *Journal of Comparative Anatomy* **112**, 141-161
33. KIRGIS H D (1941) A ramus connecting the 3rd & 2nd thoracic nerve. *Anatomical Record Suppl.* **2**, 37-38
34. KIRGIS H D, KUNTZ A (1942) Inconstant sympathetic neural pathways. *Archives of surgery* **44**, 95-102
35. KUNTZ A, WILLIAM F, ALEXANDER M S, FURCOLO C L – Complete sympathetic denervation of the upper extremity. *Annals of Surgery* **107**, 25-31

-
36. KUNTZ A (1927) Distribution of the sympathetic rami to the brachial plexus. *Archives of Surgery* **15**, 871-877
37. KUNTZ A, ALEXANDER W F (1959) Surgical implications of lower thoracic and lumbar independent sympathetic pathways. *Archives of Surgery* **61**, 1007-1018
38. KUNTZ A, MOREHOUSE A (1930) Thoracic sympathetic cardiac nerves in man. *Archives of Surgery* **20**, 607-613
39. LANGLEY JN (1896) On the nerve cell connection of splanchnic nerve fibres. *Journal of Physiology* **20**, 223-246
40. LAZORTHES G, CASSAN L (1939) Essai de schematisation des ganglions étoile et intermediaire. *CR Ass. Anat. (Programme de la de Budapest)*
41. LINDNER H H, KEMPRUD E (Nov., 1971) A clinicoanatomical study of the arcuate ligament of the Diaphragm. *Archives of Surgery* **103**, 600-605
42. MALLET-GUY M, DE BEAUJEU M J – Treatment of chronic pancreatitis by unilateral splanchnicectomy. *Archives of Surgery* 233-241
43. MCLACHLAN EM – The formation of synapses in the mammalian sympathetic ganglia reinnervated with preganglionic or somatic nerves. *Journal of Physiology* (1974) **237**, 217-247
-

-
44. MIDTGAARD K (1986) A new device for the treatment of hyperhidrosis by iontophoresis. *British Journal of Dermatology* **114**, 485-488
45. MIZERES NJ (1972) The Cardiac Plexus in Man. *American Journal Anatomy*, **112**, 141-151
46. MOODLEY J, SINGH B, SHAIK AS, HAFJEJE A, RUBIN J (1999) Thoracoscopic splanchnicectomy – A pilot evaluation of a simple alternative for chronic pancreatic pain control. *World Journal of Surgery* **23**, 688-692
47. ORKIN LR, PAPPER EM, ROVENSTEIN EA (1950) The complications of stellate and lumbar sympathetic ganglia. *Journal of Thoracic Surgery* **20**:911-922
48. PERLOW S, VEHE K L (Dec, 1935) Variations in the gross anatomy of the stellate and lumbar sympathetic ganglia. *American Journal of Anatomy* **30(3)**, 454-458
49. PERMAN E (1924) Anatomische untersuchungen uber die herznerven bei den hoheren saugetieren und beim menschen. *Ztschr. F. Anat u. Entewg*, **71**, 382-457
50. PICK J (1957) The identification of sympathetic segments. *Annals of Surgery* **145** (3), pp. 355-364
51. PICK J (1970) *The Autonomic Nervous System: Morphological, Clinical and Surgical Aspects*. JB Lippencott Company: Philadelphia.

52. PICK J, SHEEHAN D (1946) Sympathetic rami in man. *Journal of Anatomy* 8, 12-20
53. POTTS T K (1925) The main peripheral connections of the human sympathetic nervous system. *Journal of Anatomy* 59, 129-135
54. QVIST G (1977) The course and relations of the left phrenic nerve in the neck. *Journal of Anatomy* 124 (3), 803-805
55. REED AF (1951) The origin of the splanchnic nerves. *Anatomical Record* 109, 341.
56. REGIELE L (1926) Uber die innervation der hals-und brustogane bei einigen Affen. *Z. ges Anat. I Z Anat EntwGesh* 80:777-858
57. RIED A. (1634) A description of the body of man. Th Cotes:London 117
58. ROB C, TUCKWELL E G – *Upper thoracic sympathetic ganglionectomy*. O.S. pt V11, 8-19
59. SACCOMANNO G (1943) The components of upper thoracic sympathetic nerves *Journal of Comparative Neurology* 79:355-378
60. SHAIK A S (July 1997) Present status of sympathectomy .

-
61. SHEEHAN D (1933) On the innervation of the blood vessels of the upper extremity; some anatomical considerations. *British Journal of Surgery* **20**:412-424
62. SHEEHAN D (1936) Discovery of the autonomic nervous system. *Archives of Neurology and Psychiatry: Chicago* **35**:1081-1115
63. SHELLEY W B, FLORENCE R (1960) Compensatory hyperhidrosis after sympathectomy. *New England Medical Journal* **263**, 1056-1058
64. SKOOG T (1947) Ganglia in the communicating rami of the cervical sympathetic trunk. *Lancet* **2**: 457-460
65. SINGH B, MOODLEY J, HAFEEJEE AA (May 1998) The current status of sympathectomy in general surgery. *Hospital Supplies* pp. 3-11
66. SIWE SA (1931) The cervical part of the ganglionated cord, with specific references to its connections with the spinal nerves and certain cerebral nerves. *American Journal of Anatomy* **48**:479-497
67. SMITHWICK R H (Jan, 1940) A technique for splanchnic resection for hypertension. *Surgery* **7** (1) pp. 1-8

-
68. STONE HH, CHAUVIN EJ (1990) Pancreatic denervation for pain relief in chronic alcohol associated pancreatitis. *British Journal of Surgery* 77, 303-305.
69. STRICKLAND T C, DITTA T L, RIOPELLE J M (1996) Performance of local anaesthetic and placebo splanchnic blocks via indwelling catheters in a patient with retractable pancreatic pain. *Anaesthesiology* 84, 980-983
70. TELFORD E D The technique of sympathectomy. *British Journal of Surgery* 23, 448-450
71. TONI G, FRIGNANI, R (1955A) Osservazioni sul segmento toracico della catena simpatica neo neonati quad *Anat Prac Napoli* 10: 285-294
72. WETTERVIK C, CLAES G, DROTT C, EMANUELSSON H, LOMSKY M, RADBERG G, TYGESEN H (1995) Endoscopic transthoracic sympathectomy for severe angina. *Lancet* 345(8942), 97-98
73. WILLIAMS T H, PALAY S L (1969) Ultrastructure of the small neurons in the superior cervical region. *Brain Research* 15, 17-34
74. WITTMOSER R (1995) Thoracoscopic sympathectomy and vagotomy. in *Endoscopic Surgery*. UTET:110-133.

75. WOOLLARD HH, NORRISH RE (1933) The anatomy of the peripheral sympathetic nervous system. *British Journal of Surgery* **21**:83-103
76. WRETE M (1951) Ganglia of rami communicantes in man and mammals particularly the monkey. *Acta Anatomica* **13**, 329-336
77. ZUCKERMAN S (1938) Observations on the autonomic nervous system and on the vertebral and neural segmentation in monkeys. *Trans. Zoo.Soc. Lond.* **23**:315-378

TEXTBOOKS

1. AGUR AMB (1991) *Grant's atlas of anatomy*. 9th edition: Williams and Wilkins: Baltimore, Philadelphia, Hong Kong, London, Munich, Sydney, Tokyo.
2. BERGMAN RA, THOMPSON SA, ASISI AK, SAADEH FA (1988) *Compendium of human anatomic variations: text atlas and world literature*. Urban and Schwarzenburg: Baltimore, Munich
3. BONICA J J (1953) *The management of pain*. Lea & Febiger: Philadelphia
4. GABELLA G (1976) *Structure of the autonomic nervous system*. Wiley and Sons: New York
5. KUNTZ A (1934) *The Autonomic Nervous System*. 2nd edition: Bailliere, Tindall and Cox, Convent Garden, London.
6. MCMINN RMH (1995) – *Last's Anatomy : Regional and applied*. Churchill & Livingstone : Edinburgh, London, Melbourne and New York, 8th edition pp 280-281; 441
7. MITCHELL GAG (1953) *Anatomy of the Autonomic Nervous System*: Livingstone: Edinburgh.

-
8. MITCHELL GAG (1956) *Cardiovascular Innervation*. Edinburgh, London: Livingston, 196-225
 9. NETTER FH (1989) *Atlas of human anatomy*. Fiber Guy Co-operations. Summit: New Jersey
 10. O'MALLEY CD (1964) *Andreas Versalius of Brussels*. University of California Press: Berkeley 480
 11. REBER HA (1987) *Palliative operations for pancreatic cancer: Surgical disease of the pancreas*. Lea and Febiger, 725-733.
 12. ROSS JP (1958) *Surgery of the sympathetic nervous system*, pp 154-160, 3rd edition, Baillere, Tindall and Cox
 13. WHITE JC, SMITHWICK RH (1942) *The autonomic nervous system*. London: Kimpton, 275-306
 14. Williams PL, Bannister LH, Berry MM, Collin P, Dyson M, Dussec JE, Furgurson MJ (1995) *Grays Anatomy* Churchill Livingstone: New York

APPENDIX A

Specimen details

	SP. NO	TAG NO	C-R (mm)	COMMENTS
FOETUS	1	3001	266	
	2	3002	310	
	3	3003	265	TISSUE DAMAGE -RIGHT
	4	3004	300	
	5	A	207	
	6	B	276	
	7	C	295	
	8	D	167	
	9	E	305	
	10	F	400	
	11	G	315	
	12	H	340	
	13	I	265	
	14	J	315	
	15	L	267	
	16	M	299	
	17	P	327	
	18	N1	107	TISSUE DAMAGE -LEFT
	19	N10	392	
	20	N11	156	
	21	N12	189	
	22	N13	413	
	23	N2	222	
	24	N3	305	
	25	N4	410	
	26	N5	153	
	27	N6	123	
	28	N7	264	
	29	N8	173	
	30	N9	311	
	31	O	276	
ADULT	32	UND 1999C		
	33	UND 1999D		PLEURAL ADHESIONS -RIGHT
	34	UND 1999A		
	35	UND 1999B		PLEURAL ADHESIONS - LEFT
	36	UND 1999E		
	37	UND 2000G		PLEURAL ADHESIONS -RIGHT
	38	UND 2000C		
	39	UND 2000E		PLEURAL ADHESIONS -RIGHT
	40	NTECH 1999A		
	41	NTECH 1999B		
	42	NTECH1999C		
	43	UDW 3006		PLEURAL ADHESIONS -RIGHT
	44	UDW 3005		
	45	UDW N33		
	46	UDW N34		
	47	UDW N35		
	48	UDW N36		

APPENDIX B

SCG LENGTHS AND WIDTHS

	SP. NO	TAG NO	LENGTH		WIDTH	
			RIGHT	LEFT	RIGHT	LEFT
FOETUS	1	3001	9.32	10.23		
	5	A	8.97	8.65		
	6	B	4.67	4.88		
	7	C	10.19	10.63		
	8	D	5.61	6.11		
	11	G	7.34	7.51		
	12	H	10.32	11.28		
	13	I	8.44	8.56		
	14	J	10.27	11.04		
	15	L	9.67	4.88		
	16	M	6.22	6.21		
	17	P	9.98	9.77		
	19	N10	9.73	9.64		
	20	N11	10.03	9.66		
	22	N13	9.54	9.61		
	23	N2	8.94	9.11		
	24	N3	9.56	9.72		
	25	N4	10.08	10.64		
	26	N5	7.95	7.43		
	27	N6	10.22	10.01		
	28	N7	7.92	7.82		
	29	N8	8.66	8.32		
	30	N9	7.28	7.09		
ADULT	32	UND 1999C	18.38	17.99	6.35	6.89
	34	UND 1999A	32.51	27.73	8.66	7.45
	36	UND 1999E	27.88	27.96	7.56	6.93
	44	UDW 3005	29.53	17.99	7.92	7.83
	45	UDW N33	28.11	27.61	8.39	7.76
	46	UDW N34	30.18	28.91	8.8	7.92
	47	UDW N35	28.73	28.33	8.69	7.94
	48	UDW N36	26.92	28.94	7.88	7.94

APPENDIX C

MCG lengths and widths

	LENGTH			WIDTH		
	I	II	III	I	II	III
FOETAL	4.37	4.53	4.46			
	3.96	4.38	4.34			
	4.28	4.08	4.12			
	4.1	3.75	4.12			
	4	4.38	4.15			
	3.98	4.12	4.04			
	4.12	4.41	3.96			
	4.18	3.98	4.31			
	4.23	4.15	3.79			
	4.16	3.74	1.09			
	4.28	3.93				
	4.24	3.83				
	1	4.43				
		4.45				
		4.32				
		3.85				
		3.42				
		3.85				
		3.25				
		2.44				
		1.17				
ADULT	9.81	9.88	9.86	3.67	5.44	5.76
	8.54	9.44	9.72	3.62	4.24	3.64
	1.91	8.84	9.05	2.21	3.85	4.72
		8.15	8.92		3.12	3.54
		8.65	9.76		3.42	3.83
		2.27	8.92		2.29	2.84
			3.54			2.53

APPENDIX D

CTG length and widths

		RIGHT		LEFT	
	SP.	LENGTH	WIDTH	LENGTH	WIDTH
FOETUS	1	10.32		11.28	
	5	9.24		7.95	
	6			6.56	
	7			6.15	
	8	5.84		10.84	
	11	10.08		4.95	
	12	5.26		6.06	
	13	10.26		8.80	
	14	7.89		5.68	
	15				
	16	6.28		5.46	
	17	4.93		8.82	
	19	5.03		7.11	
	20	6.52		5.52	
	22	4.67			
	23	6.00		9.25	
	24	7.78		10.14	
	25	8.39		6.30	
	26	5.81		7.25	
	27	7.66		9.96	
	28	9.75			
	29	5.53			
	30			4.88	
ADULT	32	21.25	10.18	20.94	9.03
	34	15.85	8.78	14.86	4.77
	36			17.63	7.19
	44	19.77	4.26	12.69	4.71
	45	15.08	3.35	9.48	8.31
	46	17.66	7.62		
	47			14.99	4.66
	48				

SAPSE RATED PUBLICATIONS AND SCIENTIFIC PRESENTATIONS BASED ON THIS RESEARCH TO DATE

JOURNAL PUBLICATIONS

1. IN PRESS

Thoracic splanchnic nerves : Implications for splanchnic denervation

Naidoo N, Partab P, **N Pather**, Singh B, Moodley J, Satyapal K S

Journal of Anatomy (United Kingdom) Manuscript #: JANAT 2001/001045

2. UNDER REVIEW

Sympathetic contributions to the cardiac plexus

N Pather, P Partab, B Singh, KS Satyapal

Surgical and Radiological Anatomy (France) Manuscript #: 01-103

3. IN PREPARATION

The middle cervical ganglion: incidence and classification

N Pather, P Partab, B Singh, KS Satyapal

The cervical sympathetic chain patterns

N Pather, P Partab, B Singh, KS Satyapal

The incidence of fused thoracic ganglia

N Pather, P Partab, B Singh, KS Satyapal

The thoracic cardiac rami

N Pather, P Partab, B Singh, KS Satyapal

4. REFEREED ABSTRACTS / SHORT PAPERS

Limitations of Stellate Ganglion Blockade

Partab P, Singh B, Ramsaroop L, **Pather N**, Satyapal KS
Proceedings of the Surgical Research Society, July 2001

Alternate Sympathetic Vascular Branches to the Upper Limb

Pather N, Ramsaroop L, Partab P, Singh B, Satyapal KS

Proceedings of the Surgical Research Society, July 2001

Superior cervical ganglion branches

L Ramsaroop, N Pather, P Partab, B Singh, KS Satyapal

Proceedings of the XVIth International Symposium on Morphological Sciences, July 2001

Cervical sympathetic chain : Arterial branches

N Pather, L Ramsaroop, P Partab, B Singh, KS Satyapal

Proceedings of the XVIth International Symposium on Morphological Sciences, July 2001

Stellate ganglion blockade : a re-appraisal

P Partab, B Singh, N Pather, L Ramsaroop, KS Satyapal

Proceedings of the XVIth International Symposium on Morphological Sciences, July 2001

Cervical ganglia : A review

N Pather, L Ramsaroop, P Partab, B Singh, KS Satyapal

Proceedings of the XVIth International Symposium on Morphological Sciences, July 2001

T2 ganglion : anatomical landmarks

L Ramsaroop, N Pather, P Partab, B Singh, KS Satyapal

Proceedings of the XVIth International Symposium on Morphological Sciences, July 2001

Thoracoscopic advances : impact on anatomical precision

KS Satyapal, B Singh, P Partab, L Ramsaroop, N Pather

Proceedings of the XVIth International Symposium on Morphological Sciences, July 2001

Anatomical rationale for highly selective limited sympathectomy in intractable angina

N Pather, P Partab, B Singh, KS Satyapal

Proceedings of the Surgical Research Society of Southern Africa, July 2000

Thoracic sympathetic contributions to the cardiac plexus

N Pather, P Partab, B Singh, KS Satyapal

Proceedings of the Tripartite Meeting of the Anatomical Society of Great Britain and Ireland, July 2000

Identification of thoracic sympathetic ganglia in fetuses

N Pather, P Partab, KS Satyapal

Proceedings of the Anatomical Society of Southern Africa, April 2000

Sympathetic contribution to the cardiac plexus : A pilot study

N Pather, P Partab, B Singh, KS Satyapal

Proceedings of the Anatomical Society of Southern Africa, April 2000

Incidence, topography and distribution of the stellate ganglion

N Pather, L Ramsaroop, P Partab, B Singh, KS Satyapal

Proceedings of the Anatomical Society of Southern Africa, April 2000

SCIENTIFIC CONFERENCES: PAPERS DELIVERED

A) INTERNATIONAL CONFERENCES

Cervical ganglia : A review

N Pather, L Ramsaroop, P Partab, B Singh, KS Satyapal

XVIth International Symposium on Morphological Sciences, Sun City, South Africa, July 2001

Cervical sympathetic chain : Arterial branches

N Pather, L Ramsaroop, P Partab, B Singh, KS Satyapal

XVIth International Symposium on Morphological Sciences, Sun City, South Africa, July 2001

Superior cervical ganglion branches

L Ramsaroop, N Pather, P Partab, B Singh, KS Satyapal

XVIth International Symposium on Morphological Sciences, Sun City, South Africa, July 2001

Stellate ganglion blockade : a re-appraisal

P Partab, B Singh, N Pather, L Ramsaroop, KS Satyapal

XVIth International Symposium on Morphological Sciences, Sun City, South Africa, July 2001

T2 ganglion : anatomical landmarks

L Ramsaroop, N Pather, P Partab, B Singh, KS Satyapal

XVIth International Symposium on Morphological Sciences, Sun City, South Africa, July 2001

Thoracoscopic advances : impact on anatomical precision

KS Satyapal, B Singh, P Partab, L Ramsaroop, N Pather

XVIth International Symposium on Morphological Sciences, Sun City, South Africa, July 2001

Thoracic sympathetic contributions to the cardiac plexus

Pather N, Partab P, Singh B, Satyapal KS

Tripartite Meeting of the Anatomical Society of Great Britain and Ireland, , Anatomische Gesellschaft, Nederlandse Anatomen Vereniging : University of Cambridge, UK, July 2000

B) NATIONAL CONFERENCES

Alternate Sympathetic Vascular Branches to the Upper Limb

Pather N, Ramsaroop L, Partab P, Singh B, Satyapal KS

29th Congress of the Surgical Research Society of Southern Africa, Wits Business School, Parktown, Johannesburg, July 2001

Anatomical rationale for highly selective limited sympathectomy in intractable angina

N Pather, P Partab, B Singh, KS Satyapal

Surgical Research Society of Southern Africa, Annual Congress, Cape Town, July 2000

Identification of thoracic sympathetic ganglia in foetuses

N Pather, P Partab, B Singh, KS Satyapal

30th Anatomical Society of Southern Africa Conference, Stellenbosch, South Africa, April 2000

Sympathetic contribution to the cardiac plexus : A pilot study

N Pather, P Partab, B Singh, KS Satyapal

30th Anatomical Society of Southern Africa Conference, Stellenbosch, South Africa, April 2000

Incidence, topography and distribution of the stellate ganglion

N Pather, L Ramsaroop, P Partab, B Singh, KS Satyapal

30th Anatomical Society of Southern Africa Conference, Stellenbosch, South Africa, April 2000

APPENDIX C

MCG lengths and widths

	LENGTH			WIDTH		
	I	II	III	I	II	III
FOETAL	4.37	4.53	4.46			
	3.96	4.38	4.34			
	4.28	4.08	4.12			
	4.1	3.75	4.12			
	4	4.38	4.15			
	3.98	4.12	4.04			
	4.12	4.41	3.96			
	4.18	3.98	4.31			
	4.23	4.15	3.79			
	4.16	3.74	1.09			
	4.28	3.93				
	4.24	3.83				
	1	4.43				
		4.45				
		4.32				
		3.85				
		3.42				
		3.85				
		3.25				
		2.44				
		1.17				
ADULT	9.81	9.88	9.86	3.67	5.44	5.76
	8.54	9.44	9.72	3.62	4.24	3.64
	1.91	8.84	9.05	2.21	3.85	4.72
		8.15	8.92		3.12	3.54
		8.65	9.76		3.42	3.83
		2.27	8.92		2.29	2.84
			3.54			2.53